MINIMUM VIRGIN BINDER LIMITS IN RECYCLED SUPERPAVE (SR) MIXES IN KANSAS

by

MASOUMEH TAVAKOL

B.S., Isfahan University of Technology, 2005

A THESIS

Submitted in partial fulfillment of the requirements for the degree

MASTER OF SCIENCE

Department of Civil Engineering
College of Engineering

KANSAS STATE UNIVERSITY
Manhattan, Kansas

2016

Approved by:

Major Professor
Dr. Mustaque Hossain

Abstract

Use of recycled materials in asphalt pavement has become widespread recently due to rising costs of virgin binder and increased attention to sustainability. Historically, recycled asphalt pavement (RAP) has been the most commonly used recycled material for hot-mix asphalt (HMA). However, recycled asphalt shingle (RAS), another recycled material, has recently become popular. Although there are some guidelines regarding use of RAP and RAS in HMA, their effects on mixture performance, especially on mixtures containing RAS, are not thoroughly understood.

In this research, three recycled Superpave mixture designs from the Kansas Department of Transportation (KDOT) with 9.5 mm (SR-9.5A) and 19 mm (SR-19A) Nominal Maximum Aggregate Size (NMAS) were selected as control mixtures. Mixtures containing higher percentages of recycled materials (RAP and RAS) were developed using KDOT blending charts. A total of nine mixtures with varying virgin binder contents were designed and assessed for moisture susceptibility, rutting resistance, and fatigue cracking propensity using modified Lottman, Hamburg Wheel Tracking Device, flow number, Dynamic Modulus, and S-VECD direct tension fatigue tests.

Results confirmed the effect of NMAS and material source on mixture performance. For SR-9.5A, the mixtures showed increased susceptibility to moisture and rutting damage below virgin binder content of 75%. For SR-19A, mixtures with virgin binder content of 70% showed satisfactory performance properties. Mixtures with virgin binder contents lower than 60% definitely showed inferior performance.

Table of Contents

List of Figures

List of Tables

Acknowledgements

I would like to extend my sincerest thanks and appreciation to my major professor Dr. Mustaque Hossain for his encouragement, support and invaluable advice throughout all stages of my graduate studies at Kansas State University. I would like to thank Dr. Sunanda Dissanayake, Dr. Robert W. Stokes, and Dr. Kyle A. Riding for being on my thesis committee and their review and inputs for making my thesis better.

I acknowledge the Kansas Department of Transportation (KDOT) for sponsoring this study under the Kansas New Transportation Research and Developments (K-TRAN) program. Special thanks are due to Mr. Christopher Liebrock, Mr. Cliff Hobson, Dr. Brain Coree (formerly with KDOT) and Mr. Blair Heptig for their support throughout this study.

I would like to thank Dr. Christopher Vahl and Mr. Alexander McLellan for consulting the statistical analysis for the study.

I would also like to acknowledge Nassim Sabahfar, Ryan Benteman, Dustin Phommanivong Hai Vo-Le, Xingdong Wu, and Alexander McKean for their help and contribution to this research work.

Finally, I wish to express my sincere respect and appreciation to my family and friends for their love, understanding and encouragement.

Dedication

This thesis is dedicated to my parents, Mrs. Azam Niknami and Mr. Mohammadali Tavakol, because of their unconditional love and support throughout my entire life.

Chapter 1 - Introduction

1.1 Background

Asphalt pavements are quick to construct and easy to maintain while providing a smooth, safe and quiet ride. According to the National Asphalt Pavement Association (NAPA), approximately 93% of more than 2.6 million miles of paved roads and highways in the United States are asphalt-surfaced pavements (NAPA, 2015). NAPA (2015) has also reported that approximately 550 million tons of asphalt pavement materials are produced annually, for a total worth of more than $30 billion. Because asphalt pavements are vital to the transportation infrastructure, the asphalt pavement industry seeks continuous product improvement in order to achieve higher quality and versatility in application. Innovative ways, such as recycling, have contributed economic and environmental benefits to the industry. Recycled asphalt pavements (RAP) and recycled asphalt shingles (RAS), two commonly used materials for asphalt pavements, are often utilized in order to avoid increasing costs of virgin binders. RAP, the most common recycled material, is comprised of reusable asphalt pavement materials that are the product of resurfacing, rehabilitation, and reconstruction operations (Copeland, 2011). In the early 1990s, the Federal Highway Administration (FHWA) and the US Environmental Protection Agency (EPA) estimated annual reclamation of more than 90 million tons of asphalt pavements, of which 80% were recycled (Copeland, 2011). RAS, the product of manufacturing waste or reroofing, contains higher recyclable asphalt binder contents. NAPA reported that 1.1 million tons of RAS were used in asphalt pavements in 2010, resulting in the conservation of more than 234,000 tons of asphalt binder (Hansen and Newcomb, 2011). Figure 1.1 shows the RAP and RAS reclaiming process.

(a)

(b)

Figure 1.1 (a) RAP production and material (FHWA, 2015); (b) RAS production and material (LL Pelling, 2015)

In addition to economic benefits, use of recycled materials creates an optimized cycle for the use of nonrenewable natural resources such as virgin aggregate and asphalt binder and decreases the need for landfilling. However, incorporation of recycled materials into asphalt mixtures is a concern because chemical and mechanical properties of mixtures change, consequently affecting mixture performance properties. The primary reason for change in mixture properties is that aged binder from the recycled materials is introduced into the mixture; this aged binder has different composition and properties than the virgin binder (Sabahfer and Hossain, 2015; Daniel and Lachance, 2005). The change in mixture properties may result in mixtures that are more vulnerable to asphalt pavement distresses.

In summary, despite all benefits associated with use of recycled materials in pavements, performance should not be compromised. The target is achievable with proper mixture design considerations in which recycled products exhibit no performance differences compared to conventional mixtures or the recycled products demonstrate improved performance for certain applications (Hansen and Newcomb, 2011; Al-Qadi et al., 2007).

1.2 Problem Statement

The Kansas Department of Transportation (KDOT) has been increasingly permitting incorporation of recycled materials into hot-mix asphalt (HMA) Superpave mixtures. Strong incentives to include more recycled materials include increasing virgin material costs and increasing awareness of the importance of sustainability. The two recycled materials that have gained the most attention are RAP and RAS. Despite the increased tendency for incorporation of these materials into asphalt pavement mixtures, concerns have arisen regarding use of these materials. The reason is that replacement of the virgin binder with the aged binder from RAP and RAS changes the performance properties of the mixtures. Nevertheless, how the performance is affected remains questionable. However, a high uncertainty for RAS use exists because RAS contains a considerable amount of highly aged binder with limited historical experience of use in pavement structures. Guidelines for incorporation of RAP and RAS should be developed, including universal specification for considering effects of RAP and RAS in the asphalt mixtures.

1.3 Objective

The specific objective of this study was to investigate various sources and amounts of recycled binders from RAP and RAS in order to establish limits for these recycled materials based on mixture performance. In other words, the effect of varying virgin binder contents on Superpave mixtures irrespective of recycled binder source needed to be assessed. Performance properties were defined as the ability to resist damage caused by moisture, rutting, and fatigue cracking.

1.4 Thesis Outline

This thesis consists of five chapters including this introductory chapter. Chapter 2 provides a literature review of materials and terminologies as well as selected mixture performance properties that have been evaluated in the laboratory. Chapter 3 describes materials used and methodology followed to assess performance of the mixtures. Chapter 4 presents results obtained from all performed tests and a statistical analysis of the results. Chapter 5 presents conclusions and recommendations based on this study.

Chapter 2 - Literature Review

2.1 Introduction

Use of recycled materials, especially RAP and RAS, in asphalt pavement construction is currently preferred over virgin materials due to rising asphalt binder costs, scarcity of quality aggregates, and environmental concerns. However, the effect of recycled materials on pavement performance is a topic of interest for researchers. Although national and some state specifications allow incorporation of high amounts of recycled materials in HMA mixtures, most agencies are reluctant to do so because of uncertainty about the long-term performance of such mixtures. As a result, the amount of RAP used in a majority of states is only 15% to 25% and RAS is usually limited to 5%. This chapter presents a comprehensive literature review of studies on RAP and RAS use in HMA mixtures. The first section provides information on materials used and terminologies. The latter section contains an assessment of common asphalt mixture deficiencies discussed in this study.

2.2 Reclaimed Asphalt Pavement

The FHWA defines RAP as existing asphalt pavement materials removed and processed during resurfacing, rehabilitation, or reconstruction operations (Copeland, 2011). The first use of RAP dates back to 1915, but it was not until the 1970s that asphalt pavement recycling became more popular due to a sharp rise in crude oil costs followed by increased demand as good aggregate sources dwindled (Sabahfar, 2012; Copeland, 2011). Currently, RAP is the most frequently recycled material in the United States: The FHWA and the US EPA have estimated annual usage of RAP to be 72 million tons in 1990s (Copeland, 2011).

Use of recycled materials in pavements is driven by two main motivations. The first incentive is reduced costs of materials, transportation, and disposal. Materials account for

approximately 70% of the total cost of HMA production, and the most expensive constituent of HMA is asphalt binder. Consequently, strong incentives exist to increase RAP in HMA mixtures with typical 4% to 6% asphalt binder content as an economical substitute for virgin material. Transportation and disposal costs can also be reduced with RAP usage (Copeland, 2011). In addition to economics, another important motivation for use of recycled materials in pavements is environmental benefits such as conservation of energy, preservation of resources, and reduction of landfills.

Full depth pavement removal and milling are two methods commonly employed for production of RAP materials. Full depth removal requires use of heavy equipment to break the pavement structure into slabs that are transported, crushed, and processed to manageable size (Copeland, 2011). In the milling procedure, distressed upper layers of pavement are removed to a given depth. Generally for the milling method no further processing is required to crush and screen RAP to create suitable and consistent materials (Copeland, 2011). Once RAP is produced, the asphalt binder content and aggregate gradation must be determined. Ignition oven is the most common method used to determine RAP asphalt content and to quantify recovered aggregate gradation. Once characteristics of the RAP material are known, it can be incorporated into the HMA as a viable source of aggregate and binder (Copeland, 2011).

RAP was successfully used before implementation of the Superior Performing Asphalt Pavements (Superpave) design method in the late 1990s, but large-scale use of RAP was limited in favor of implementation of Superpave. First, Superpave did not provide guidelines for use of RAP material, and second, RAP contains higher fine content, which is discouraged in the Superpave HMA mixture design procedure. However, the problem was overcome and guidelines

for use of RAP were gradually developed by the FHWA and the National Cooperative Highway Research Program (NCHRP), resulting in increased RAP usage (Copeland, 2011).

State Departments of Transportation (DOTs) require RAP mixtures to meet all conventional mixture design specifications. Furthermore, the current national guideline, AASHTO M323, requires adjustments in virgin binder grade to account for the stiffening effect of aged binder in RAP when RAP is used in higher quantity. Aging of the binder, which is defined as binder hardening due to oxidation throughout the pavement service life, occurs beyond the near-surface of the pavement, critically impacting pavement durability (Glover et al., 2009). Binder properties in asphalt pavements are highly influenced by the aging process. Increased stiffness is the main concern, but changes in chemical and physical properties, such as ductility and adhesion, are also evident, thereby affecting binder performance and consequently, mixture performance (Karlsson and Isacsson, 2006).

According to current national requirements specified in AASHTO M323, if the percentage of RAP in Superpave mixtures is less than 15%, the binder grade selection does not need to be changed to account for aging of binder. If the percentage of RAP is between 15% and 25%, a softer virgin binder than normal is required, and in the case of more than 25% RAP, blending charts should be followed and RAP binder grade should be determined using several tests and procedures. First, the RAP binder should be extracted and recovered using solvents then test methods such as Dynamic Shear Rheometer (DSR), the Bending Beam Rheometer (BBR), and the Direct Tension Tester (DTT) are used to grade high and low sides of the RAP asphalt binder (Copeland, 2011).

Despite the many benefits associated with RAP usage in mixtures, several issues prevent further use of RAP. Based on a survey conducted by the North Carolina DOT in 2009, quality

was a major concern of DOTs (Copeland, 2011). Other barriers to RAP use include lack of consistency of RAP, binder grade and blending, mix design procedures, durability, and cracking performance. Furthermore, many DOTs are reluctant to allow high RAP percentages in mixtures because the required procedure for RAP binder extraction and testing is time-consuming and expensive. Therefore, although a majority of state DOTs allow RAP incorporation into asphalt pavement, most states impose restrictions on the amount of RAP usage (Copeland, 2011). Based on a survey conducted by the Ministry of Transportation of Ontario, 20%–50% RAP typically are permitted in base and intermediate layers; the permitted level is higher for roads with light traffic and base layers with low percentages for the surface course (Copeland, 2011). In general, percentages of RAP allowed by state DOTs is 10%–20% for heavy traffic and surface layers. The current practice of RAP incorporation has been confirmed by many studies that have shown that mixtures with up to 25% RAP perform identically to virgin mixtures (Li et al., 2008; Al-Qadi et al., 2007; McDaniel et al., 2000).

2.3 Recycled Asphalt Shingles

RAS are shingle waste streams that can be processed and used in pavements. Shingle recycling first began approximately 30 years ago, and the first technical literature on RAS incorporation in HMA was published in the late 1980s (Zhou et al., 2012). The NAPA reported that 1.1 million tons of RAS was used in the US in 2010, representing a 57% increase compared to 2009 usage (Hansen and Newcomb, 2011). AASHTO MP23 is the current standard specification for RAS use in HMA mixtures, and more than 20 states have specifications for RAS use or are considering RAS application in HMA (Williams et al., 2013).

Two basic types of shingles are available for recycling and processing: manufacturer waste asphalt shingles (MWAS), such as tab cutouts or out-of-specification roofing shingles

shipped directly from asphalt shingle manufacturers, and post-consumer asphalt shingles or tear-off asphalt shingles (TOAS), which represent shingles removed during reroofing or roof removal projects. TOAS accounts for more shingle waste because it is readily available to contractors, but MWAS is more favorable for use because the material composition is more well-known and the asphalt binder is less oxidized (Button et al., 1996). In addition, TOAS contains deleterious or harmful materials such as wood, nails, and in some cases, asbestos, which is harmful for road construction workers. Table 2.1 lists the typical composition of asphalt shingles.

Table 2.1 Typical compositions of new residential asphalt shingles (Zhou et al., 2012)

Component	Organic Shingles, % by wt.	Fiberglass Shingles, % by wt.
Asphalt cement	30–36	19–22
Reinforcing mat	2–15	2–15
Mineral granules/aggregate	20–38	20–38
Mineral filler/stabilizer	8–40	8–40
Adhesives (modified asphalt-based)	0.2–2	0.2–2

Production of RAS includes collecting, sorting, grinding, screening, and storing the material. After processing, RAS physical and rheological properties, such as aggregate gradation, binder content, and binder Performance Grade (PG), must be determined. The ignition oven method or the extraction method is used to determine binder content and aggregate gradation. DSR, BBR, and DTT methods are used to find the PG binder grade. However, due to the oxidation effect, RAS binder is very stiff and difficult to grade. Researchers have reported that the low-temperature PG grade of RAS binder is above 0 °C (Zhou et al., 2012).

Superpave mixture design can be followed to design and incorporate RAS into HMA mixtures. Past standard specifications for use of RAS, AASHTO MP15, limited recycled binder

replacement to 30% in mixtures; otherwise, adjustments to the virgin binder grade or the addition of asphalt rejuvenator were recommended. Current standard AASHTO MP23 adopted Table 2 of AASHTO M323 for binder grade adjustment for mixtures with RAS, allowing for use of more than 25% RAS or a combination of RAP and RAS with suitable binder adjustment.

Many research studies have been performed to evaluate the effect of RAS on HMA mixture performance. Results have suggested that incorporating up to 5% RAS in HMA mixtures has minimum impact on mixture performance (Wen et al., 2015; Williams et al., 2011; Johnson et al., 2010; Scholz, 2010; Newcomb et al., 1993). A majority of states that currently allow RAS use in HMA mixture impose a maximum limit of 5%. Each state DOT has additional requirements for RAS used in combination with RAP and other virgin binder requirements.

2.4 State DOT Requirements for Virgin Binder Replacement

According to AASHTO M323, the standard specification of Superpave mixture design, no national requirement exists for minimum virgin binder content in recycled mixtures; therefore, high percentages of recycled materials can be incorporated into mixtures as long as blending chart recommendations are followed. However, each state DOT has special construction specifications that define maximum allowable incorporation of recycled materials into mixtures or minimum virgin binder requirements. A majority of state specifications are based on maximum allowable RAP/RAS incorporation, but some states also set the limit on virgin binder replacement. Most states permit use of RAP in mixtures. For RAS incorporation, currently more than 20 states have specifications, are developing specifications, or are considering incorporation of RAS into their asphalt applications (Williams et al., 2013). KDOT has adopted AASHTO M323 requirements for use of RAP that allows high RAP percentages in HMA mixtures and adheres to the limitation of 5% maximum RAS in mixtures. KDOT allows a

maximum of 5% RAS and 10% RAP for a combination of RAP and RAS. Table 2.2 and Table 2.3 summarize maximum percentages or binder replacement requirements of RAP or RAS in some states.

Table 2.2 State specifications for RAS (Williams et al., 2013)

State	Specification
AL	Allows 5% M or 3% C
GA	Allows 5% M or C
IA	Allows 5% M or C
IL	Allows 5% M or C
IN	Allows binder replacement of 15% M or C for surface coarse mixes (maximum 25% binder replacement for mixes less than 9 million ESALs
KS	Allows 5% M or C
KY	24% binder replacement
MA	Allows 5% M
MD	Allows 5% M
MN	Allows 5% M or C
MO	Allows 7% M or C
NC	Allows 5% M or C
NJ	Allows 5% M
NH	0.6% binder replaced with M or C from % of total mix
NY	Allows 5% M
OH	Allows 5% M or C
PA	Allows 5% M or C
SC	Allows 5% M or C
TX	Allows 5% M or C
VA	Allows 5% M or C
WI	Allows binder replacement of 20% M or C (5% max when used in combination of RAP)

- M stands for post-Manufacturer RAS and C stands for post-Consumer RAS
- Reflects requirement on RAS application without RAP

Table 2.3 State specifications for RAP (Source: State Specifications for Construction)

State	State specification for maximum RAP or minimum virgin binder	Specification year
AL	20% max. RAP for surface, other 25% max.	2012
AR	70% min. virgin binder	2003
CA	15% max. RAP	2010
CO	20% max. RAP for surface, other 25% max.	-
DE	20% max. RAP	2001
FL	Allows >30% RAP	2013
IA	10% max. unclassified RAP	2012
	20% max. certified RAP	
	70% min. virgin binder classified RAP	
KS	Allows >25% with binder testing	-
MN	70% min. virgin binder	2010
MD	20% max. RAP for surface, other 25% max.	-
NY	20-50% max. RAP based on RAP moisture content	2008
NC	>30% max. RAP	2012
OH	15% max. RAP for heavy traffic polymer surface course	2013
	20% max. RAP medium traffic surface course	
	25% max. RAP light traffic surface course	
	40% to up to 55% max. RAP intermediate and base course	
TX	20% max. RAP in surface	2014
WI (lower layer)	75% min. virgin binder when RAS used alone	2015
	60% min. virgin binder when RAP and FRAP in any combination	
	65% min. virgin binder when RAS, RAP, and FRAP in combination	
WI (upper layer)	80% min. virgin binder when RAS used alone	
	75% min. virgin binder when RAP and FRAP in any combination	
	75% min. virgin binder when RAS, RAP, and FRAP in combination	

2.5 Superpave Mixture Design Method

The Superpave design method is a comprehensive design procedure that seeks to design asphalt mixtures for required performance dictated by traffic, environment (climate), and structural sections at a particular pavement site in order to achieve an economical asphalt mixture (Cominsky et al., 1994).

In 1987, the Strategic Highway Research Program (SHRP) began a comprehensive asphalt research program to develop a performance-based asphalt binder specification and a performance-based asphalt mixture design system. Successful outcomes of the study that are currently used include the PG asphalt binder specification and Superpave mixture design method (Huber, 2013).

The Superpave design method is based on incorporation of adequate asphalt binder, sufficient voids in the mineral aggregate (VMA) and air voids, proper workability, and satisfactory performance characteristics throughout the pavement service life (Sabhafer and Hossain, 2014; Cominsky et al., 1994). Although Superpave uses traditional volumetric mix design methodologies, it also includes a direct relationship to field performance, which was not effectively considered in previous mix design procedures. Superpave mix design was developed with three levels of increasingly complex mix designs: Level 1, Level 2, and Level 3. However, because performance-based tests and models were not implemented, only Level 1 is specified in AASHTO M323 (Huber, 2013). Since completion of the SHRP research in 1993, the asphalt industry and a majority of state DOTs have implemented the Superpave system (TRB Superpave committee, 2005).

2.6 Common HMA Mixture Deficiencies

Due to high traffic volumes and increased tire pressures, asphalt mixtures are now exposed to more stresses that cause problems related to fracture, permanent deformation, and surface wear of pavement. Among all HMA deficiencies, researchers have reported rutting and fatigue cracking as the two major distresses of asphalt pavements (Moghaddam et al., 2011; Shu et al., 2008). Another deficiency is susceptibility to moisture damage, which is considered in the Superpave mixture design procedure. In this study, performance tests were conducted to address deficiencies of HMA mixtures that contain recycled materials.

2.7 Evaluating Moisture Susceptibility

Moisture susceptibility is defined as the tendency of HMA to show stripping (Putman and Amirkhanian, 2006). Stripping is a major distress of HMA that negatively affects pavement performance and results in unforeseen increases in maintenance costs. Stripping has been observed in HMA mixtures in the United States as well as many other parts of the world (Kiggundu and Roberts, 1988). Stripping is induced by moisture that causes loss of adhesion between aggregates and binder in HMA and loss of cohesion within the asphalt mastic, eventually resulting in weakened bond strength and reduced stiffness and leading to additional distresses such as raveling, rutting, and fatigue cracking (Huang et al., 2010; Putman and Amirkhanian, 2006; Kiggundu and Roberts, 1988). Stripping usually begins at the bottom of the HMA layer and gradually moves toward the surface. Typically loss of strength occurs over the years (Putman and Amirkhanian, 2006; Roberts et al., 1996).

Since the first detection of stripping in the early 1900s, many studies have sought to understand and predict stripping potential of HMA (Huang et al., 2010; Kiggundu and Roberts, 1988). Despite all efforts, the mechanism behind stripping is still not thoroughly understood due

to the complexity of phenomena, and stripping continues to appear on pavements (Kiggundu and Roberts, 1988). However, factors that contribute to moisture-related damages are largely known. In addition to water, the only reason widely referred to as the cause of stripping, aggregate and asphalt binder characteristics, mixture design and properties, additives used, construction practices and issues, and traffic loads are also factors related to stripping (Kiggundu and Roberts, 1988). Inadequate drainage is also claimed as a major contributing factor to stripping since field observations reported that stripping was predominant only in areas that remained oversaturated with water due to inadequate drainage (Kandhal, 1994). Postulated mechanisms such as detachment, displacement, spontaneous emulsification, film rupture, pore pressure, and hydraulic scouring seek to explain how stripping occurs in pavements (Kiggundu and Roberts, 1988).

The best practice to prevent stripping involves using a combination of quality materials, proper mixture design and laboratory testing, proper pavement construction, and adequate drainage. Antistripping agents are also used to chemically improve adhesion between the asphaltic binder and aggregates. These chemicals or additives are commonly used to prevent moisture-induced damage in asphalt pavement (Huang et al., 2010; Kiggundu and Roberts, 1988). Liquid antistripping agents are usually a class of amine-based chemicals added directly to the aggregates or to the heated asphalt binder prior to mixing. Interaction between the polar ends of antistripping agents and aggregate surfaces can reduce surface tension between the aggregate surface and the asphalt binder, thereby promoting adhesion between aggregate particles and the asphalt binder (Huang et al., 2010; Kiggundu and Roberts, 1988; Anderson et al., 1982). Mineral or solid antistripping additives are usually inorganic powders that are added to aggregates before mixing with the asphalt binder. Commonly used solid antistripping agents include Portland cement, hydrated lime, fly ash, and flue dust. Hydrated lime is a very effective agent and the

most accepted way of controlling moisture susceptibility of HMA in many parts of the country. Chemical interaction between calcium in the lime with silicates in the aggregates is the mechanism for how lime improves moisture susceptibility (Little and Petersen, 2005; Little and Epps, 2001; Kiggundu and Roberts, 1988)

2.7.1 Laboratory Methods to Evaluate Moisture Damage

Adequate laboratory testing on designed mixtures prior to incorporation in pavement is essential to decrease the potential for moisture susceptibility. Such tests include indirect tension testing, the modified Lottman test, and the Texas Boiling Water test. The Lottman test was developed to evaluate the stripping potential of HMA mixtures. Originally, three subsets of samples were prepared and differently conditioned. Control samples were evaluated when dry; the second set demonstrated long-term moisture effects by undergoing freeze-thaw cycles, and the third set evaluated short-term effects of moisture by warm water. Then samples were tested to obtain tensile strength. Test results were average strength of the wet sets to the dry sets which yield the tensile strength ratio (TSR). Lottman suggested 70% as the minimum TSR. The test procedure was later modified by changing the test temperature and loading rate and by omitting the short-term effect evaluation (Kiggundu and Roberts, 1988). The test is now commonly called the modified Lottman method and is standardized in AASHTO T283. Although the modified Lottman test is the current adopted test method for evaluating moisture susceptibility of Superpave mixtures in Kansas, test procedure has been further modified to have a shorter conditioning period and a mandatory freeze cycle that is optional in AASHTO T283.

2.7.2 Moisture Susceptibility of Recycled Mixtures

Extensive efforts have been made to evaluate the moisture susceptibility of recycled mixtures during recent years; however, results have not always been consistent. Results of a study performed in Minnesota on RAP mixtures with various percentages of RAP material and virgin binder grades showed that the addition of RAP to a mixture had no positive or negative influence on the mixture's tensile strength or moisture susceptibility (Sondag et al., 2002). Other studies found that as the percentage of RAP increased, TSR decreased and mixtures with RAP became more susceptible to moisture damage (Sabahfar et al., 2014; Rahman, 2010; Li et al., 2004).

However, some studies have postulated that an increase in RAP content improves moisture susceptibility of HMA mixtures. A study to evaluate the impact of high RAP content on HMA was performed with RAP contents of 0%, 30%, 40%, and 50%. Results showed that with the exception of mixtures with 40% RAP, TSRs increased with increased RAP content. An increase in tensile strength with increased RAP content was also observed (Al-Qadi et al., 2012). Another study to evaluate moisture susceptibility of plant-produced foamed warm-mix asphalt (WMA) with high percentages of RAP confirmed that RAP improved moisture resistance of WMA and HMA mixtures (Shu et al., 2012). RAS mixtures exhibited identical resistance to moisture damage as conventional HMA mixtures; however, researchers found that oxidized TOAS had negative effects on moisture resistance (Zhao et al., 2013; Zhou et al., 2012; Newcomb et al., 1993).

2.8 Evaluating Rutting Potential

Rutting, identified as the most important distress of HMA (Witczak et al., 2002), is the permanent deformation of the HMA layer caused by densification due to traffic loading and by shear flow with no volume change (Brown et al., 2009). A common form of rutting is longitudinal depressions in the wheel paths with small side upheavals. Rutting is a primary distress of HMA that significantly impacts pavement performance and reduces service life of the pavement. Rutting also results in safety issues because it affects vehicle handling on the road, potentially leading to hydroplaning due to accumulated water in the ruts (Williams, 2003; Sousa et al., 1991).

The mechanism to form rutting is described as the accumulation of permanent deformation in paving materials with increasing numbers of load applications due to a combination of densification and shear deformation in one or all pavement layers (Tayfur et al., 2007; Sousa et al., 1991). However, researchers found shear deformation to be the primary rutting mechanism and thus recommended pavement placement at higher densities in order to reduce the effect of shear deformation (Eisenmann and Hilmer, 1987; Hofstra and Klomp, 1972).

Several factors known to contribute to rutting can be divided into characteristics of asphalt mixture and field condition. Mixtures with dense-graded aggregates and rough surface texture, hard asphalt binders, and adequate binder content have shown superior rutting resistance. However, moisture damage and hot weather can increase the potential for rutting (Zhang et al., 2009; Sousa et al., 1991).

2.8.1 Tests for Rutting Potential Prediction

Several test methods are available to predict rutting susceptibility of asphalt mixtures. These methods include the Marshall flow test, the static creep test, the dynamic creep test, the

wheel tracking test, and the indirect tensile test (Tayfur et al., 2007). The most common type of laboratory tester currently used to asses rutting resistance is the loaded wheel tester (LWT) (Cooley et al., 2000). Several types of testers are available in the United States, including the Georgia Loaded Wheel Tester (GLWT), the Asphalt Pavement Analyzer (APA), the Hamburg Wheel Tracking Device (HWTD), the LCPC (French) Wheel Tracker, the Purdue University Laboratory Wheel Tracking Device (PURWheel), and the one-third scale Model Mobile Load Simulator (MMLS3) (Cooley et al., 2000). All the testers have a similar operating principle in that a loaded wheel rolls back and forth over a test sample and the resulting rut depth is measured. Two test parameters, air voids and test temperature, significantly affect test results from these testers. Research has shown that higher air voids and high test temperatures result in increased rut depth (Cooley et al., 2000; West, 1999; Shami et al., 1997; Collins et al., 1996; Stuart and Izzo, 1995). When in-service loading and environmental conditions are considered, LWT results were reasonably well correlated to actual field performance (Cooley et al., 2000). In the NCHRP 9-19 Project, three tests were evaluated to develop a practical and economic simple performance tester for evaluating the Superpave mixture design procedure (Brown et al., 2009). The studied tests were the flow time test, the flow number (FN) test, and the dynamic modulus test (Brown et al., 2009). FN and dynamic modulus tests were recommended for rutting assessment (Witczak et al., 2002).

Flow time test output represents the length of time that pavement can withstand steady pressure before flow occurs, and the FN test identifies the number of load cycles the pavement can endure before flow occurs. In this study, the HWTD and FN tests were used to evaluate rutting susceptibility of HMA mixtures with recycled materials.

2.8.1.1 Hamburg Wheel Tracking Device

The HWTD was originally developed and used in Hamburg, Germany in the 1970s to evaluate moisture susceptibility of HMA. The combined effects of rutting and moisture damage are evaluated by rolling a steel wheel across the surface of compacted samples submerged under 50 °C water. However, the HWTD test can be conducted within a temperature range of 25–75 °C (Izzo and Tahmoressi, 1999; Aschenbrener, 1994). Test results include rut depth, post-compaction, creep slope, stripping inflection point (SIP), and stripping slope, as illustrated in Figure 2.1.

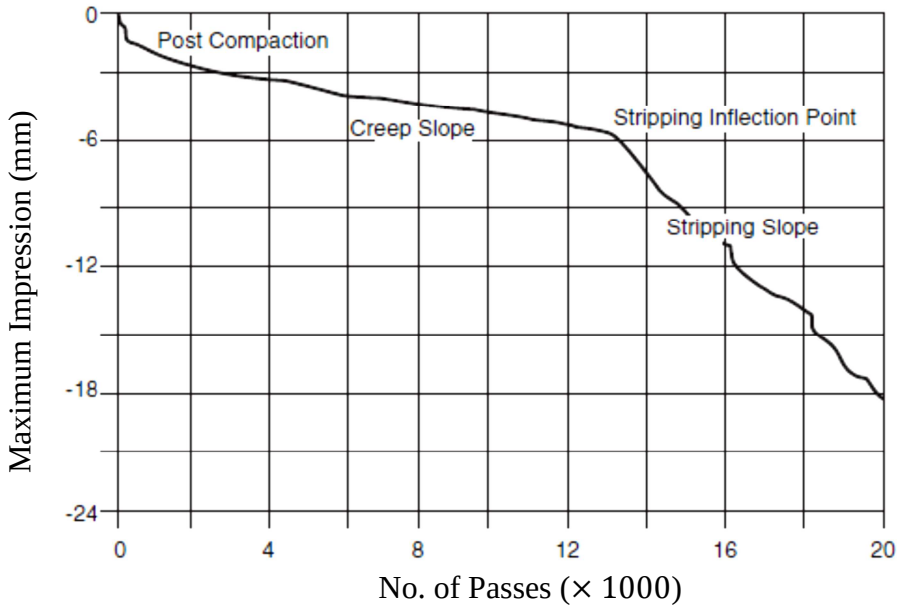

Figure 2.1 Typical Hamburg Wheel Tracking Test results (Yildirim et al., 2007)

Deformation (mm) at 1,000 wheel passes is the post-compaction consolidation that occurs rapidly during the first few minutes of the test. The inverse of the deformation rate of the linear region post compaction and prior to stripping (if occurs) is referred to as the creep slope, which measures rutting susceptibility primarily due to plastic flow. The inverse of the deformation rate within the linear deformation of the deformation curve after stripping begins is

the stripping slope, which measures rutting due to moisture damage. The number of wheel passes corresponding to the intersection of the creep slope and the stripping slope is the stripping inflection point. The stripping slope is the number of wheel passes required to create 1 mm of rut depth after the stripping inflection point and low values of it suggest severe moisture damage. The final region of the deformation curve, the tertiary region, is where the specimen starts to rapidly fail due to moisture damage. In general, high creep slopes, stripping points, and stripping slopes indicate mixtures with less moisture susceptibility (Uppu, 2012; Yildirim et al., 2007).

In the early1990s, the Colorado Department of Transportation (CDOT) and the Turner-Fairbank Highway Research Center (TFHRC) of FHWA began evaluating and demonstrating the HWTD, and they performed extensive research with HWTD (Aschenbrener, 1994). Results showed that test stripping inflection point can be well correlated with known stripping performance; pavements showing improved stripping performance generally carried more than 10,000 passes. The conclusion was made that in order to obtain passing results, asphalt cement cannot be expected to overcome aggregate deficiencies because of the influence of aggregate quality. Moisture resistance was shown to improve as asphalt cement stiffness increased. In addition, the suggestion was made that test temperature should be selected based on the high temperature the pavement will experience in service (Yildirim et al., 2007; Stuart and Mogawer, 1997; Aschenbrener, 1994).

Although the HWTD test is widely used in the United States, the test procedure and specifications may vary slightly among agencies. The Texas Department of Transportation (TxDOT) follows the TEX-242-F procedure, the procedure used in this study. Table 2.4 summarizes the test criteria.

Table 2.4 Hamburg Wheel Tracking Device test criteria (Zhou et al., 2006)

Binder Grade	Number of Wheel Passes	Maximum Rut Depth (mm)
PG 64-22	10,000	12.5
PG 70-22	15,000	12.5
PG 76-22	20,000	12.5

2.8.1.2 Flow Number or Repeated Load Permanent Deformation Test

The FN test, also referred to as the Repeated Load Permanent Deformation (RLPD) test, is a method to evaluate rutting susceptibility of HMA mixtures. Test protocol includes confined (triaxial RLPD) or unconfined (RLPD) procedure. Load application due to repeated heavy vehicle over a pavement structure is simulated by applying a haversine pulse compressive load with 0.1 second duration and 0.9 second rest time. FN test temperature is usually above 40 ℃, but requirements for test temperature and stress vary among states agencies (Bonaquist, 2012). Cumulative permanent deformation is recorded by the tester's data acquisition system as a function of load repetitions (Brown et al., 2009; Zhou et al., 2004). The cumulative permanent strain curve can be constructed by drawing permanent strain values versus the number of load cycles. This curve consists of the primary, secondary, and tertiary zones. Permanent strain accumulates rapidly in the primary zone, but the primary stage is followed by the secondary zone with an approximately constant value for permanent strain. Finally, permanent strain per cycle starts to increase again, and the sample enters the tertiary zone. FN is defined as the number of load repetitions at which tertiary flow begins (Brown et al., 2009; Zhou et al., 2004). Figure 2.2 illustrates the typical relationship between the total cumulative permanent strain and the number of load repetitions.

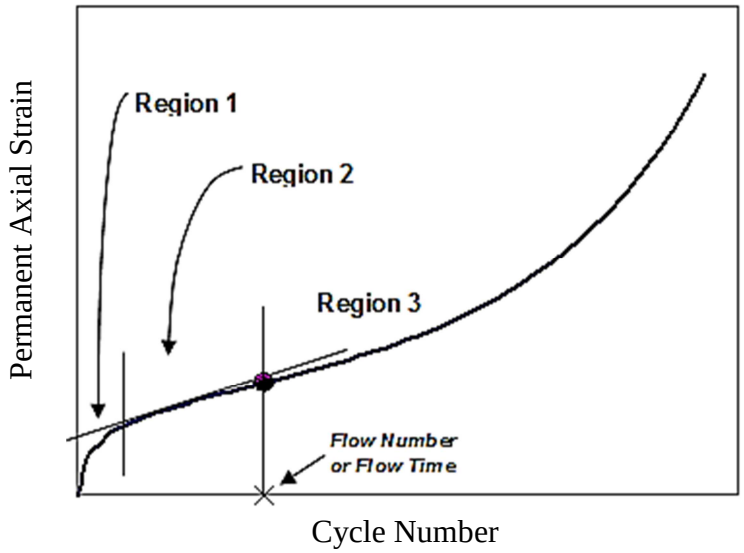

Figure 2.2 Typical relationship between permanent deformation and number of load cycles (FHWA, 2012)

In the NCHRP Project 9-19 study, FN correlated well with rutting resistance of mixtures used on experimental sections. FN has been recommended as a rutting indicator test for HMA mixtures (Bonaquist, 2012; Witczak et al., 2002).

2.8.2 Rutting Potential of Recycled Mixtures

Researchers have evaluated performance properties and rutting potential of RAP/RAS mixtures for over a decade. Rutting of HMA mixtures with recycled materials is not that mixed. Most studies confirmed improved rutting performance of recycled mixtures with high RAP percentage, possibly due to hardened asphalt from RAP that causes a stiff mixture, resulting in improved rutting performance (Rahman, 2010; Uppu, 2012). This was also confirmed by results of previous research work in which improved rutting resistance was observed for mixtures with stiff binders (Yildirim et al., 2007; Stuart and Mogawer, 1997; Aschenbrener, 1994).

One study showed that WMA mixtures with high amounts of RAP (0%–50%) were rut-resistant (Doyle et al., 2011). In another study, Elseifi et al. (2011) evaluated asphalt mixtures

containing RAP, crumb rubber modifier (CRM), engineered rejuvenator including demetalized oil and resin, plant-based rejuvenator, and sulfur-based additive. In general, they found that asphalt mixtures prepared with polymer-modified PG 76-22 and low percentages of RAP showed the best performance. Mixtures containing 15% RAP performed similarly to the conventional mixture prepared with the same binder grade. Ozer et al. (2012) conducted laboratory experiments to evaluate high asphalt binder replacement levels with RAS for a low N-design asphalt mixture. Levels of virgin asphalt replacement were ranged from 43% to 64%. Results indicated that permanent deformation resistance of the mixtures improved with RAS.

2.9 Dynamic Modulus

Dynamic modulus represents the viscoelastic nature of asphalt material and describes how the stiffness of HMA mixtures varies over a range of service temperatures and loading traffic rates (NCAT, 2014). From the mechanistic of materials point of view, dynamic modulus ($|E^*|$) is a complex modulus that relates stress to strain of a linear viscoelastic material as a function of loading rate and temperature. Dynamic modulus is a fundamental property of HMA mixtures. The dynamic modulus test was one of the fundamental tests evaluated in the NCHRP Project 9-19, for the purpose of developing simple performance tests to incorporate into the Superpave volumetric mix design method (Witczak, 2005). Results from that project showed that dynamic modulus can provide necessary inputs for structural analysis and is a rational way to establish mixture criteria. In addition to FN, dynamic modulus was proposed as a suitable parameter for evaluating permanent deformation (Witczak, 2005).

Dynamic modulus has recently gained more attention as a main input for HMA material in the Mechanistic Empirical Pavement Design Guide (MEPDG) (Brown et al., 2009). In order to determine dynamic modulus, a repetitive sinusoidal load is applied to the HMA sample and

deformation is measured. Due to viscous properties of the material, a time lag occurs between strain and stress, known as phase angle. Relationships for calculation of dynamic modulus and phase angle are as follows (Brown et al., 2009):

$$|E^*| = \frac{\sigma_0}{\varepsilon_0} \tag{2.1}$$

where:

$|E^*|$ = dynamic modulus (psi),

σ_0 = peak-to-peak sinusoidal compressive axial stress (psi), and

ε_0 = peak-to-peak corresponding axial strain.

$$\emptyset = 2\pi f \Delta t \tag{2.2}$$

where:

$\emptyset$ = phase angle (rad),

f = frequency (Hz), and

Δt = time lag between stress and strain (sec).

Although the Asphalt Mixture Performance Tester (AMPT) is commonly used to perform a dynamic modulus test according to AASHTO TP 79-13 test protocol, two other test methods are also utilized. Test protocols that use cylindrical specimens tested in compression are AASHTO TP-62 and AASHTO TP 79-13. The primary difference between these protocols is that TP-62 permits use of any kind of Linear Variable Differential Transformer (LVDT), whereas TP-79 uses spring-loaded LVDT types, which are not favored by some researchers (Brown et al., 2009). Other slight differences exist, such as number of samples required, maximum allowable load, test temperature, and loading frequencies. Although this test is considered a nondestructive test because microstrain levels are kept small and recoverable, mean strain increases as the test proceeds. Thus, in order to reduce the accumulation of strain in the

sample, the dynamic modulus test starts at the lowest temperature and highest frequency where HMA is stiffer (Brown et al., 2009).

2.9.1 Dynamic Modulus Master Curves

As mentioned earlier, temperature and loading frequency are two main factors that affect determination of dynamic modulus and phase angle of HMA. This characteristic is captured in a curve known as mastercurve, constructed based on the time-temperature superposition concept (Brown et al., 2009). The time-temperature superposition that relates modulus values of a material obtained at various temperatures and frequencies is based on the idea that time and temperature are equivalent. It states that, at a given temperature, modulus obtained under a slow loading rate (longer time) is equivalent to the modulus at a high temperature measured for a fast loading rate (shorter period of time) (NCAT, 2014). After data has been collected for various temperatures and loading frequencies, a smooth single mastercurve as shown in Figure 2.3 is produced using a shift factor to shift data for a reference temperature, generally 21 °C (Witczak, 2005). The general equation is as follows (NCAT, 2014):

$$\mathrm{Log}(f_r) = \mathrm{Log}(f) + \mathrm{Log}(\alpha T) \tag{2.3}$$

where:

f_r = reduced frequency,

f = testing frequency, and

αT = shift factor (T given temperature).

AASHTO PP 61 is the standard method for developing dynamic modulus master curves for hot mix asphalt (HMA) using AMPT.

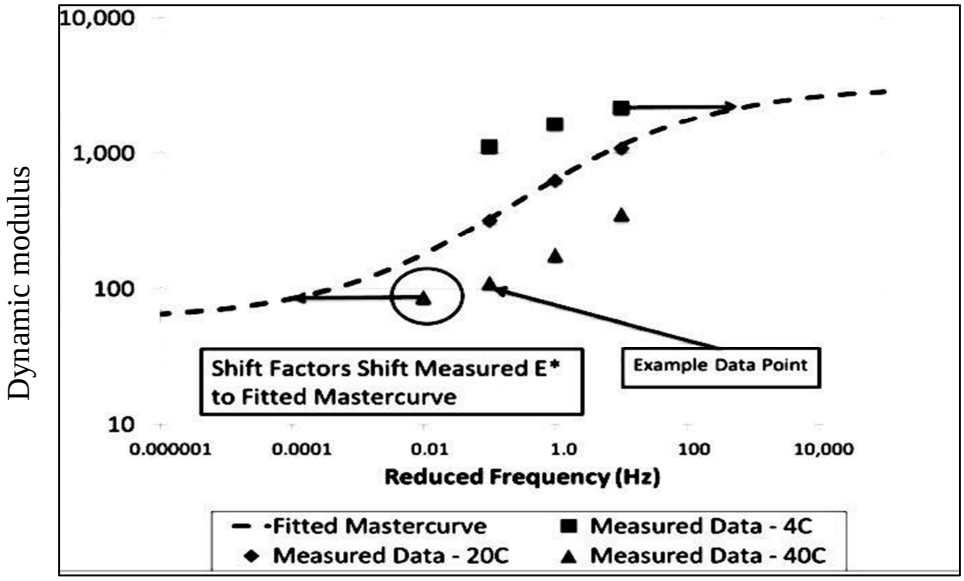

Figure 2.3 Typical dynamic modulus master curve (NCAT, 2014)

2.9.2 Effect of RAP/RAS on Dynamic Modulus

As stated, the main parameter measured in the dynamic modulus test is mixture stiffness. Previous studies indicated increased stiffness of mixtures containing RAP, RAS, or a combination of both (Mogawer et al., 2011). Cascione et al. (2010) evaluated the effects of RAS on HMA performance on highway and low-traffic pavements containing Fractionated RAP (FRAP). Samples were collected from an Illinois Tollway field demonstration project; Also laboratory mixes were produced and tested for dynamic modulus (E*) in AMPT to build master curves. As the percentage of FRAP increased, the dynamic modulus at both low and high temperatures increased. However, when FRAP content changed from 35% to 45%, no significant change in mastercurve was observed.

Miró et al. (2011) evaluated the behavior of recycled mixtures with high RAP percentages. Four mixtures with RAP percentages of 0%, 15%, 30% and 50% were analyzed. Stiffness modulus, toughness, moisture sensitivity, resistance to rutting, and fatigue resistance of the mixtures were studied. Results of dynamic modulus tests showed higher modulus for higher

RAP contents. Valdés et al. (2011) studied recycled asphalt mixtures with high RAP percentages and concluded that higher RAP contents lead to increased stiffness, as indicated by results of the dynamic modulus test. They studied mixtures with 20-mm maximum aggregate size with 40% and 60% RAP. The effect of RAP variability on the recycled mixtures was evaluated using stiffness modulus, indirect tensile strength (ITS), cracking, and fatigue behavior.

2.10 Evaluating Cracking Susceptibility

Cracking is a dominant form of HMA distress that occurs due to moisture damage, stresses, inadequate structure, or aging of HMA. Fatigue cracking, a common form of cracks in HMA, is defined as the accumulation of cracks under repetitive traffic and thermal loads. Fatigue cracks typically appear at the end of service life (Li et al., 2014). Fatigue cracking, comprised of a series of interconnected cracks traditionally believed to initiate at the bottom of pavement where tensile strains are higher and eventually propagate toward the surface, is referred to as bottom-up cracking. However, top-down cracking, which starts at or near the surface, is also a commonly accepted form of fatigue cracking. Fatigue cracking can be best controlled by adequate HMA thickness and material properties (Brown et al., 2009; Witczak et al., 2002)

Cracking characteristics can be evaluated through various methods that are essentially categorized into two types of fatigue and fracture mechanics testing (Brown et al., 2009). The beam flexural test, the indirect tensile fatigue test (IDT), and the direct tension or tension-compression Viscoelastic Continuum Damage (VECD) test are various fatigue test types. Indirect tension creep/strength and Semicircular Bending (SCB) tests are fracture mechanics tests used to characterize both fatigue cracking and thermal cracking (Brown et al., 2009). These methods use phenomenological and mechanistic approaches to predict fatigue life of pavements. The simplest model is the phenomenological fatigue model, but damage evolution throughout the

fatigue process is not taken into consideration. However, mechanistic models are based on fracture mechanics or damage mechanics that use stress-strain relationships. In spite of complexity of the model, the latter approach is more widely accepted (Kim et al., 2003).

2.10.1 Viscoelastic Continuum Damage (VECD) Theory and VECD Direct Tension Fatigue Test

In addition to the traditional fatigue and fracture mechanics approaches, damage mechanics approaches are also applied to HMA mixtures to characterize fatigue behavior. Kim et al. (1997) developed a fatigue model for HMA mixtures using the elastic–viscoelastic correspondence principle and continuum damage mechanics (Little et al., 2015; Palvadi et al., 2012; Kim et al., 1997; Kim et al., 1990).

Conventional procedures for fatigue performance evaluation, such as beam fatigue test methods have a major limitation that is the long durations of the tests at low strain or stress levels. In addition, collecting sufficient data to develop required plots of fatigue model requires a lot of samples (Brown et al., 2009). Therefore, such type of testing may be suitable only for research purposes (Brown et al., 2009; Kim et al., 2003). Moreover, research has shown the effect of asphalt self-healing on fatigue resistance characteristics of asphalt pavements. Asphalt self-healing is defined as complete or partial reversal of microcrack or microdamage due to fatigue loads (Palvadi et al., 2012; Kim et al., 1997). The issues are addressed by the VECD theory (Palvadi et al., 2012). Schapery (1975) developed the work potential theory, a continuum damage theory that describes mechanical behavior of an elastic material under increased damage (Little et al., 2015). The theory asserts that the same amount of strain energy is required to change the state of the material from one to another regardless of the path. Using correspondence principles and damage evolution law, elastic continuum damage theory can be extended to

describe viscoelastic damage evolution. The VECD model characterizes fatigue damage in asphalt concrete (Little et al., 2015).

In VECD theory, the state of damage within a sample, represented by an internal state variable S, is related to a reduction in pseudo stiffness C of the specimen that undergoes continuous loading. Researchers found S-C relationship as a true property of material independent of testing conditions (Little et al., 2015; Palvadi et al., 2012). Pseudo strain and stress at time step t, C, and S are calculated as follows (Little et al., 2015):

$$\varepsilon^{R} = \frac{1}{E_R}\int_0^t E(t-\tau)\frac{d\varepsilon(\tau)}{d\tau}d\tau \tag{2.4}$$

$$\sigma^{R} = \sigma(t) \tag{2.5}$$

where:

σ^R = pseudo stress,

ε^R = pseudo strain,

ε = actual strain,

E^R= reference modulus, and

$E(t)$ = relaxation modulus at time step t.

Pseudo-stress, pseudo-strain behavior of asphalt concrete subjected to a uniaxial cyclic fatigue test is modeled as follows (Little et al., 2015):

$$(C)S = \frac{\sigma^{R}}{\varepsilon^{R} * I} \tag{2.6}$$

Pseudo stiffness, C, can be calculated as follows (Lancaster and Khalid, 2015):

$$(C) = \frac{|E^*|_N}{|E^*|_{LVE}} \tag{2.7}$$

where:

$|E^*|_N$ = dynamic modulus at Nth cycle, and

$|E^*|_{LVE}$ = average representative dynamic modulus of undamaged material at temperature and the frequency of interest.

An efficient method to compute the change in damage for each time step is (AASHTO TP-107)

$$S_{N+1} = S_N + \left[-\frac{DMR}{2}(C_N - C_{N-1})(\varepsilon^R)^2\right]^{\frac{\alpha}{\alpha+1}} (\Delta t_R)^{\frac{1}{\alpha+1}} \quad (2.8)$$

$$DMR = \frac{|E^*|_{Fingerprint}}{|E^*|_{LVE}} \quad (2.9)$$

where:

DMR = dynamic modulus ratio,

α = continuum damage power term related to material time dependence, and

C_N = pseudo secant modulus at time step N.

Cumulative damage accumulated due to loading for each time step can be evaluated and subsequent damage characteristics curves (C-S) can be developed. In this study, a simplified version of the VECD direct tension fatigue test, developed by North Carolina State University under the NCHRP 1-42A Project (Ahmed, 2015), was selected as the performance test for evaluating cracking potential of HMA mixtures. The VECD theory was used as the underlying principle to evaluate pavement performance using finite element-based analysis.

2.10.2 Effect of RAP/RAS on Fatigue Cracking

Experience in evaluating fatigue life of HMA mixtures including RAP and RAS is mixed; RAS mixtures have shown more diverse behavior. Shu et al. (2008) reported a decrease in HMA fatigue life with RAP. In their study, fatigue characteristics of plant-produced mixtures

with 0%, 10%, 20%, and 30% RAP were evaluated with various testing methods. Results showed that inclusions of RAP may shorten fatigue life of HMA mixtures (Shu et al., 2008). However, some researchers have reported similar or better fatigue performance of recycled mixtures with RAP if proper mix design was considered (Zhou et al., 2013; Zhao et al., 2012; Visintine, 2011).

Although some studies confirmed increased fatigue potential of mixtures with increased RAS content (Ozer et al., 2013), other studies suggested similar or better performance of RAS mixtures compared to non-RAS mixes. Incorporation of 3% to 5% RAS in HMA resulted in no significant difference in fatigue cracking in mixtures without RAS (Wen et al., 2014; Williams et al., 2011; Cascione et al., 2011; Samoo, 2011). In one study, superior low and intermediate temperature fatigue resistance was observed in mixtures containing RAS compared to mixtures containing RAP (Foxlow et al., 2011). In other studies, RAS mixes showed better fatigue lives than non-RAS mixtures, leading to the conclusion that fibers in RAS could improve fatigue performance (Williams et al., 2013).

All aforementioned studies were done using conventional fatigue cracking evaluation test methods such as the beam fatigue cracking test. To date, no study using the VECD test method for mixtures containing RAS has been reported in the literature. Thus, this study is one of the first studies that evaluated fatigue properties of RAS mixtures using the VECD test method.

2.11 Summary

RAP and RAS have been used in new or rehabilitation HMA pavement projects. However, performance properties of HMA mixtures with RAP/RAS change due to incorporation of aged asphalt binder into the mixture. Researchers have suggested that proper mixture design would allow recycled mixtures to perform identically to or better than conventional mixtures.

Although rutting resistance has been proven to improve with the addition of recycled materials, susceptibility to moisture damage and fatigue cracking may increase. Due to highly aged binder, limited experience of usage, and diverse behavior of RAS, agencies typically limit RAS content to 5% in HMA mixtures. RAP has a longer history of application and higher amount of usage, but the applied percentage in mixtures is usually limited to 15% to 25%. The VECD test is a novel approach for fatigue evaluation of HMA mixtures.

Chapter 3 - Methodology

3.1 Introduction

In this study, three KDOT HMA mixture designs containing 15% recycled materials were selected as control mixtures. For each selected KDOT mixture, the percentage of recycled materials was increased to 20% and then to 35%. Mixture design was performed in the laboratory according to KDOT specifications for the Superpave recycled mixture design. Mixture performance was also assessed in the laboratory with respect to rutting potential, fatigue cracking propensity, and moisture susceptibility. This chapter discusses materials used and laboratory test performed in this study.

3.2 Virgin and Recycled Material Sources

As mentioned, three KDOT mixture designs were selected as control mixtures. The first KDOT mixture design was a surface course with 9.5-mm Nominal Maximum Aggregate Size (NMAS), known as SR-9.5A. The second and third control mixtures were intermediate courses with 19-mm NMAS, known as SR-19A. Mixture designs were obtained from two projects in Kansas: US-59 in Douglas County and US-36 in Jewell County. Table 3.1 shows specific project information and locations.

Table 3.1 Project information and locations

Project Number	Mix Designation	Project Name	Project Location
U59-23 K 7888-06	SR-9.5A	US-59-surface course	Douglas County
U59-23 K 7888-01	SR-19A	US-59-intermediate course	Douglas County
U36-45 KA 2187-01	SR-19A	US-36-intermediate course	Jewell County

Superpave mixtures were designed using 10 different virgin aggregates, two different sources of RAP, and two different sources of RAS. Virgin aggregates were collected form the US-59 and US-36 projects. RAP sources were millings from these projects, and RAS sources were tear-off shingles obtained from project US-59 and another project on US-81. (The US-36 project did not use any RAS.) All material sources are represented in Table 3.2.

Table 3.2 Virgin and recycled material sources

Project Name	Aggregate Source	Binder Source	RAP Source (Milling)	RAS Source (TOAS)
US-59- Surface course	Ottawa (OK), Douglas, and Shawnee County	Vance Brothers	US-59 Douglas County	US-59
US-59- intermediate Course	Ottawa (OK) and Douglas County	Flint Hills	US-59 Douglas County	US-59
US-36- intermediate Course	Lincoln and Republic County	Flint Hills	US-36 Jewell County	US-81

3.3 Bulk Specific Gravity of Aggregates

The bulk specific gravities of all virgin aggregates were determined in the laboratory following the Specific Gravity and Absorption of Aggregates Test (Kansas standard test method KT-6). For recycled aggregates, specific gravity test results obtained by KDOT were used in design procedure.

Figure 3.1 Specific gravity test (KT-6)

Table 3.3 Specific gravities of aggregates

US-59		US-36	
Aggregate	Specific Gravity	Aggregate	Specific Gravity
CS-1	2.506	CS-1D	2.598
CS-1A	2.538	CS-1A	2.645
CH-1	2.520	CS-2A	2.646
CS-2	2.642	CS-2	2.685
SSG	2.634	SSG-2	2.604
RAP	2.663	RAP	2.650
RAS	2.653	RAS	2.640

3.4 Virgin and Recycled Aggregate Gradation

Virgin aggregates used in all mixtures include crushed limestone, finely crushed limestone, limestone screenings, and natural/river sand. A sieve analysis test was performed on aggregates following Kansas test methods of sampling and splitting aggregates (Kansas test method KT-1) and sieve analysis of aggregates (Kansas standard test method KT-2). KDOT also provided information on RAP and RAS aggregate gradation using the Sieve Analysis of Extracted Aggregate Test (Kansas test method KT-34). Table 3.4 and Table 3.5 show square-mesh sieve analysis results. Figure 3.2 and Figure 3.3 illustrate 0.45-power gradation charts for virgin and recycled aggregates.

Table 3.4 Aggregate gradation for US-59 project

Sieve Size (mm)	25.4	19.0	12.5	9.5	4.75	2.36	1.18	0.6	0.3	0.15	0.075
CS-1	100	77	25	8	1	1	1	1	1	1	0.7
CS-1A				100	40	1	1	1	1	1	0.9
CH-1			100	100	98	75	50	30	13	5	2.4
SSG			100	100	96	86	73	52	17	4	1.5
CS-2			100	100	100	67	37	23	13	9	7.8
RAP		100	97	90	61	47	35	25	15	9	7.0
RAS			100	99	99	99	87	71	63	54	38.8

Table 3.5 Aggregate gradation for US-36 project

Sieve Size (mm)	25.4	19.0	12.5	9.5	4.75	2.36	1.18	0.6	0.3	0.15	0.075
CS-1D	100	92	36	13	1	1	1	1	1	1	0.7
CS-1A				100	82	36	20	16	10	5	3.4
CS-2A				100	98	74	52	43	31	9	3.5
CS-2				100	93	68	57	51	38	21	13.4
SSG-2		100	98	97	88	64	36	18	4	1	0.8
RAP		100	97	93	77	62	50	38	22	11	7.2
RAS				100	99	98	80	60	52	44	33.0

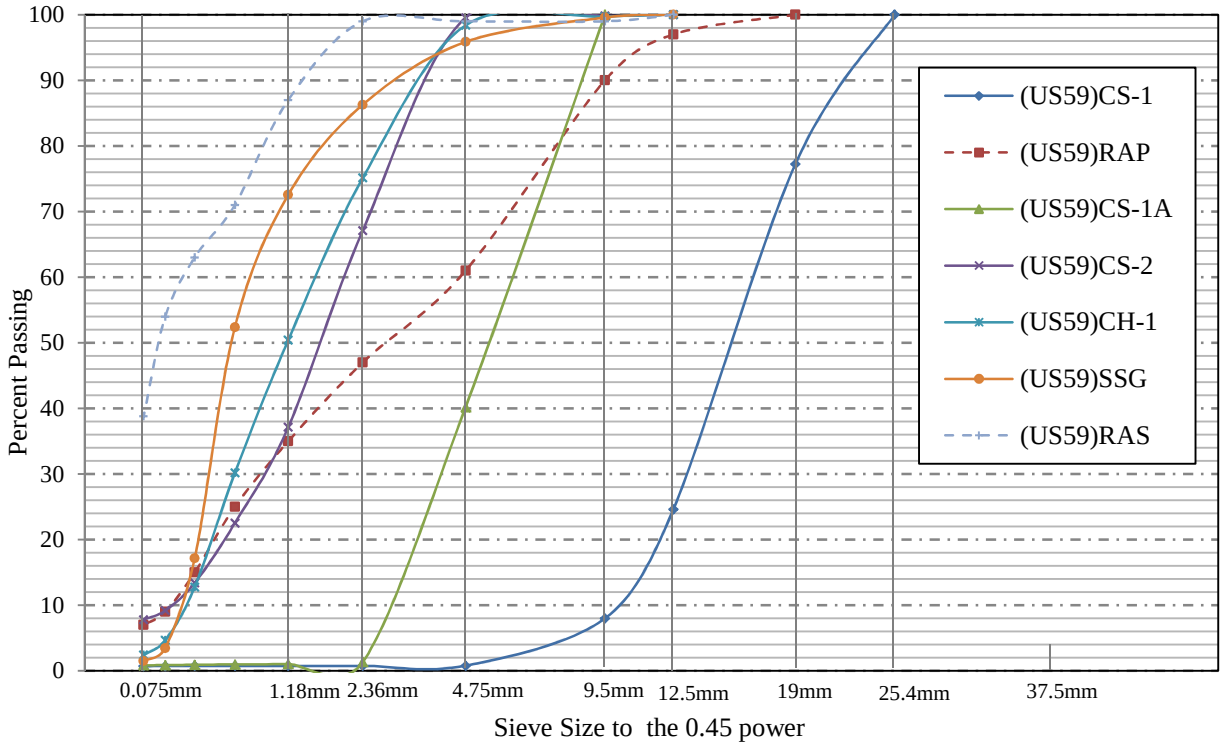

Figure 3.2 0.45 power chart for US-59 aggregates

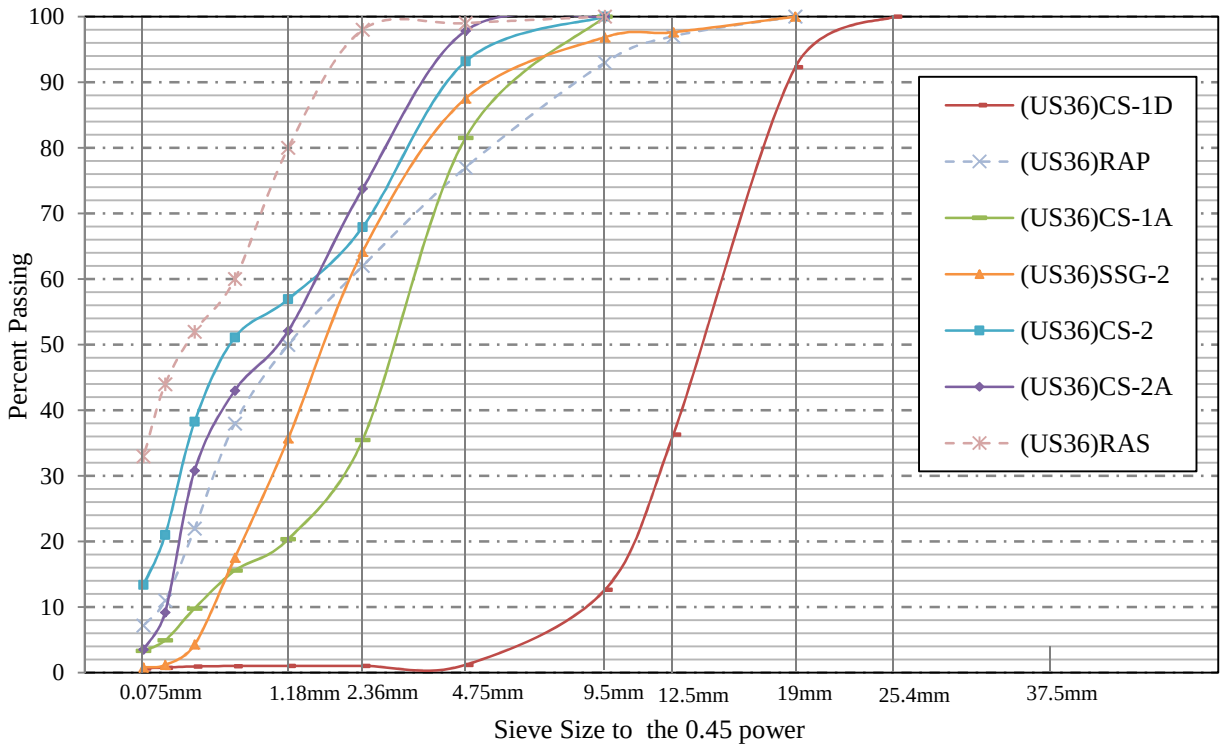

Figure 3.3 0.45 power chart for US-36 aggregates

3.5 Mixture Design Procedure

HMA mixtures were developed in the laboratory following KDOT requirements for recycled Superpave mixture design. The procedure included four major steps:

1. Selection of materials (aggregate, binder, modifier, etc.)
2. Selection of design aggregate structure
3. Selection of design asphalt binder content
4. Evaluation of moisture susceptibility of the design mixture

3.6 Selection of Design Aggregate Structure

In order to have the optimal structure of blended aggregates and reduce binder cost, a dense graded blend that incorporates as much aggregates as possible while considering sufficient voids as a room for binder and air is desirable. In Superpave, the FHWA 0.45-power chart is typically used to evaluate blended aggregate gradation. This chart includes the maximum density line, which is a straight line based on the Fuller formula but with an exponent of 0.45 that represents particle size distribution required for maximum density (Mamlouk and Zaniewski, 2006).

As mentioned, the percentage of recycled materials was increased in two steps (up to 35%) for each control mixture in this study. KDOT defines mixtures by their NMAS. In order to satisfy KDOT requirements for aggregate gradation, combined structure should fall between specific control points, as shown in Figure 3.4 to Figure 3.6. Table 3.6 to Table 3.9 show percentages of virgin and recycled aggregates in the combined blend for all nine mixtures.

Table 3.6 Aggregate percentage in US-59-surface course mixtures

Aggregate	Control Mixture (15% Recycled)	Second Mixture (20% Recycled)	Final Mixture (35% Recycled)
(US-59) CS-1	0	0	0
(US-59) CS-1A	20	20	15
(US-59) CH-1	30	30	23
(US-59) SSG	5	5	4
(US-59) CS-2	30	25	23
(US-59) RAP	10	15	30
(US-59) RAS	5	5	5

Table 3.7 Aggregate percentage in US-59-intermediate course mixtures

Aggregate	Control Mixture (15% Recycled)	Second Mixture (20% Recycled)	Final Mixture (30% Recycled)
(US-59) CS-1	28	25	23
(US-59) CS-1A	15	15	12
(US-59) CH-1	25	27	23
(US-59) SSG	0	0	0
(US-59) CS-2	17	13	12
(US-59) RAP	10	15	25
(US-59) RAS	5	5	5

Table 3.8 Aggregate percentage in US-36-intermediate course mixtures

Aggregate	Control Mixture (15% Recycled)	Second Mixture (20% Recycled)	Final Mixture (25% Recycled)
(US-36) CS-1D	25	25	25
(US-36) CS-1A	17	16	15
(US-36) CS-2A	30	28	25
(US-36) CS-2	5	5	5
(US-36) SSG-2	8	6	5
(US-36) RAP	15	15	20
(US-81) RAS	0	5	5

Table 3.9 Blended aggregate gradation for various mixture designs

Sieve size (mm)		25.4	19	12.5	9.5	4.75	2.36	1.18	0.6	0.3	0.15	0.075
US-59-surface Course	15% Recycled			100	99	85	55	34	20	10	6	4.7
	20% Recycled			100	98	81	56	38	25	14	8	5.9
	35% Recycled			99	97	79	55	38	25	15	9	6.6
US-59-intermediate Course	15% Recycled	100	94	79	73	60	40	27	18	11	7	4.9
	20% Recycled	100	94	81	75	60	41	28	19	11	7	5
	30% Recycled	100	95	82	76	60	42	29	20	12	7	5.4
US-36-intermediate Course	15% Recycled	100	98	84	78	67	46	31	25	15	6	4.2
	20% Recycled	100	98	84	77	67	48	35	27	19	9	5.1
	25% Recycled	100	98	83	77	66	48	35	27	19	9	5.4

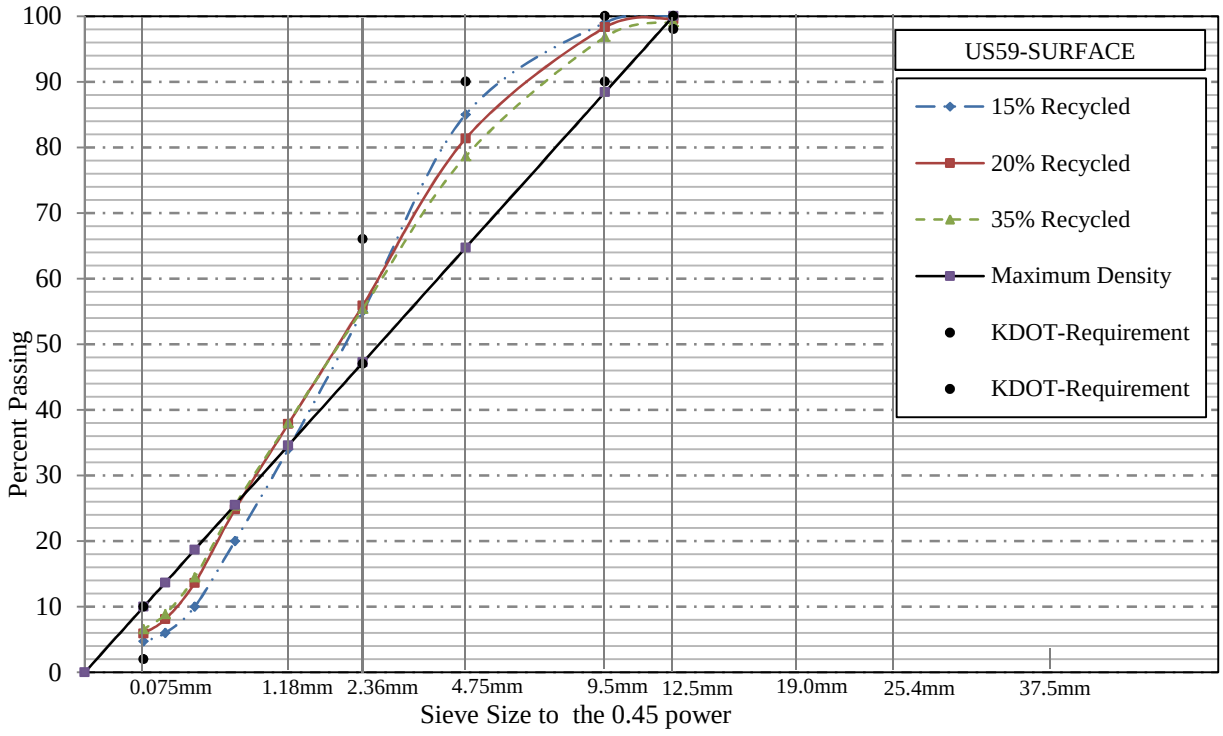

Figure 3.4 0.45 power chart for US-59-surface blended aggregates

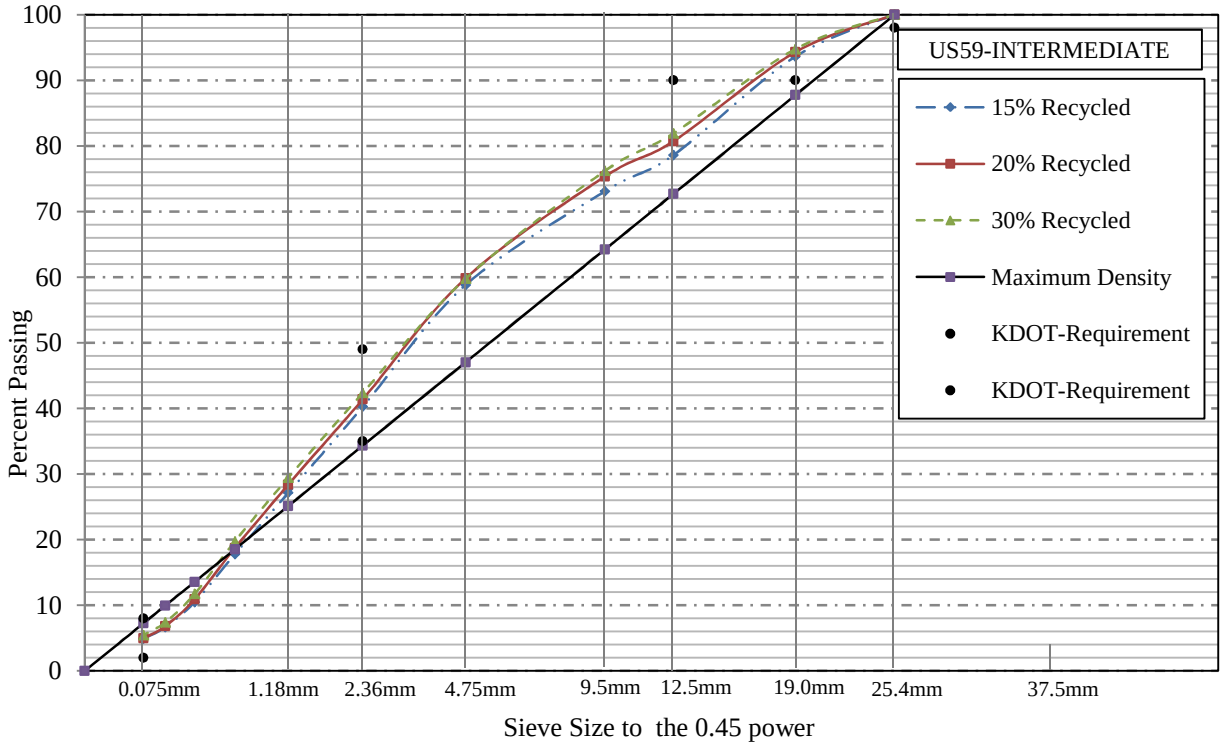

Figure 3.5 0.45 power chart for US-59-intermediate blended aggregates

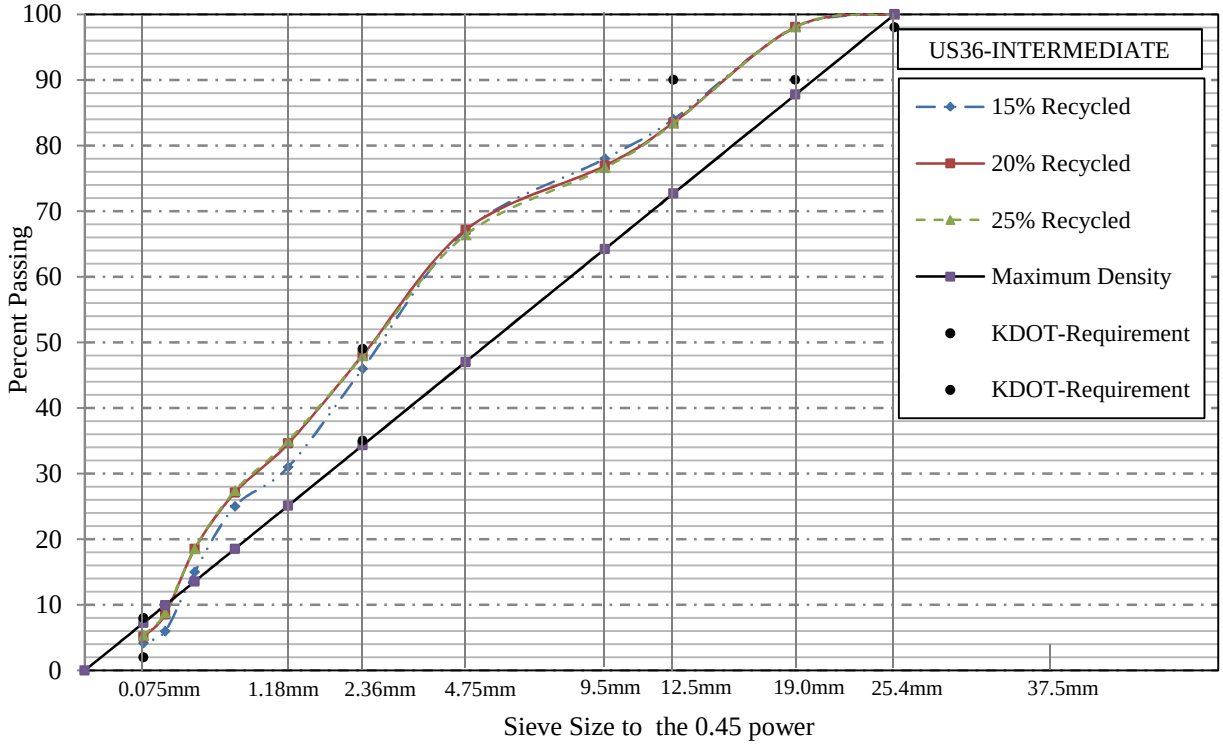

Figure 3.6 0.45 power chart for US-36 blended aggregates

3.7 Virgin Binder PG Grade Selection

In the Superpave method of mixture design, asphalt binders are specified based on expected binder performance over a range of temperatures representing the high side and low side of the range at which the binder is expected to perform in service. For example, PG 70-28 indicates that the maximum temperature for this binder for expected performance is 70 °C and the lowest temperature is -28 °C.

Binder selection in Superpave is based on the specific project traffic and climate condition. When recycled materials are incorporated into the Superpave mixture, the specified grade of virgin binder must be adjusted due to the stiffening effect of the aged binder in RAP and RAS.

Table 3.10 Binder selection guidelines for RAP and RAS mixtures (AASHTO PP-78)

Recommended Virgin Asphalt Binder Grade	%RAP/RAS/RAP+RAS
No change in binder selection	<15
Select virgin binder one grade softer than normal	15-25
Follow recommendations from blending charts	>25

Based on Table 3.10, binder grade adjustment of mixtures is done only if RAP content is greater than 15%. However, when RAS is incorporated into the mixture, KDOT requires use of a binder that is one grade softer, even if the percentage of RAP is less than 15%. The blending chart developed by KDOT was used to make the adjustment in virgin binder grade for mixtures with high percentages of recycled material. The chart was developed based on blending at a known RAP (RAS) percentage when desired target blended binder grade, percent of RAP (RAS), and RAP recovered binder properties are known (Sabahfar, 2012):

$$T_{virgin} = \frac{T_{target} - (\%RAP \times T_{RAP})}{(1 - \%RAP)} \quad (3.1)$$

where:

T_{virgin} = critical temperature of virgin asphalt binder (high, intermediate, or low),

T_{target} = critical temperature of blended asphalt binder (high, intermediate, or low),

%RAP = percentage of RAP expressed as a decimal, and

T_{RAP} = critical temperature of recovered RAP binder (high, intermediate, or low).

Virgin binder grade as well as extracted binder grades of RAP and RAS are needed in order to use the KDOT blending chart. These extracted binders were tested in the KDOT laboratory to obtain their PG binder grade. High-side and low-side performance grades of binder extracted from the US-59 RAP was PG 86-16; for US-36, RAP was PG 90-7. For RAS, high side of the extracted binder for both sources was 175, but it was not possible to grade the low side of the RAS binder in the laboratory. Based on the literature, 1.5 ^{o}C was selected as the low side for RAS binder for both sources (Zhou et al., 2012). Table 3.11 summarizes the type of binders used in this study.

Table 3.11 Virgin PG binder used in each mixture

Binder grade	**US-59-surface course (SR-9.5A)**			**US-59-intermediate course (SR-19A)**			**US-36-intermediate course (SR-19A)***		
	15% Rec.	20% Rec.	35% Rec.	15% Rec.	20% Rec.	30% Rec.	15% Rec.	20% Rec.	25% Rec.
Target	70-28	70-28	70-28	70-28	70-28	70-28	70-28	70-28	70-28
RAP	86-16	86-16	86-16	86-16	86-16	86-16	90-7	90-7	90-7
RAS	175+1.5	175+1.5	175+1.5	175+1.5	175+1.5	175+1.5	175+1.5	175+1.5	175+1.5
Virgin	64-34	64-34	58-34	64-34	64-34	58-34	70-28	64-34	58-34

* Antistripping agent (Arr-Maz LA-2) was used by 0.5% of the total weight of the virgin binder.

3.8 Mixture Volumetric Properties

Mixture volumetric requirements are the other important part of the Superpave method of mixture design. Mixture performance properties are highly influenced by volumetric properties. In order to find the optimum percentage of total binder that should be used in a mixture, mixtures with different binder contents were prepared and evaluated with respect to specific volumetric properties, including compacted mix percent air voids (Va), voids in mineral aggregate (VMA), voids filled with asphalt (VFA), dust proportion (DP), in-place density at the initial number of gyrations (%Gmm @ N_{ini}), and in-place density at the final number of gyrations (% Gmm @ N_{max}) .

3.8.1 Air Voids of Mixture

Total volume of air between coated aggregates of a compacted paving mixture is referred to as air voids (Va). Air void is calculated as a percentage of bulk volume of the compacted mixture following the relationship:

$$V_a = 100 \times (1 - \frac{G_{mb}}{G_{mm}}) \quad (3.2)$$

where:

Va = air voids of mixture,

G_{mb} = bulk specific gravity of the mixture, and

G_{mm} = maximum specific gravity of the mixture.

Paving mixture stability and durability is dependent on the percentage of air voids. KDOT requirement for air voids in the design procedure is typically set at 4% at design gyration level (Ndesign).

3.8.2 Voids in the Mineral Aggregate

VMA is the volume of void space between aggregate particles of a compacted paving mixture. VMA, expressed as a percentage of total volume, consists of air voids and effective asphalt content.

$$\mathrm{VMA} = 100 - \left[\frac{(\mathrm{G_{mb}P_s})}{\mathrm{G_{sb}}}\right] \tag{3.3}$$

where:

VMA = voids in mineral aggregates,

Gmb = bulk specific gravity of the compacted mixture,

Gsb = bulk specific gravity of the blended aggregate, and

Ps = percent of aggregates.

Minimum required VMA for incorporation into Superpave mixture design ensures adequate binder content and proper air void content. KDOT requires minimum VMA of 13% and 15% for SR-9.5A and SR-19A mixtures, respectively.

3.8.3 Voids Filled with Asphalt

VFA, the portion of voids in mineral aggregate filled with asphalt binder, represents the volume of effective asphalt content and is defined as a percentage of VMA:

$$\mathrm{VFA} = 100 \times \left[\frac{\mathrm{VMA} - \mathrm{Va}}{\mathrm{VMA}}\right] \tag{3.4}$$

where:

VFA = voids filled with asphalt,

VMA= voids in mineral aggregate, and

Va = air voids content.

VFA requirement depends on project design traffic in ESALs.

3.8.4 Dust Proportion

DP represents the ratio of materials passing 0.075 mm sieve to the effective asphalt content. Fine particles stiffen the binder when combined with binder, allowing DP to affect rutting potential of a mixture (Kandhal and Cooley, 2002).

$$DP = \left[\frac{P_{0.075}}{P_{be}}\right] \quad (3.5)$$

where:

DP = dust proportion,

$P_{0.075}$ = materials passing 0.075 mm sieve (%), and

P_{be} = effective binder content (%).

Acceptable dust proportion for SR A-type mixture based on KDOT criteria is 0.6 to 1.2.

3.9 Loose Mixture Preparation

Superpave mixture design procedure of recycled mixtures is similar to the procedure for virgin mixture design, with the exception of adjustment for binder grade (as necessary) and virgin binder content. Total optimum binder content, estimated based on minimum VMA, represents the total binder, including virgin binder and recycled binder. In order to consider the amount of binder incorporated into the mixture by recycled material, weight of recycled binder introduced into the mixture is calculated and then the amount of required virgin binder is adjusted.

In this study, loose mixtures were prepared according to KDOT requirements. First, all virgin aggregates were measured and blended at specified mixture design percentages described

in Table 3.9. Aggregates were then heated and mixed with the heated virgin binder within the recommended mixing temperature range, corresponding to a specific range of viscosities. All recycled materials were measured and heated individually to a lower temperature of approximately 60 °C to prevent additional aging of the recycled binder. Recycled materials were mixed simultaneously with the aggregates and virgin binder using a mechanical mixer. A uniform mixture with all aggregates coated properly with asphalt was expected after mixing was complete. The loose mixtures were aged for 2 hours at the recommended compaction temperature in the oven.

(a) **(b)** **(c)**

Figure 3.7 HMA mixing procedure: (a) heating aggregate; (b) adding binder to the aggregate; (c) mixing of binder and aggregate

3.10 Mixture Compaction with Superpave Gyratory Compactor

The initial design and maximum number of gyrations (N_{ini} , N_{des} , N_{max}) to produce a mix density equivalent to the expected density in the field are defined based on anticipated traffic load on the project over the design life. N_{ini} represents the period during construction, N_{des} represents the required effort to produce a sample with the same density as expected of the pavement in service after the indicated amount of traffic, and N_{max} is the number of gyrations to produce a laboratory density that should never be surpassed in the field. The required number of

gyrations as function of predicted Equivalent Single Axle Loads (ESALs) is shown in Table 3.12.

Table 3.12 Superpave gyratory compactive effort (Kansas Method)

Design ESALs (millions)	Number of Gyrations		
	N_{ini}	N_{des}	N_{max}
<0.3	6	50	75
0.3 to <3	7	75	115
3 to <30	8	100	160
≥30	9	125	205

The N_{des} for the US-59 project with predicted ESALs of 3.5 million is 100 and for project US-36 with 1.8 million ESALs is 75.

After knowing the required number of gyrations, the amount of loose mixture, and compaction temperature, the Superpave gyratory compactor (SGC) was used to compact the aged mixtures to cylindrical samples with 150 mm diameter and 115±5 mm height for a target air void of 4%. Samples were compacted in cylindrical molds that were preheated to the compaction temperature for a minimum of 35 minutes in advance. After ensuring the right compaction temperature for the mixture, 4,500 gm of loose mixture was measured and charged into the mold using a pouring pan. The mold was placed into the SGC, and the sample was compacted to the specified maximum number of gyration, as listed in Table 3.12. The compacted samples were then removed from the molds after compaction and extruded after a few minutes of cooling. The samples were used in volumetric analysis, as explained later.

Table 3.13 Compaction parameters for SGC

Compaction Parameters and Values	
Pressure	600±18 kPa
Angle of gyration	1.16° ± 0.02°
Speed of rotation	30±0.5 gyrations per minute

Figure 3.8 Compacting specimens using SGC

In order to determine the optimum amount of binder, four different percentages of binder content were tried. After a loose mixture with specific binder content was made, two samples were compacted from that mixture, and average results were used for further analysis. As shown in Figure 3.9**,** a graph with % binder in x-axis and % air voids in y-axis was plotted, and optimum % binder that produced 4% air voids was selected.

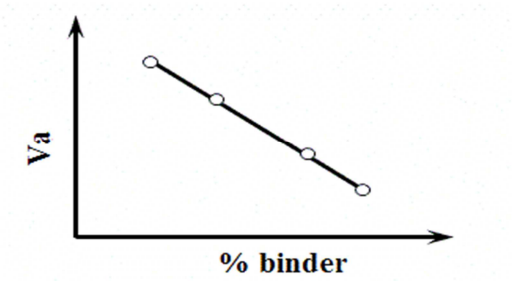

Figure 3.9 Air void content versus %binder

3.10.1 Determining Percentages of Air Voids

KT-15 and KT-39 test methods were used to determine the bulk specific gravity (G_{mb}) of compacted asphalt mixtures and theoretical maximum specific gravity (G_{mm}) of asphalt mixtures, respectively. In order to determine G_{mb} of a compacted sample, weights of samples that were dry (no water in sample), Saturated Surface Dry (SSD) (HMA air voids filled with water), and submerged in water (underwater) must be determined according to the KT-15 standard test method. Bulk specific gravity of the compacted sample is computed as:

$$G_{mb} = \frac{\text{Dry weight}}{\text{SSD weight} - \text{Submerged weight}}$$

In this study, the KT-39 method was followed to determine theoretical maximum specific gravity, or specific gravity of the mixture without air voids, of loose HMA mixtures. Therefore, a sample of loose HMA (minimum of 1,500 gm) was taken and the volume of sample was determined by calculating the volume of water that was displaced. Theoretical maximum specific gravity was calculated by dividing sample weight by sample volume:

$$G_{mm} = \frac{\text{Dry weight}}{(\text{Dry weight} - \text{Weight of water displaced by sample})}$$

As mentioned, using bulk specific gravity (G_{mb}) and theoretical maximum specific gravity (G_{mm}), percentage of air voids in sample can be calculated using Eq. 3.2.

Table 3.14, Table 3.15, and Table 3.16 summarize volumetric properties of all mixtures and KDOT requirements for SR-9.5 and SR-19 Superpave mixtures. All volumetric requirements were met.

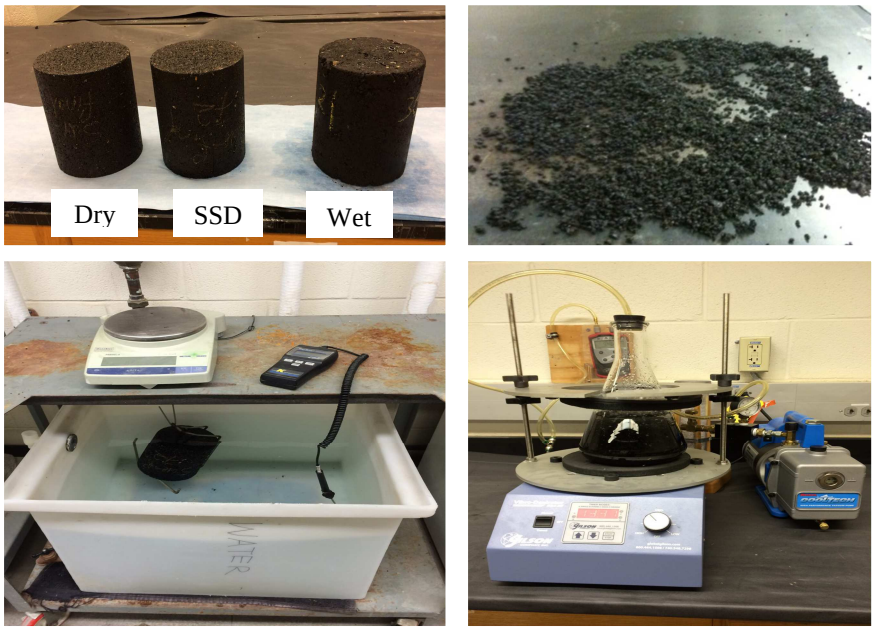

G_{mb} test **G_{mm} test**

Figure 3.10 Determining G_{mb} of compacted samples and G_{mm} of loose mixtures

Table 3.14 Volumetric properties of US-59-surface course

Parameter	US-59-surface course			KDOT Requirements for (SR-9.5A)
	15% Recycled	20% Recycled	35% Recycled	
Total Asphalt Content (%)	7.18	6.9	6.6	-
Airvoid @ N_{des} (%)	4.18	3.87	3.9	4.0%
Voids in Mineral Aggregates (%)	17	18.71	19.1	min. 15%
Voids Filled with Asphalt (%)	74	76	75	65–76
Dust Proportion	0.7	0.96	1.03	0.6–1.2
% Gmm @ N_{ini}	86.7	86.5	87.1	≤90
% Gmm @ N_{des}	95.8	96.1	96.1	-
% Gmm @ N_{max}	97	97.4	97.2	<98

Table 3.15 Volumetric properties of US-59-intermediate course

Parameter	US-59-intermediate course			KDOT Requirements for (SR-19A)
	15% Recycled	20% Recycled	35% Recycled	
Total Asphalt Content (%)	7.08	5.9	5.7	-
Airvoid @ N_{des} (%)	3.64	4.32	4.42	4.0%
Voids in Mineral Aggregates (%)	16	16.02	16.9	min. 13%
Voids Filled with Asphalt (%)	76	75	73.8	65–76
Dust Proportion	0.7	0.98	1.05	0.6–1.2
% Gmm @ N_{ini}	86.6	86.4	86.8	≤90
% Gmm @ N_{des}	96.4	95.7	95.6	-
% Gmm @ N_{max}	97.7	97.3	96.7	<98

Table 3.16 Volumetric properties of US-36-intermediate course

Parameter	US-36-intermediate course			KDOT Requirements for (SR-19A)
	15% Recycled	20% Recycled	35% Recycled	
Total Asphalt Content (%)	5.18	4.8	4.7	-
Airvoid @ N_{des} (%)	4.64	3.17	4.86	4.0%
Voids in Mineral Aggregates (%)	15.4	13.77	14.67	min. 13%
Voids Filled with Asphalt (%)	71	77	68	65–78
Dust Proportion	0.7	1.19	1.2	0.6–1.2
% Gmm @ N_{ini}	89.2	90.3	89.1	≤90.5
% Gmm @ N_{des}	95.4	96.8	95.1	-
% Gmm @ N_{max}	96.2	97.6	95.9	<98

3.10.2 Evaluation of Moisture Susceptibility

The final step in the Superpave mixture design is to evaluate the design mixture for moisture susceptibility. The KDOT test method of Resistance of Compacted Asphalt Mixture to Moisture-induced Damage (Kansas Test Method KT-56) was performed to complete this evaluation. The SGC was used to compact samples with design aggregate structure and asphalt content with 150 mm diameter and 95±5 mm height at 7±0.5%. The KT-56 test method requires a total of six samples. A subset of three samples was taken as control samples and another subset was conditioned via freeze-thaw cycles prior to testing. For the US-36 mixture, antistripping agent was used for all conditioned and unconditioned samples. Conditioning process included partial vacuum saturation (70%–80% of air voids) followed by a freeze cycle for a minimum of 16 hours at -18±3 °C. The final step in conditioning consisted of soaking samples in a hot water bath at 60±1 °C for 24±1 hour and then placing the samples at 25±1 °C in a water bath for 2 hours to reach the test temperature (25±1 °C). Unconditioned samples were also put into plastic

containers and placed in a water bath at 25±1 °C for 2 hours. A Marshall stability tester was used to test samples for ITS. All specimens were loaded at 51mm/minute loading rate until failure, and peak loads were recorded to calculate ITS:

$$\mathrm{ITS} = \frac{2000 \times \mathrm{P}}{\pi \times \mathrm{t} \times \mathrm{D}} \tag{3.6}$$

where:

ITS = indirect tensile strength (KPa),

P = maximum load (N),

t = specimen thickness (mm), and

D = specimen diameter.

Average strength of the three samples was reported as the tensile strength of the mixture for each subset. The TSR, the ratio of average ITS of the conditioned samples to the average ITS of the unconditioned samples, was then calculated using Equation 3.7.

$$\mathrm{TSR} = \frac{\mathrm{ITS_C}}{\mathrm{ITS_{UC}}} \tag{3.7}$$

where:

TSR = tensile strength ratio,

ITS_c = average indirect strength of conditioned subset, and

ITS_{uc} = average indirect tensile strength of unconditioned subset.

KDOT criteria for acceptable minimum TSR is 80%, which was obtained for all mixtures.

3.11 Laboratory Performance Evaluation Tests

In this study, tests were conducted to evaluate mixture performance with respect to three main HMA pavement distresses: moisture damage (stripping), rutting, and fatigue cracking. A brief description of the laboratory tests is provided in the following sections.

3.12 Dynamic Modulus Test

Dynamic modulus ($|E^*|$) is a complex modulus that relates stress to strain of a linear viscoelastic material as a function of loading rate and temperature. In this study, the dynamic modulus test was performed according to the AASHTO TP-79 standard method of test for Determining the Dynamic Modulus and Flow Number for HMA Using the Asphalt Mixture Performance Tester (AMPT specification). AASHTO TP-62, Standard Test Method for Determining Dynamic Modulus of HMA was also followed in order to prepare the test specimen. These two methods have several similarities as well as slight differences. The selection of test temperature and frequencies was the main difference between these two test protocols.

Loose mixtures were prepared and aged for 2 hours at the compaction temperature. The SGC compacted samples with 150 mm diameter and 170 mm height. For each mixture, three samples were fabricated, cored, and trimmed to 100 mm in diameter and 150 mm in height at 7±0.5% target air voids. Metal studs were glued to the sides of the samples in order to attach three LVDTs that provided axial deformation data. Samples were conditioned in the environmental chamber prior to testing for the specified target test temperature according to AASHTO TP-62, and then the samples were tested in the AMPT machine according to AMPT specification. Dynamic modulus tests were conducted at six frequencies of 25, 10, 5, 1, 0.5, and 0.1 Hz and three temperatures of 4 ^{o}C, 21 ^{o}C, and 37 ^{o}C, as shown in Table 3.17.

Table 3.17 Dynamic modulus test specifications

Description	AMPT Specification
Compacted sample dimension	Diameter: 150mm / height: 170 mm
Cored sample dimension	Diameter: 100mm / height: 150±2.5 mm
Cored samples target air voids	7±0.5%
Testing temperatures	4, 21, 37 °C
Testing frequencies	25, 10, 5, 1, 0.5, 0.1 Hz
Maximum load	3000 Ib (13.5 KN)
End friction reducer	Teflon sheet
Strain levels	75 to 125 microstrains
Maximum permanent strain	5000 microstrains
LVDTs	≥2
Replicates	≥2

Although the dynamic modulus test is a nondestructive test, as the test proceeds, an increase in mean strain occurs that is caused by the stress-controlled mode used in the test. Thus, the test mode is set so that early sequences of the temperatures-frequencies have minimum effects on the later testing temperatures and frequencies. Therefore, all available test protocols require that the test begin at the lowest temperature and highest frequencies at which HMA becomes stiff. In this study, dynamic modulus and phase angle were calculated automatically by AMPT. The average of dynamic modulus results of three samples was reported as the mixture dynamic modulus.

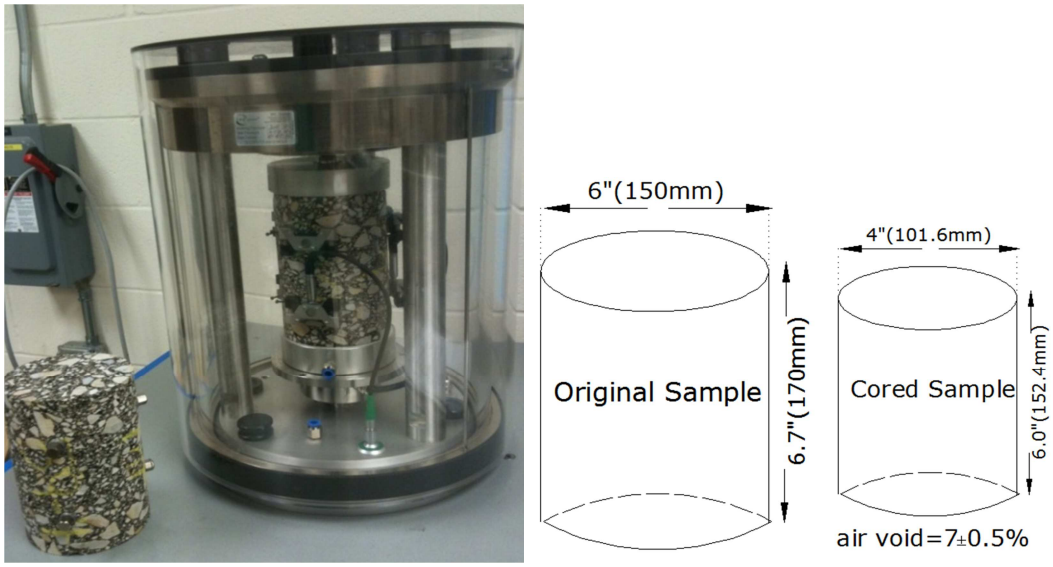

Figure 3.11 Dynamic modulus test setup and standard sample

3.13 Hamburg Wheel Tracking Device

In this study, two tests were used to assess permanent deformation of HMA materials: the HWTD test to evaluate densification and the FN test (also referred to as Repeated Load Permanent Deformation) to assess shear deformation under constant volume.

The HWTD test was performed according to the Tex-242-F test method of the TxDOT. In order to fabricate the laboratory-molded specimen, loose mixtures were prepared and samples were aged for 2 hours in the oven. The SGC compacted samples with 150 mm diameter and 62±2 mm height at 7±1% target air voids. A set of tests for each mixture consisted of four samples and three replicate tests, totaling 12 samples for each mixture. A set of two samples was placed into standard polyethylene molds, forming the test specimen configuration of HWTD, as shown in Figure 3.12. Edges of the fabricated molds had to be cut using a masonry saw in order to fit the fabricated specimens into the molds. After samples were trimmed, molds were placed into the mounting tray and samples were put into each mold. Required test information, such as the test temperature and number of maximum wheel passes over the sample, was inputted into

the operating software. In this study, the machine was set for 40,000 wheel passes or a maximum of 20 mm rut depth (whichever came first) as the failure criteria.

The water bath in the HWTD was filled with water. Once the water reached the desired test temperature (50±1 °C), the specimens were saturated in the water bath for an additional 30 minutes. Each test used two polyethylene molds containing four asphalt samples, and the samples were tested simultaneously under the right and left steel wheels of the HWTD, measuring 204 mm in diameter and 47 mm in width and traversing the HMA specimen length 50 times per minute. Load applied by each wheel was approximately 705±22 N (158±5 Ib). An LVDT automatically measured rut depth induced by steel wheels at 11 points along the wheel path with an accuracy of 0.01 mm. Rut depth measurement was taken at least every 100 passes of the wheel. The test stopped automatically when the HWTD applied the number of desired passes or the maximum allowable rut depth was reached. For each specimen, the numbers of passes to failure and rut depth at the end of test were reported. Table 3.18 lists test specifications.

Table 3.18 HWTD test specifications

Parameter	Specification
Sample dimension	Diameter: 150 mm / height: 62±2 mm
Target air voids	7±1%
Testing temperature	50±1 °C
Applied load	705±22 N (158±5 Ib)
Number of passes per minute	50±5
Maximum speed of the wheel	1.1 ft./sec
Minimum rut-depth measurements	every 100 passes
Maximum number of passes setting	40,000 (KDOT criteria is 10,000)
Maximum rut depth setting	20 mm (KDOT criteria is 12.5 mm)

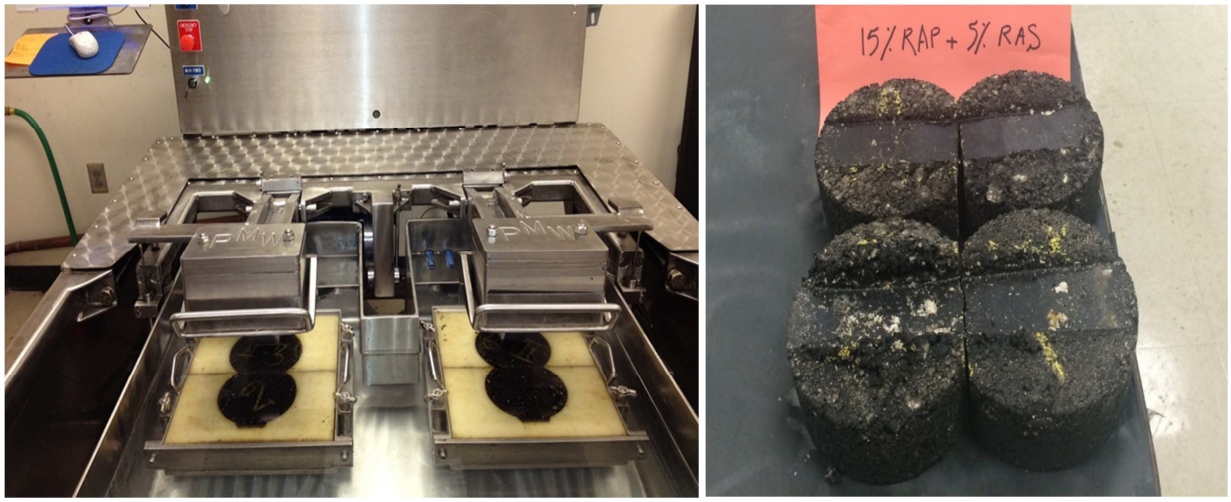

Figure 3.12 HWTD test setup (Sabahfar, 2012) and tested samples

3.14 Flow Number Test

In this study, an unconfined FN test was done according to AASHTO TP-79, requiring testing of the HMA mixture at one effective pavement temperature, T_{eff}, and at one design stress level. T_{eff} covers an approximate range of 25–60 °C (77–140 °F), and the design stress level consists of a range between 69 and 207 kPa (10–30 psi) for the unconfined tests. The FN test was conducted at a single effective temperature of 54 °C according to the literature (Witczak et al., 2002). Since the dynamic modulus test is nondestructive, the same specimens used for the dynamic modulus test were used for the FN test.

Samples were placed in the environmental chamber for three hours according to AASHTO TP-62 to allow for temperature equilibrium. Flexible friction-reducing end treatments were placed between specimen ends and loading platens, and the specimen was carefully centered in the load actuator to avoid eccentric loading. Then all sample information and test specifications listed in Table 3.19 were entered into the AMPT software, and the environmental chamber was closed. The test began after some time to allow the temperature to stabilize. The machine automatically applied contact load equal to 5% of the total load to ensure proper LVDT response.

A load of 207kPa with haversine pulse of 0.1 second load and a 0.9 second rest period was repeatedly applied for a maximum of 10,000 cycles, 50,000 accumulated microstain, or until the sample failed. The AMPT data acquisition system recorded the applied load and axial deformation. The number of cycles each sample endured before failure was used for further performance comparison between various mixtures.

Table 3.19 FN test specifications (current study)

Description	AMPT Specification
Compacted sample dimension	Diameter: 150 mm / height: 170 mm
Cored sample dimension	Diameter: 100 mm / height: 150±2.5 mm
Cored samples target air voids	7±0.5%
Testing temperatures	54 °C
Load application	0.1 second haversine pulse load / 0.9 second rest time
Applied pressure	207 kPa

Figure 3.13 FN test setup and a failed sample

3.15 S-VECD Direct Tension Fatigue Test

The S-VECD direct tension fatigue test used direct tension cyclic loading to evaluate fatigue cracking propensity of the mixtures. Three test samples with150 mm diameters and 180

mm heights were fabricated in the SGC and cut and cored to 102±2 mm in diameter and 130±2.5 mm in height with 7±0.5% air voids. Epoxy cement was used to glue mounting studs to the sides of the samples in order to attach the LVDTs to the sample; end plates were glued to the samples according to AASHTO TP-107 procedure. Table 3.20 lists test parameters.

Table 3.20 S-VECD fatigue cracking test specifications

Description	AMPT Specification
Compacted sample dimension	Diameter: 150 mm / height: 180 mm
Cored sample dimension	Diameter: 102±2 mm / height: 130±2.5 mm
Cored samples target air voids	7±0.5%
Testing temperatures	18 °C
Testing frequencies	10Hz
LVDTs	≥3
Replicates	≥2

The test temperature of the S-VECD fatigue cracking test was determined based on the average of high and low side of the PG binder grade temperatures minus 3 °C but not exceeding 21 °C (AASHTO TP-107). In this study, target PG binder grade was PG 70-28 for all mixtures; thus, the test temperature was 18 °C. The specimen was placed in the environmental chamber for temperature equilibrium 2 hours prior to testing, and then it was placed in the AMPT for testing by securing to the bottom platen. After the specimen was firmly placed, the actuator was brought up to position and quickly secured to the upper loading platen with screws. Care was taken not to shear the specimen unintentionally. LVDTs were attached to the sample, and the chamber was closed. The sample remained in the AMPT chamber for approximately 15 minutes in order to bring it back to the test temperature.

The S-VECD fatigue cracking test consisted of two main parts. In the first part, a fingerprint dynamic modulus test was performed in tension-compression mode; the tension-

tension fatigue test began after a rest period of a minimum of 15 minutes. The electronic measuring system was adjusted and set to zero load, and then the fingerprint dynamic modulus test was conducted at the target test temperature at a frequency of 10 Hz. In the software, target strain was set for a range of 50–75 microstrains. AMPT calculated load necessary to achieve the desired microstrain level using results of the first few cycles, and then applied for 50 cycles. UTS-032 software computed the dynamic modulus and phase angle for the sample. The test resumed after the rest period following the fingerprint testing.

Based on AASHTO specification, at least three microstrain levels are required and the first sample of the three samples should be tested at a strain level of 300 microstrains. Based on results obtained from first the sample, the microstrain level must be adjusted for the second and third specimens. However, for a majority of recycled mixtures evaluated in this study, 300 microstrains did not result in sample failure, and in some cases, the test continued through 200,000 load cycles. In this study, microstrain levels were chosen based on trial and error using guidelines in Table 4 of AASHTO TP-107. The direct tension-tension fatigue test was performed at a frequency of 10 Hz and at a strain level expected to cause sample failure within a reasonable number of load repetitions. When a sample failed, a clear microcrack formed or a sudden drop in dynamic modulus-phase angle graph was evident. The number of applied load cycles, peak and valley values of stress, and peak and valley values of strain were acquired by the AMPT data acquisition system. The test was done on three replicates at various microstrain levels.

Figure 3.14 S-VECD test setup and a failed sample

Based on recorded data of all samples and using the Alpha-F software developed by North Carolina State University, a damage characteristics relationship can be determined using one of the two models described in Equations (3.8) and (3.9):

$$C = e^{aS^b} \tag{3.8}$$

$$C = 1 - yS^z \tag{3.9}$$

where:

a,b = fitting coefficients for the exponential model,

y,z = fitting coefficients for the power model,

C = pseudo stiffness, and

S = internal state variable.

For a given normalized stiffness (C), a high damage parameter (S) value indicates increased damage resistance (AASHTO TP 107-14).

Chapter 4 - Results and Discussion

4.1 Moisture Susceptibility Test Results

In order to assess the moisture susceptibility of mixtures, KDOT standard test method KT-56 for evaluating resistance of compacted asphalt mixture to moisture-induced damage was performed in the laboratory. A Marshall stability tester tested samples in conditioned and unconditioned states for ITS. Test results and sample information for all mixtures are listed in Table 4.1 to Table 4.3.

Table 4.1 Moisture susceptibility test results for US-59-surface

Mixture Design	% Virgin AC	Sample		% Air Voids	Tensile strength (kPa)	Avg. (kPa)	% TSR
US-59-surface (15% recycled)	79	a	Conditioned	7.0	681	707	90.0
		b		7.1	720		
		c		7.2	721		
		d	Unconditioned	7.3	800	786	
		e		7.2	779		
		f		7.0	779		
US-59-surface (20% recycled)	75	a	Conditioned	7.0	863	833	89.7
		b		7.2	821		
		c		6.8	816		
		d	Unconditioned	7.1	976	929	
		e		7.0	917		
		f		6.9	894		
US-59-surface (35% recycled)	62	a	Conditioned	7.1	722	698	87.5
		b		7.0	678		
		c		6.9	692		
		d	Unconditioned	6.8	795	797	
		e		7.1	793		
		f		7.0	803		

Table 4.2 Moisture susceptibility test results for US-59-intermediate

Mixture Design	% Virgin AC	Sample		% Air Voids	Tensile strength (kPa)	Avg. (kPa)	% TSR
US-59-int. (15% recycled)	79	a	Conditioned	7.0	771	764	85.4
		b		7.4	781		
		c		6.9	741		
		d	Unconditioned	7.2	881	895	
		e		7.1	900		
		f		7.0	903		
US-59-int. (20% recycled)	70	a	Conditioned	6.5	839	867	85.3
		b		6.5	870		
		c		6.7	892		
		d	Unconditioned	6.4	1074	1016	
		e		6.7	926		
		f		6.5	1050		
US-59-int. (35% recycled)	60	a	Conditioned	6.6	701	731	84.7
		b		6.7	674		
		c		6.9	685		
		d	Unconditioned	6.4	798	810	
		e		7.1	812		
		f		7.0	820		

Table 4.3 Moisture susceptibility test results for US-36-intermediate

Mixture Design	% Virgin AC	Sample		% Air Voids	Tensile strength (KPa)	Avg. (KPa)	% TSR
US-36-int. (15% recycled)	86	a	Conditioned	7.3	761	770	82.0
		b		7.1	781		
		c		7.2	769		
		d	Unconditioned	7.2	954	939	
		e		7.3	961		
		f		7.2	901		
US-36-int. (20% recycled)	58	a	Conditioned	6.5	1205	1151	93.2
		b		6.5	1103		
		c		6.6	1145		
		d	Unconditioned	7.0	1226	1235	
		e		6.8	1326		
		f		6.2	1152		
US-36-int. (25% recycled)	52	a	Conditioned	6.5	872	946	83.4
		b		6.6	1019		
		c		-	-		
		d	Unconditioned	6	1191	1134	
		e		6.7	1187		
		f		7.0	1024		

Figure 4.1 illustrates TSR values for all mixtures for the current study. As shown, all mixtures proved viable with respect to moisture damage resistance, and they met the KDOT requirement of minimum TSR of 80%. However, different trends in TSR values were observed for mixtures, especially when the source of RAP material was different. For the US-59-surface mixture, as the percentage of recycled material increased, TSR values slightly decreased. For the US-59-intermediate course, inclusion of additional RAP materials decreased performance, although the effect was not very significant. Incorporation of RAS into the US-36 mixture resulted in considerable improvement in moisture resistance, with 11% increase in TSR value for

mixtures with 15% and 20% recycled materials, respectively. In general, for US-36, RAS mixtures exhibited better moisture susceptibility.

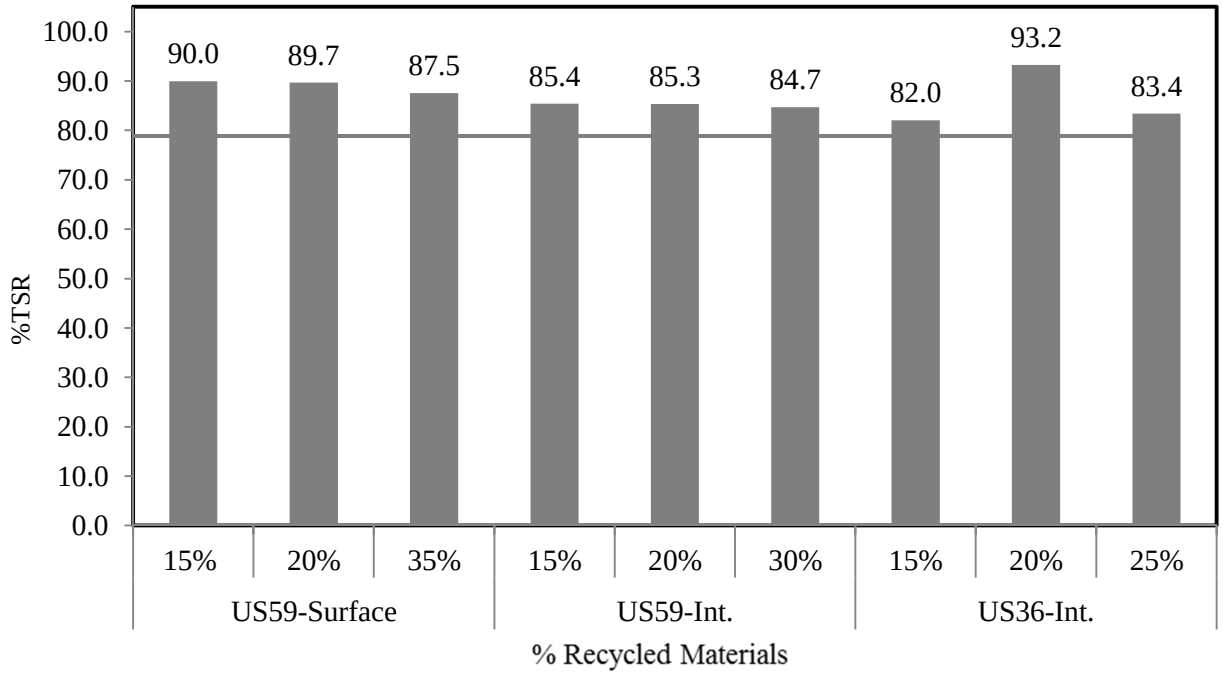

Figure 4.1 Tensile strength ratios (%TSR) for all mixtures

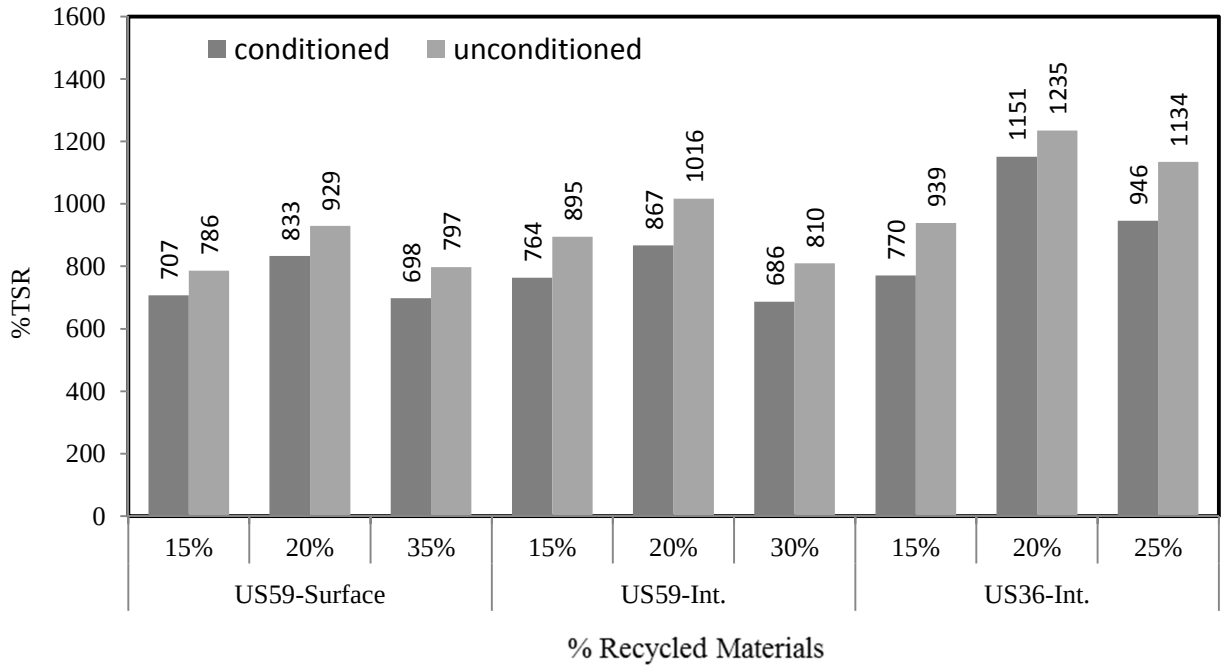

Figure 4.2 Tensile strength results (KPa) for all mixtures

Figure 4.2 shows average tensile strength of conditioned and unconditioned specimens with varying recycled material content. Based on results, the highest average tensile strength of all mixtures was observed with recycled material content of 20%. Mixtures with the highest tensile strength had virgin binder content ranging from 58% to 75% for US-36 and US-59-surface mixtures, respectively.

4.2 Hamburg Wheel Tracking Device Test Results

4.2.1 Rut Depth and Number of Wheel Passes

Tex-242-F test method was used to perform the HWTD test. All specimens were fabricated at 7±1% air voids and tested under 50 ℃ water. The HWTD machine was set for 40,000 wheel passes or rut depth of 20 mm, whichever came first. Average numbers of wheel passes and corresponding rut depths are tabulated in Table 4.4. With the exception of the US-59-surface course with the highest percentage of recycled materials, all mixtures reached the maximum number of wheel passes before 20 mm rut depth. In addition, intermediate course mixtures (SR-19A) performed better compared to the surface course mixture (SR-9.5A), where average rut depth for SR-19A for all cases remained low (maximum of 8.2 mm). Figure 4.4 represents the average rut depth for various mixtures. The highest average rut depth was 20 mm for the surface mixture, and the lowest rut depth was 1.9 mm for US-36 with 15% RAP and 5% RAS.

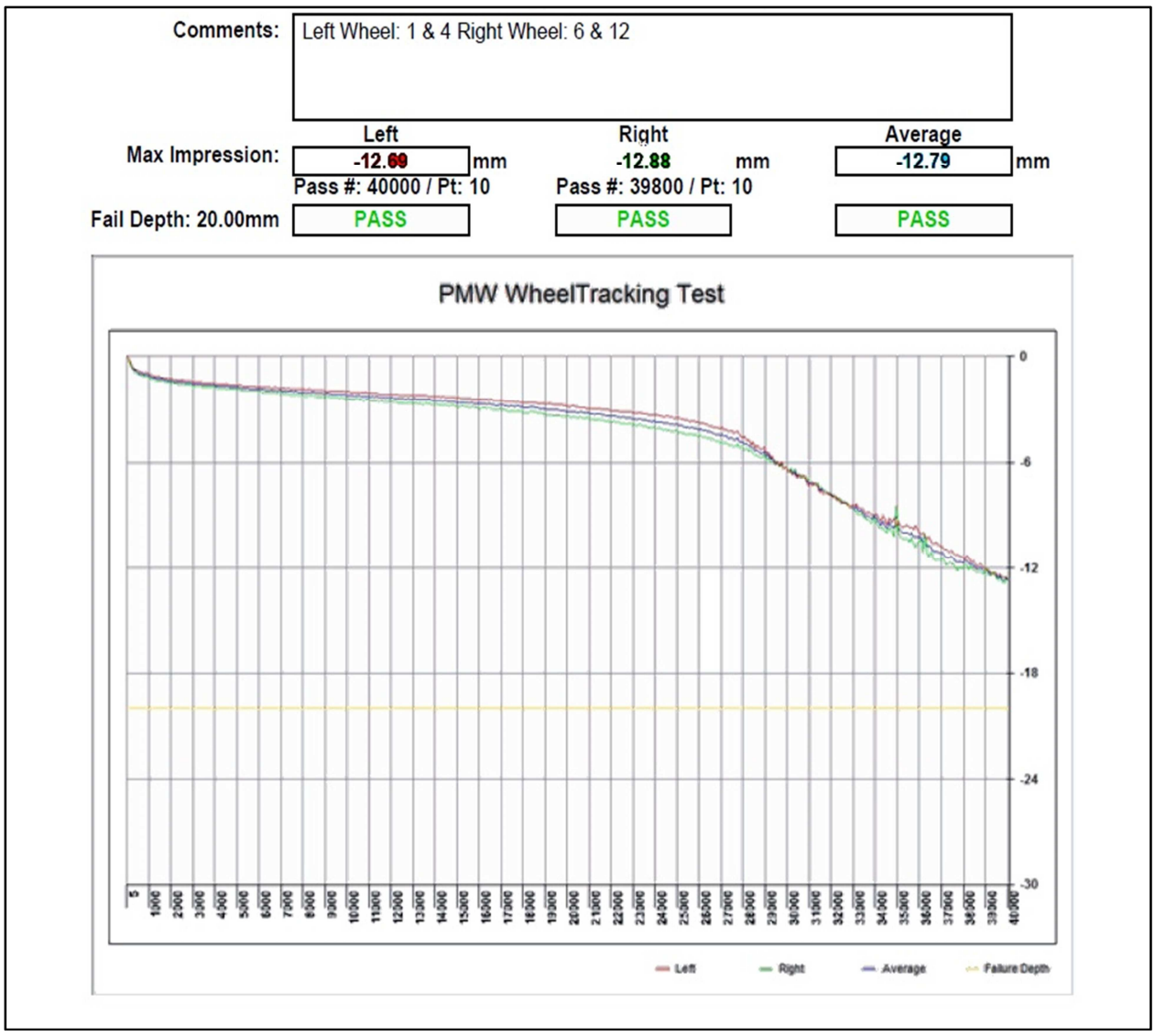

Figure 4.3 HWTD typical test summary output

Table 4.4 HWTD test results

Mixture Design	% Virgin AC	Sample	Left wheel		Right wheel		Avg.	Average Rut Depth (mm)
			Pass Num	Rut depth (mm)	Pass Num	Rut depth (mm)		
US-59-surface (15% recycled)	79	1	40000	9.8	40000	13.6	11.7	15.2
		2	40000	14.6	39900	17.4	16.0	
		3	39772	20.1	40000	16.0	18.0	
US-59-surface (20% recycled)	75	1	40000	12.7	39800	12.9	13.0	11.5
		2	39900	18.3	39200	9.4	13.9	
		3	40000	7.5	40000	8.2	7.9	
US-59-surface (35% recycled)	62	1	26700	20.1	33314	20.0	20.0	20.1
		2	20500	20.1	31894	20.1	20.0	
		3	38595	20.0	31175	20.0	20.0	
US-59-int. (15% Recycled)	79	1	39900	6.5	40000	7.2	6.8	5.4
		2	40000	4.7	39200	4.3	4.5	
		3	39700	4.7	39400	5.3	5.0	
US-59-int. (20% recycled)	70	1	40000	11.6	39700	5.0	8.3	8.2
		2	40000	7.5	39800	8.0	7.8	
		3	39700	6.5	39900	10.7	8.6	
US-59-int. (30% Recycled)	60	1	40000	13.2	39800	3.5	8.4	8.0
		2	40000	4.6	39900	10.6	7.6	
		3*	-	-	-	-	-	
US-36-Int. (15% recycled)	86	1	39900	5.7	40000	4.4	5.1	6.8
		2	40000	4.4	39800	4.5	4.5	
		3	40000	17.3	39900	4.2	10.8	
US-36-Int. (20% Recycled)	58	1	39000	1.3	39900	1.8	1.5	1.9
		2	40000	2.0	36100	1.9	1.9	
		3	39700	1.6	40000	2.5	2.1	
US-36-int. (25% recycled)	52	1	39700	5.7	39200	2.9	4.3	4.7
		2	40000	7.3	39700	2.7	5	
		3*	-	-	-	-	-	

* Data could not be obtained due to machine power failure during the test.

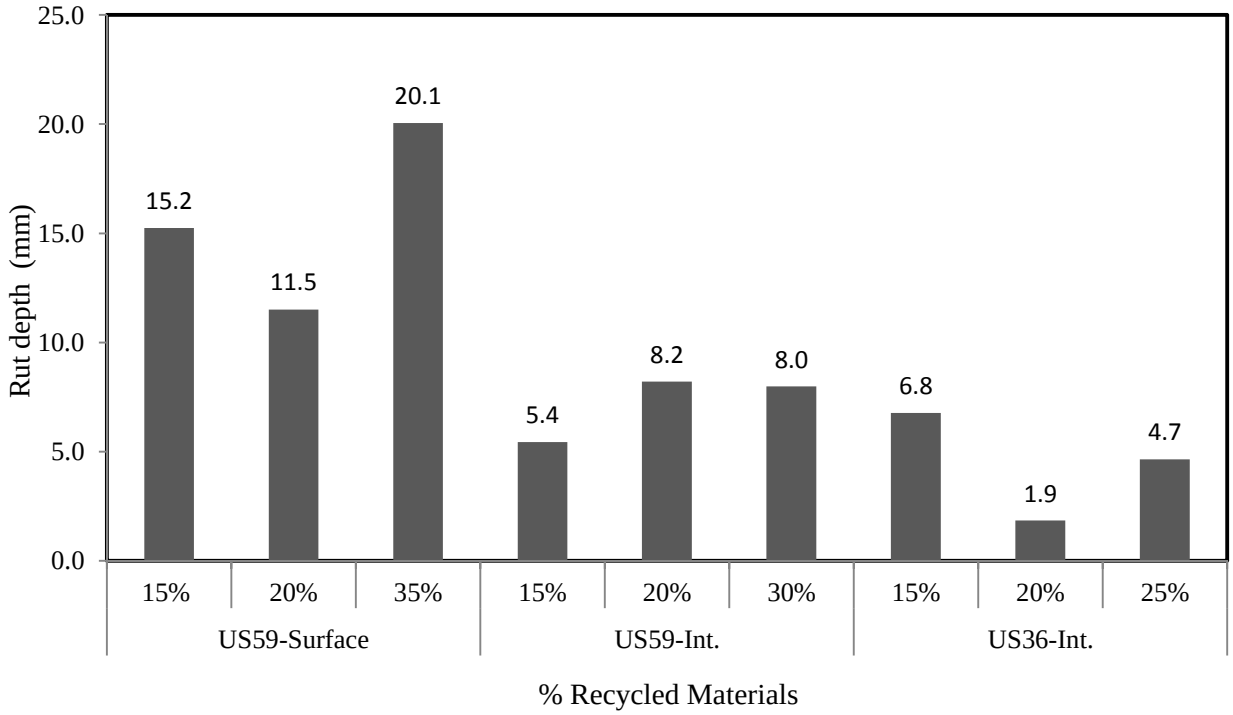

Figure 4.4 Rut depth (mm) for various mixtures

4.2.2 Hamburg Wheel Tracking Device Test Output Parameters

HWTD test output parameters were used for further mixture performance evaluation. Figure 4.5 shows how parameters were extracted from HWTD data output. Average of results of three samples was reported as the test output parameter of mixture.

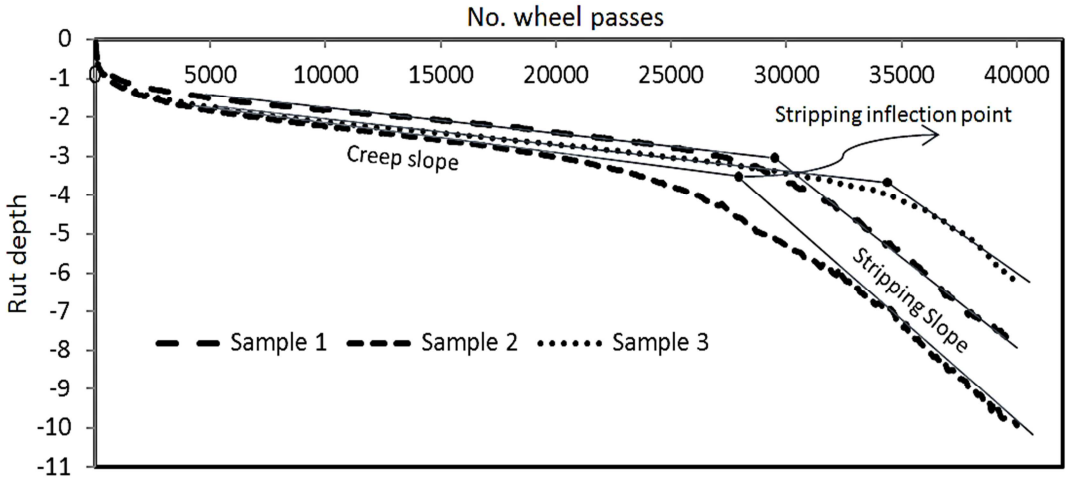

Figure 4.5 HWTD results for US-59-surface 20% recycled

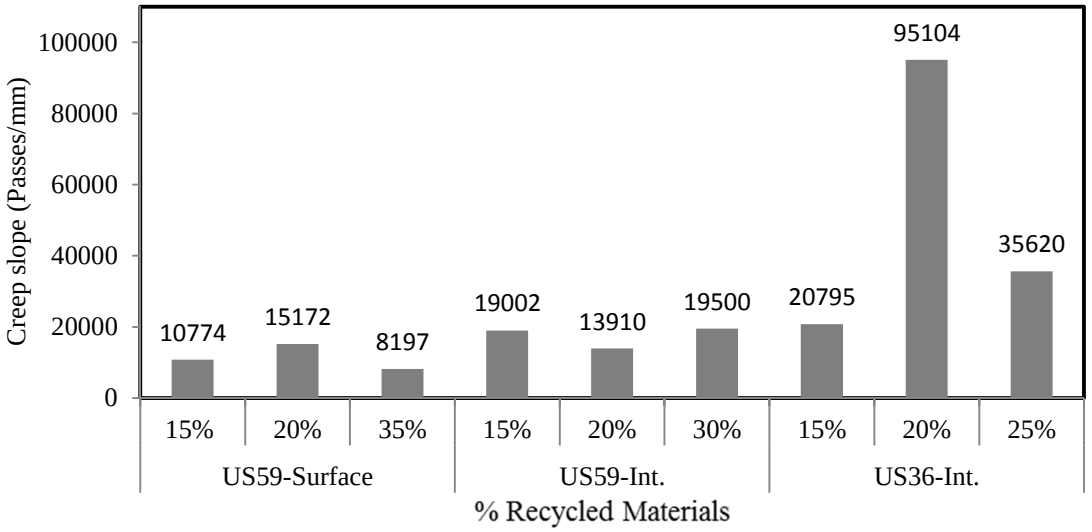

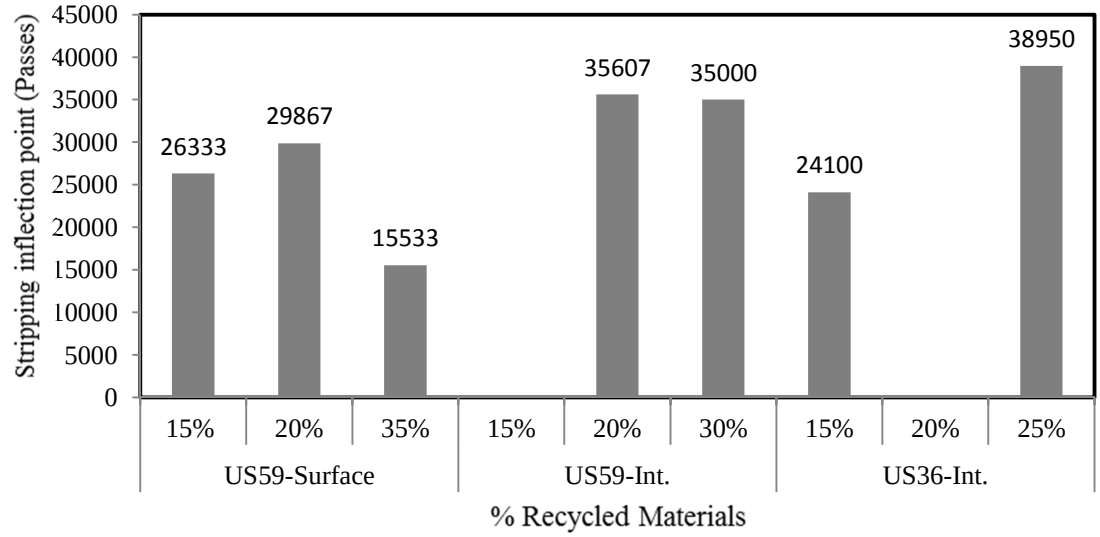

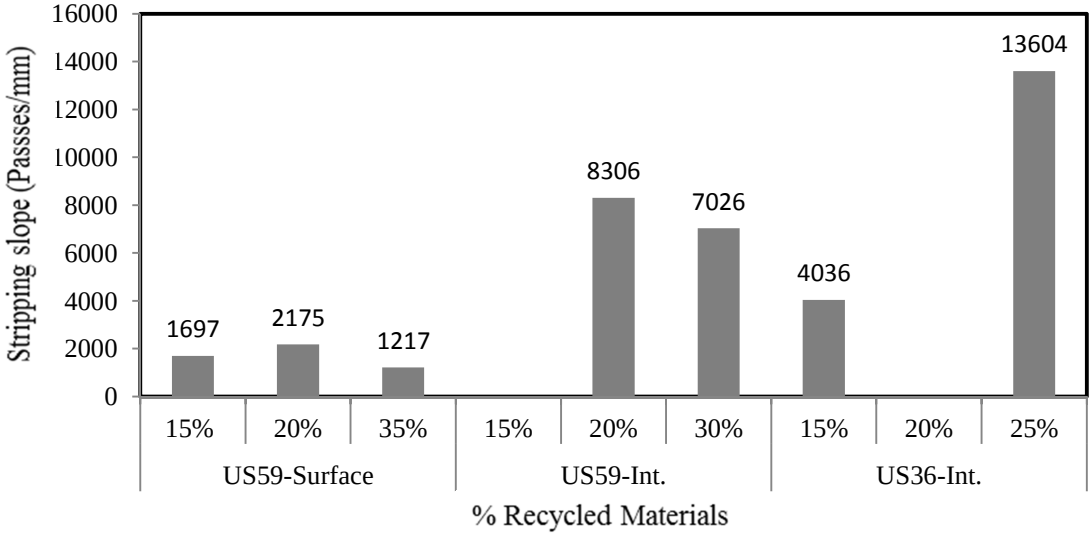

Figure 4.6 HWTD output parameters for all mixtures

Figure 4.6 illustrates HWTD test outputs, including creep slope, stripping slope, and stripping inflection point. Rut depth results were compared to output parameters in order to evaluate the moisture effect on rutting performance. For the surface mixture (SR-9.5A), lowest rut depth was observed for the mixture with 20% recycled materials (75% virgin binder). The highest creep and stripping slope as well as stripping inflection point were associated with the same mixture. For the US-59-intermediate course (SR-19A), optimum rutting performance was observed for the mixture with 15% recycled materials (79% virgin binder). This mixture showed highest resistance of moisture damage, and stripping inflection was not observed. Other US-59-intermediate mixtures with higher recycled materials performed approximately the same. However, the mixture with the lowest virgin binder content showed more vulnerability toward moisture damage. US-36 mixtures (SR-19A) showed optimal rutting resistant among all mixtures of this study, potentially because of the antistripping agent. For US-36, the mixture with 20% recycled material (58% virgin binder) performed the best with respect to rutting and had the highest HWTD output parameter values.

Regardless of virgin binder content, all SR-19A mixtures generally performed very well with respect to rutting potential, and the maximum average rut depth was as low as 8.2 mm. For SR-9.5A mixtures, all mixtures passed the KDOT criteria for rut depth, but rutting potential significantly increased for lower virgin binder content. The KDOT requirement for rut depth is 12.5 mm for 10,000 wheel passes.

4.2.3 Comparison of HWTD and KT-56 Test Results

HWTD and KT-56 tests were performed to evaluate rutting potential and moisture susceptibility of the mixtures. Based on all results, optimal rutting and moisture resistance was observed for mixtures with virgin binder content greater than 75% for the US-59-surface (SR-

9.5A). Moisture and rutting susceptibility increased for the mixture with the lowest virgin binder content. For the US-59-surface, although all mixtures with varying binder contents passed KDOT requirements for the HWTD test, low values of stripping slopes and inflection points for the mixture with the lowest virgin binder content indicated decreased moisture resistance which was confirmed by the KT-56 test results. For US-59-intermediate, mixtures with higher percentage of recycled materials showed higher rutting susceptibility, but the decrease in TSR value was not significant. HWTD output parameters also suggested that moisture damage did not have a major impact on this mixture. US-36 mixtures with RAS showed optimal rutting and moisture resistance. However, for percentage of virgin binder less than 60%, a drop in performance was observed.

4.3 Flow Number Test Results

The FN test was performed on the laboratory-fabricated samples according to the AASHTO TP-79 standard test method using an AMPT machine. The AMPT automatically applied and controlled test parameters, including unconfined pressure and test temperature. Test data was collected by the AMPT data acquisition system; results are presented in Table 4.5 and Figure 4.8. Rutting potential due to shear deformation was higher for the SR-19A mixtures. Failure criteria were 10,000 cycles, cumulative 50,000 microstrains, or sample failure due to shear flow, whichever came first. As illustrated in Figure 4.8, all US-59-surface mixtures (SR-9.5A) performed very well and the number of cycles to failure was close to 10,000 cycles. For SR-19A mixtures, average FN was typically less than 5,000 cycles, with the exception of the US-36-20% recycled mixture that showed 7,000 cycles. Optimal performance for US-59-surface, US-59-intermediate, and US-36 was observed for mixtures containing 62%, 60%, and 58%

virgin binder, respectively. However, for US-59-intermediate mixtures with 60% and 70% virgin binder, performance was approximately identical.

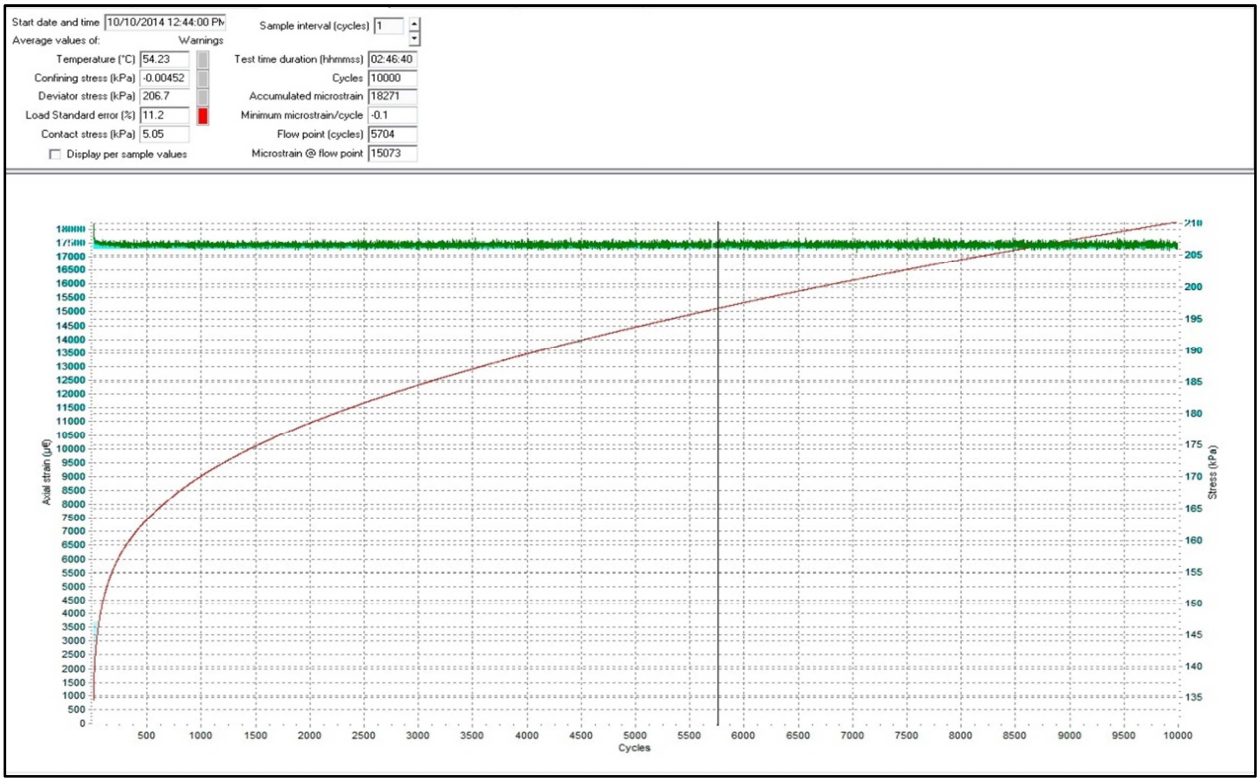

Figure 4.7 Typical FN test data output

Table 4.5 FN test results

Mixture Design	% Virgin AC	Sample	Flow point (cycles)	Microstrain at flow point	Avg. Flow No. (cycles)	Avg. Microstrain
US-59-surface (15% recycled)	79	1	8469	18931	9093	18457
		2	9717	17982		
US-59-surface (20% recycled)	75	1	7466	17634	7507	15393
		2	7548	13152		
US-59-surface (35% recycled)	62	1	9970	26921	9852	22106
		2	9733	17290		
US-59-int. (15% recycled)	79	1	2089	27832	2190	24501
		2	2290	21169		
US-59-int. (20% recycled)	70	1	3544	11580	4624	13327
		2	5704	15073		
US-59-int. (30% recycled)	60	1	2690	12984	4842	20711
		2	6994	28437		
US-36-int. (15% recycled)	86	1	3021	21422	3801	23629
		2	4580	25835		
US-36-int. (20% recycled)	58	1	9061	8858	7153	6674
		2	5244	4490		
US-36-Int. (25% Recycled)	52	1	7319	16444	4665	13571
		2	2011	10698		

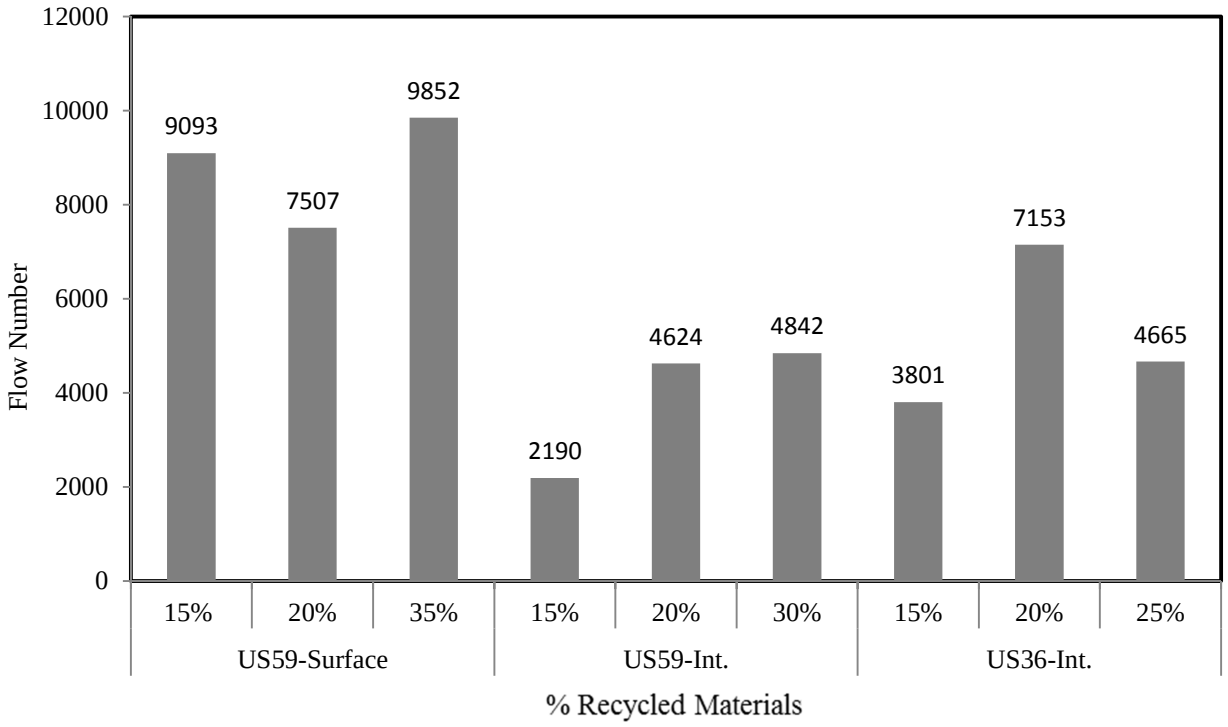

Figure 4.8 FN test results

4.3.1 Comparison of Flow Number and HWTD Test Results

The FN and HWTD tests evaluated rutting potential of the mixtures. FN evaluates rutting potential due to shear deformation, and HWTD evaluates rutting potential due to densification, shear deformation, and moisture damage.

For US-36 mixtures, results of the two tests were in very good agreement because they identified one rutting performance pattern for the mixtures. Optimal rutting performance based on the two tests was captured for the mixture with 58% virgin binder, which was an RAS mixture. However, for US-59, test outputs were inconsistent and contradictory. For mixtures with the lowest rut depth, higher numbers of load cycles were expected in the FN test, but in this study, the lowest number of load cycles in the FN test was obtained for mixtures with lowest rut depth in the HWTD test.

4.4 Dynamic Modulus Test Results

The dynamic modulus test was performed according to AASHTO TP-79. Test results were automatically collected and recorded by the AMPT data acquisition system. Typical data output is shown in Figure 4.9. Dynamic modulus and phase angle were computed by the AMPT software, and all results are depicted in Figure 4.10 to Figure 4.15. Two parameters that predominantly affected test results were test temperature and test frequency. In general, viscoelastic materials were stiffer at higher frequencies and lower temperatures; therefore, higher dynamic modulus values were expected for such conditions. This trend was also observed for all mixtures in this study. For SR-19A mixtures, the highest and the lowest values for dynamic modulus were measured for mixtures with 20% and 15% recycled materials, respectively. For SR-9.5A, mixtures with 15% recycled materials showed the stiffest behavior, with the exception of 4 °C. In addition, high phase angles were associated to higher testing temperatures due to viscous behavior of the mixtures.

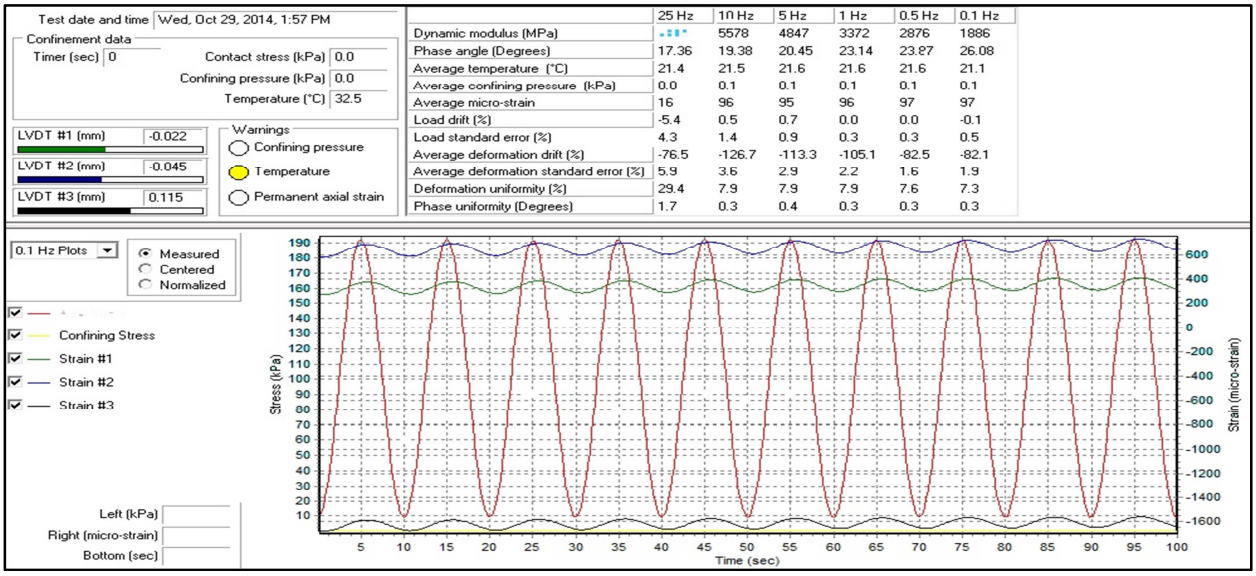

Figure 4.9 Dynamic modulus typical data summary output

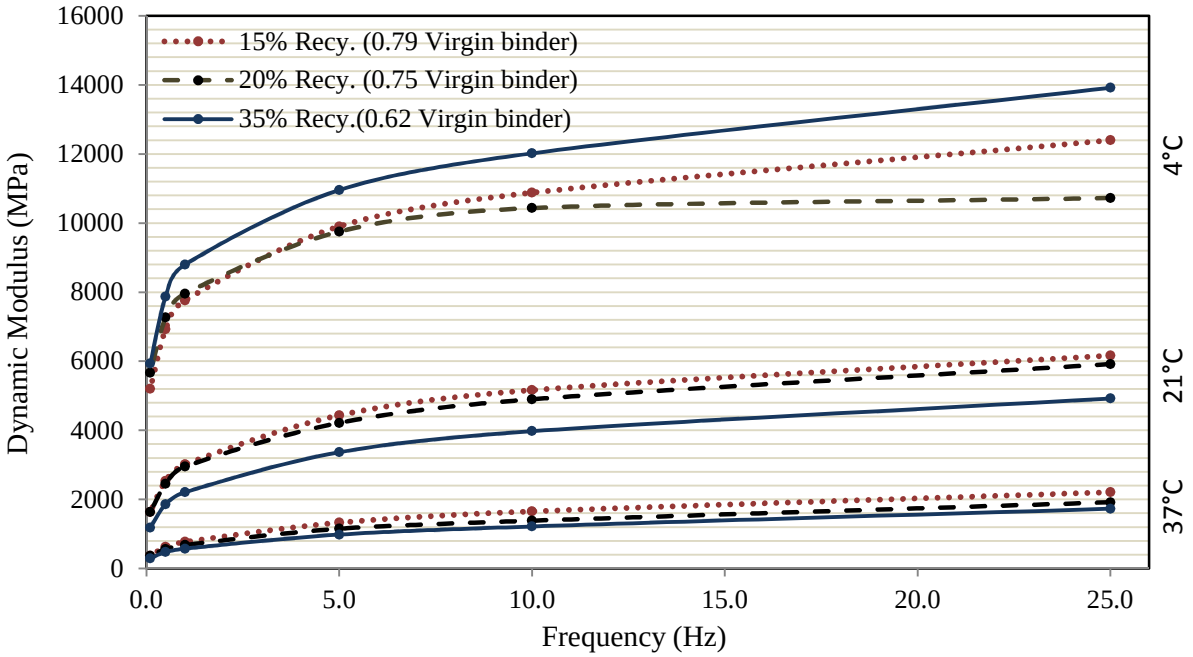

Figure 4.10 Dynamic modulus test results for US-59-surface

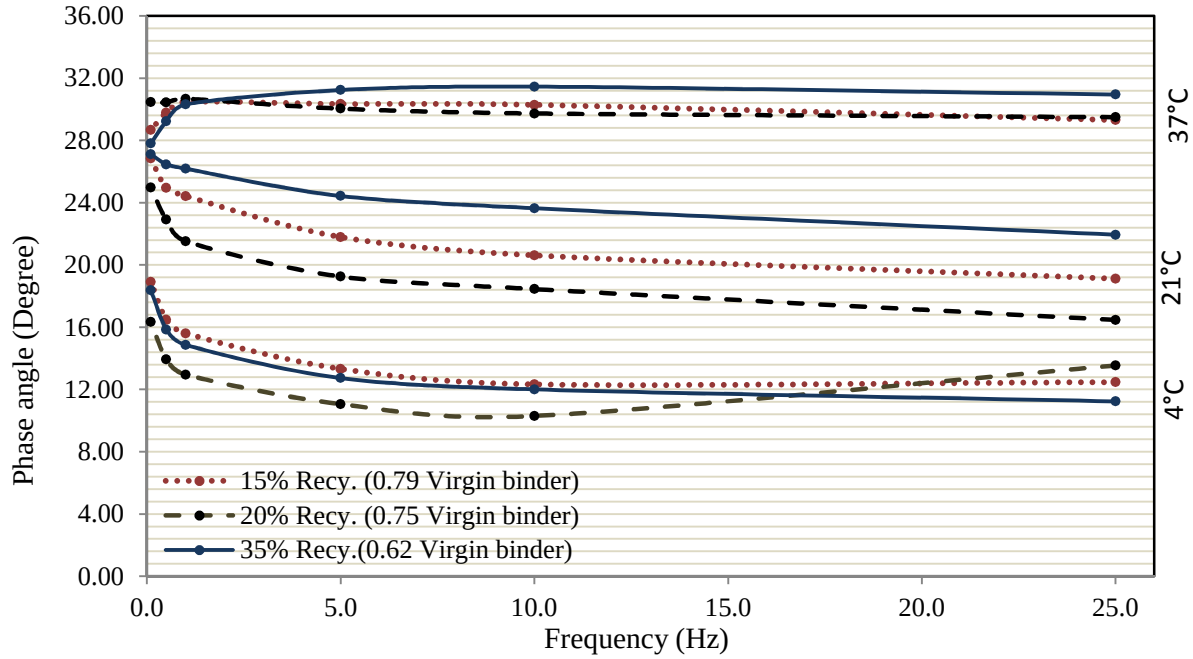

Figure 4.11 Phase angle test results for US-59-surface

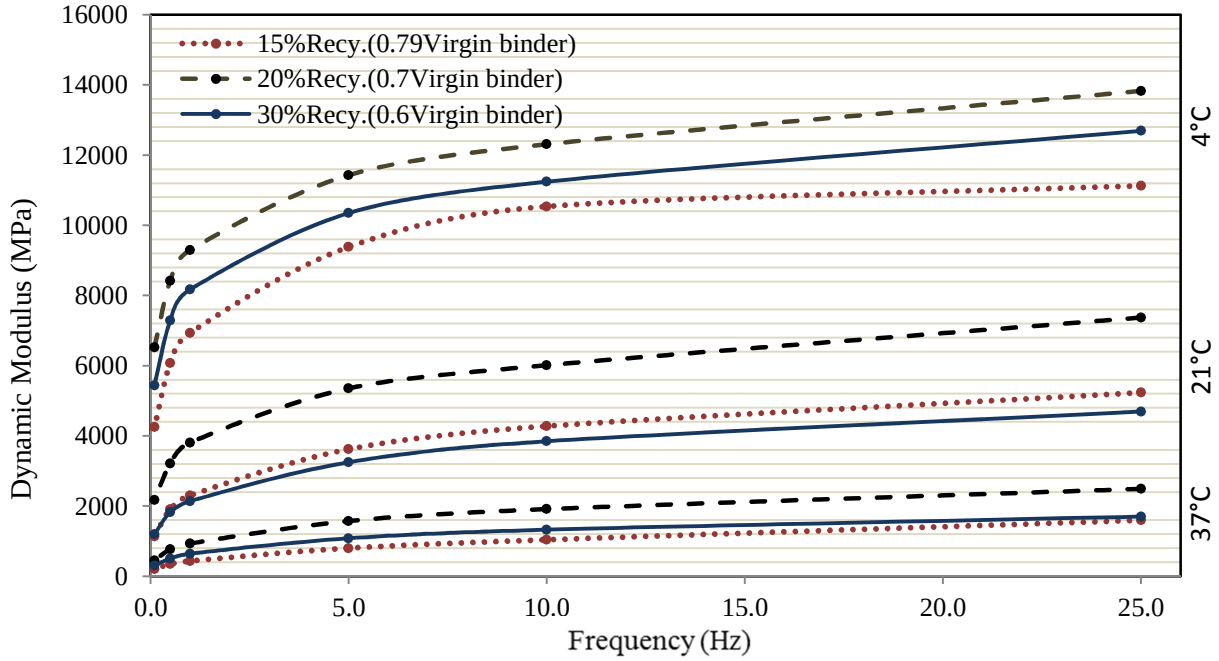

Figure 4.12 Dynamic modulus test results for US-59-intermediate

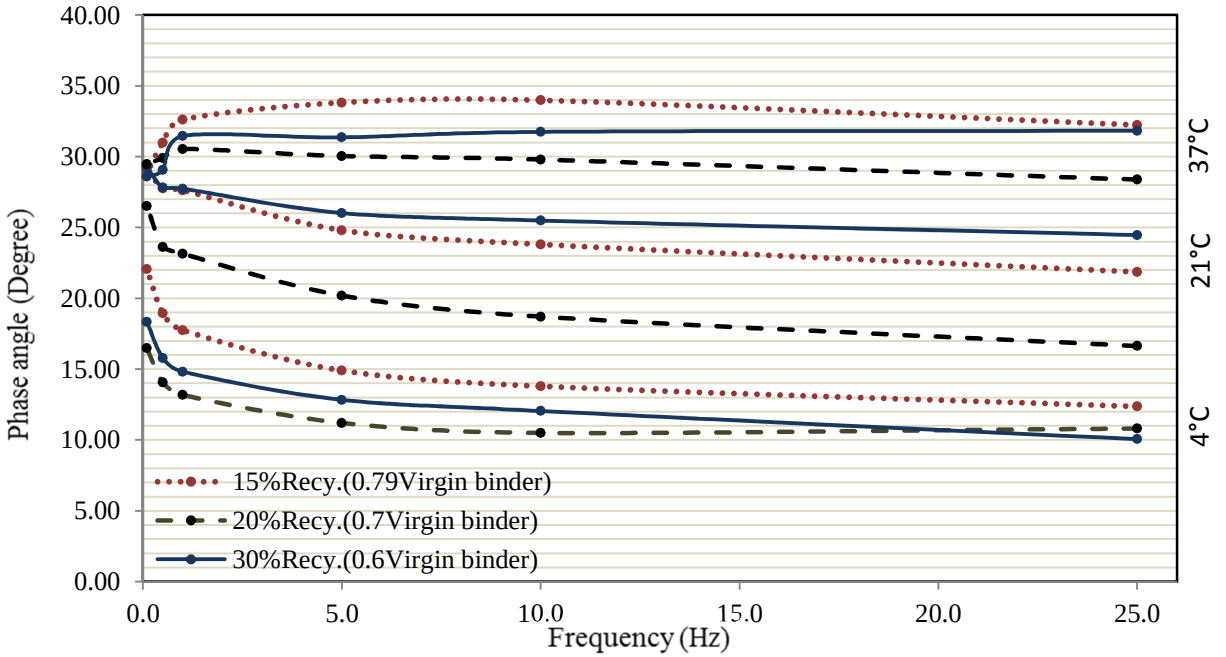

Figure 4.13 Phase angle test results for US-59-intermediate

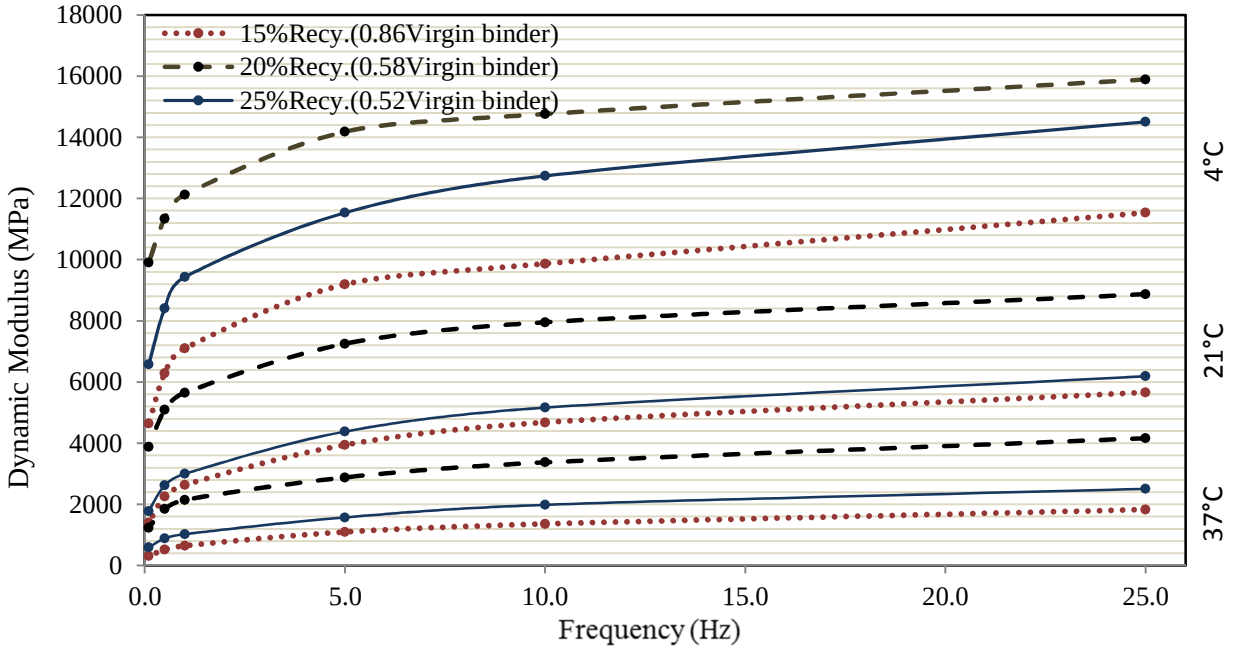

Figure 4.14 Dynamic modulus test results for US-36

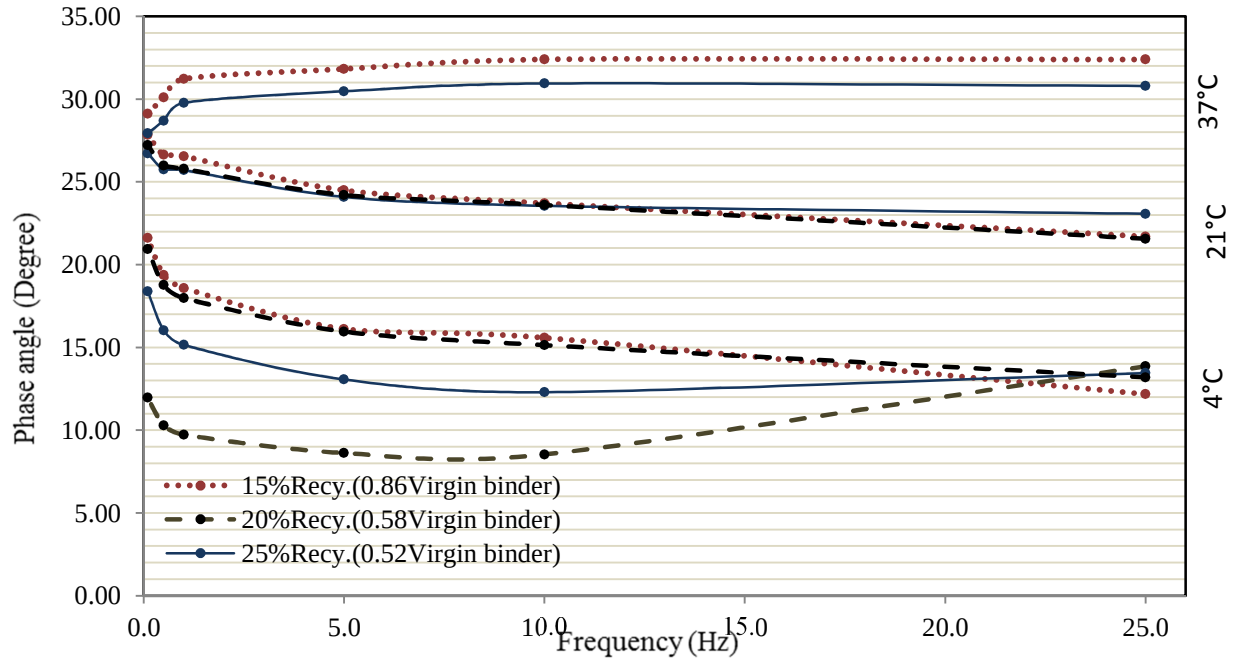

Figure 4.15 Phase angle test results for US-36

4.4.1 Dynamic Modulus Master Curves

In order to more accurately compare results, all dynamic modulus data for each mixture at various temperatures were shifted to a single reference temperature. Reference temperature is usually 21 ℃ (Witczak, 2005), but 18 ℃ was selected for this study in order to produce mastercurves at the same temperature as the test temperature of the S-VECD fatigue cracking test. In the S-VECD test, dynamic modulus master curves are used for data analysis and production of S-C curves. Mastersolver Version 2.2, developed by Advanced Asphalt Technologies, LLC, was used to develop dynamic modulus master curves in this study. Test data and mixture volumetric properties were fitted in the Hirsch model and Arrhenius equation to solve the modified version of the MEPDG master curve equation. The final product was a smooth dynamic modulus prediction curve for the specified reference temperature. Mastercurves from this study are illustrated in Figure 4.16 to Figure 4.18.

Master curves developed at 18 °C indicated unique behaviors of SR-9.5A and SR-19A mixtures. For SR-9.5A mixtures, stiffness was dependent on test frequency: mixtures with lower amounts of recycled materials showed higher levels of stiffness at lower test frequencies. For higher frequencies, all mixtures showed approximately the same level of stiffness. For SR-19A, a distinct pattern was observed for all frequencies: Mixtures with 60% and 70% virgin binder content showed the highest stiffness for US-59-intermediate and US-36 mixtures, respectively.

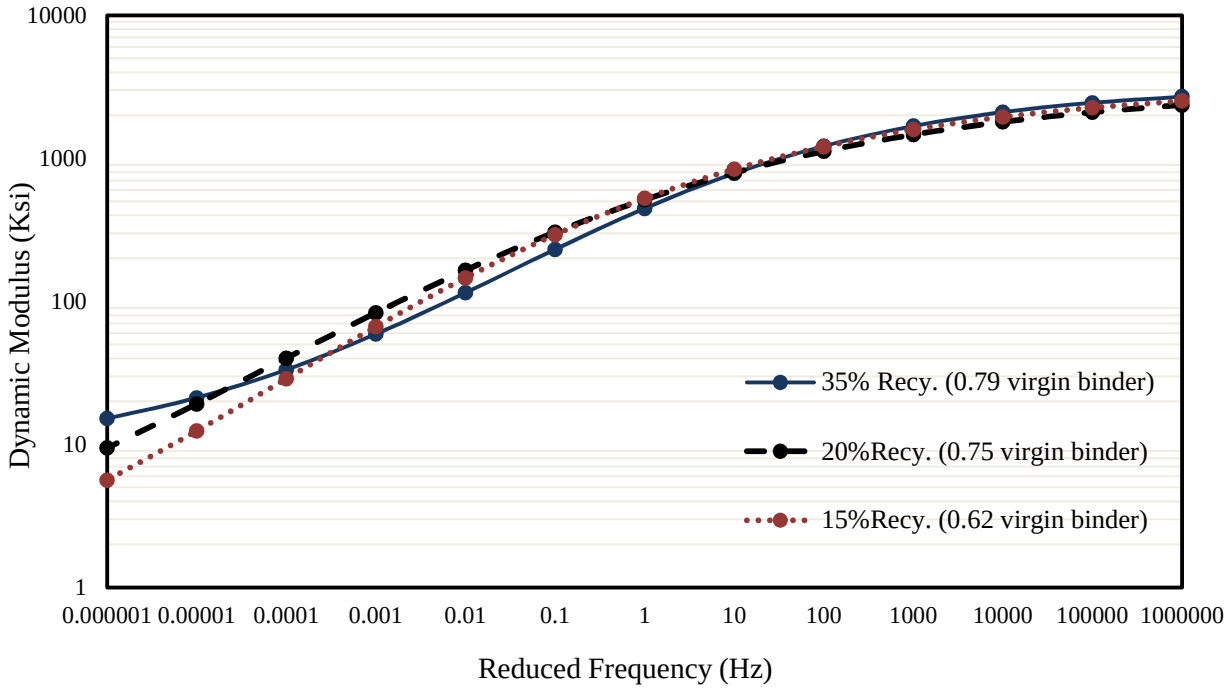

Figure 4.16 Dynamic modulus master curve at 18 ℃ for US-59-surface

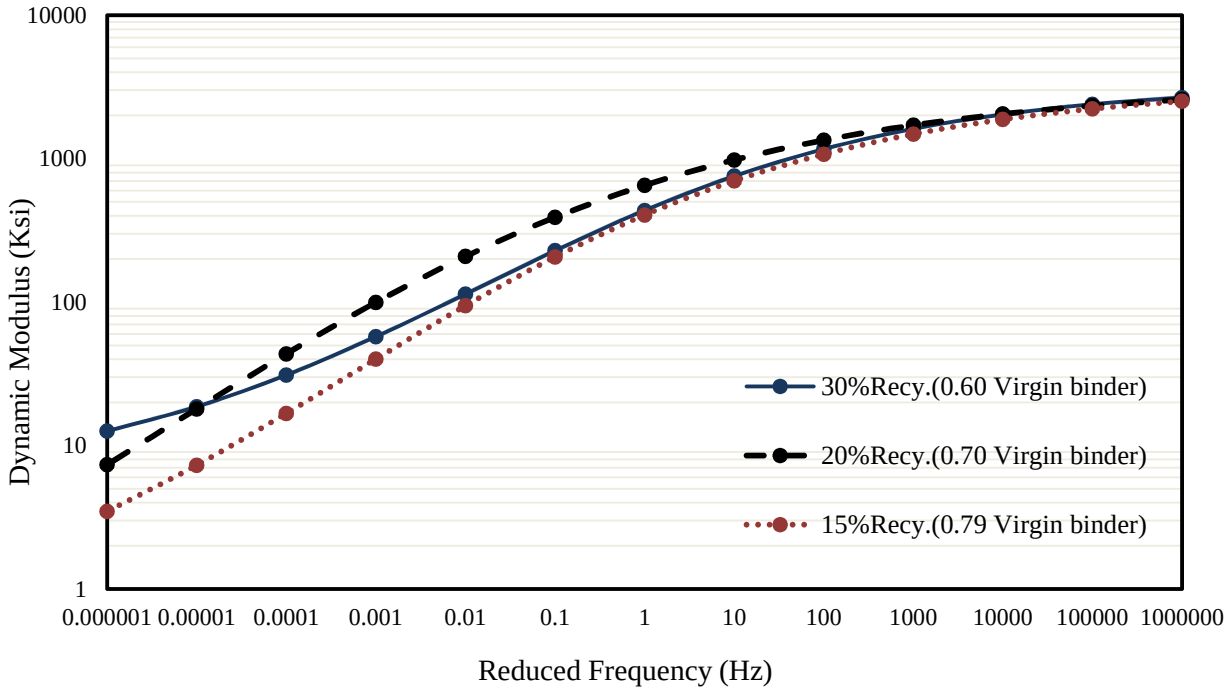

Figure 4.17 Dynamic modulus master curve at 18 ℃ for US-59-intermediate

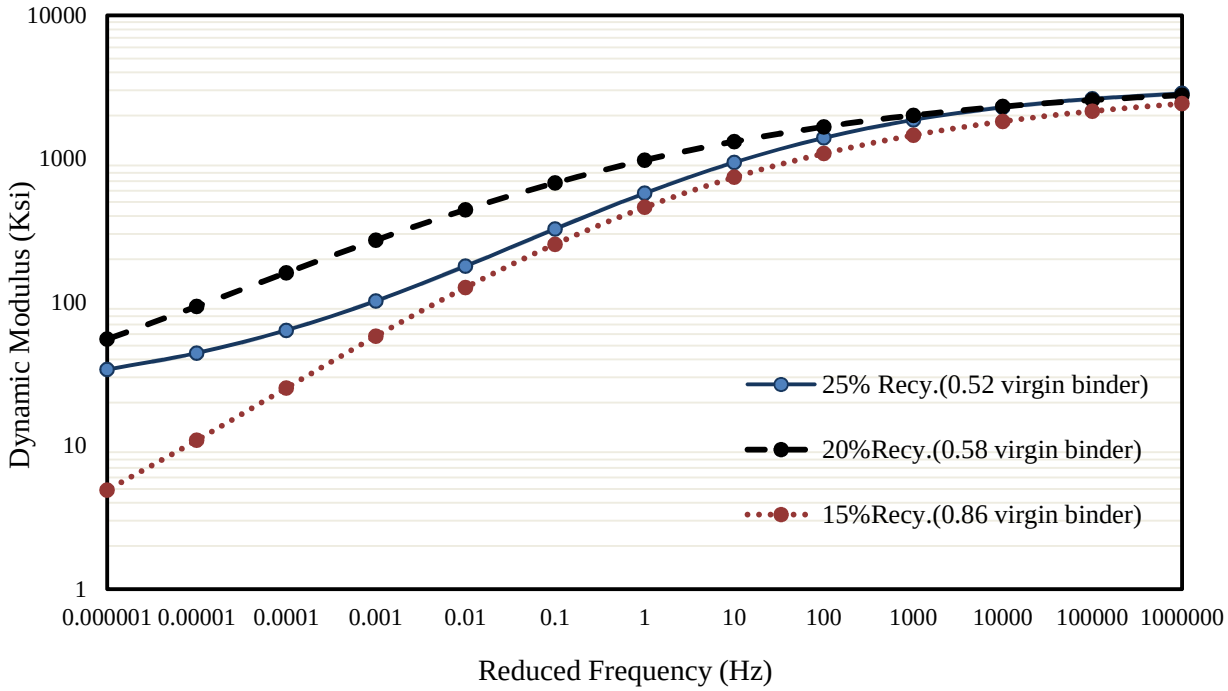

Figure 4.18 Dynamic modulus master curve at 18 ℃ for US-36

4.5 S-VECD Fatigue Cracking Test Results

The Simple VECD (S-VECD) fatigue test was performed to evaluate fatigue cracking potential of HMA mixtures according to AASHTO TP-107. Standard samples were prepared and subjected to the direct tension fatigue test at a test frequency of 10 Hz and test temperature of 18 °C. The AMPT machine performed the test and recorded the data. Test output was the number of fatigue cycles before failure, defined as formation of a clear microcrack or a sudden drop in the dynamic modulus-phase angle graph. Figure 4.19 shows typical output for the S-VECD fatigue cracking test.

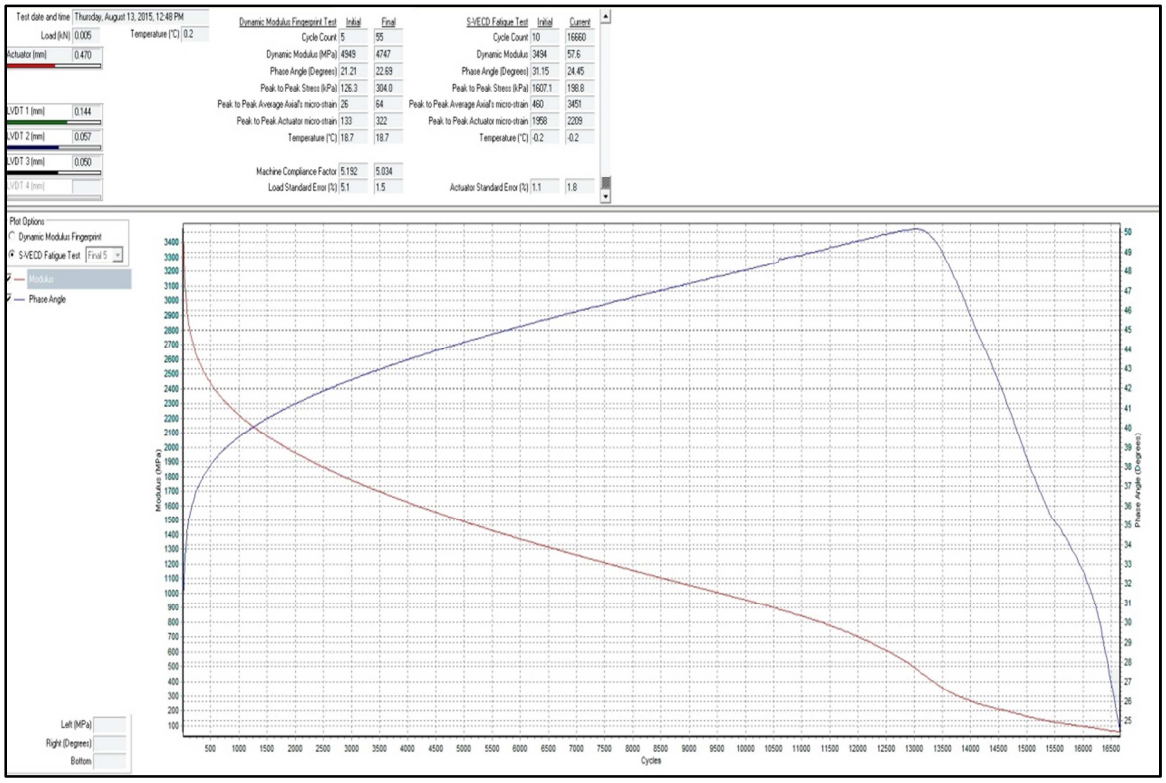

Figure 4.19 Typical data summary output for S-VECD fatigue cracking test

4.5.1 Damage Characteristic Curve

A damage characteristic curve was developed using test results from the S-VECD test in order to study mixture resistance toward fatigue cracking. Mixtures with various binder contents were then compared based on the damage curve. The following power model, as mentioned previously in Equation (3.9), was used to investigate damage parameter for various mixtures:

$$C = 1 - yS^z$$

where:

C = pseudo stiffness at failure,

S = damage internal state variable at failure, and

y,z = fitting coefficients for the power model.

S represents cumulative damage in the mixture prior to initial fatigue microcrack formation, and C is the pseudo secant modulus at failure. Alpha-Fatigue software was used to derive fatigue damage characteristics using results from three replicate tests (InstroTek, Inc., 2012). Fitting coefficients y and z and pseudo strains at failure estimated by the software are tabulated in Table 4.6. Curves were developed using fitting coefficients and pseudo stiffness values at failure for the range of 1 to the end value at failure (Xie et al., 2015). Figure 4.20 to Figure 4.22 illustrate damage characteristic curves for various mixtures.

Resistance to fatigue cracking was assessed from the damage curves. For a given normalized stiffness (C), a high damage parameter (S) value indicated increased damage resistance (Ahmed, 2015; AASHTO TP 107-14). According to damage curves in this study, both mixtures from US-59 showed an identical pattern of fatigue-cracking resistance. For higher virgin binder content, performance was almost identical, but for the lower virgin binder percentage, a decrease in mixture fatigue cracking resistance was predicted. For US-36 mixtures, optimum performance was anticipated for a virgin binder content of 58%, and the worst performance occurred for the mixture with the highest virgin binder percentage of 86%. For US-36, mixtures with RAS demonstrated better fatigue-cracking resistance, due in part to the fibers in the RAS that can improve fatigue performance properties (Williams et al., 2013).

Table 4.6 S-VECD calibration coefficients for damage characteristic curve

Mixture Design		% Virgin AC	y	z	Pseudo Strain at failure (με)
US-59-surface	15% Rec.	79	8.04E-05	7.92E-01	0.538
	20% Rec.	75	1.46E-04	7.34E-01	0.552
	35% Rec.	62	4.24E-03	4.45E-01	0.383
US-59-int.	15% Rec.	79	8.44E-05	8.15E-01	0.515
	20% Rec.	70	1.21E-04	7.74E-01	0.510
	30% Rec.	60	2.17E-03	5.17E-01	0.387
US-36-int.	15% Rec.	86	1.69E-02	3.43E-01	0.316
	20% Rec.	58	3.37E-05	8.50E-01	0.403
	25% Rec.	52	2.70E-03	4.81E-01	0.371

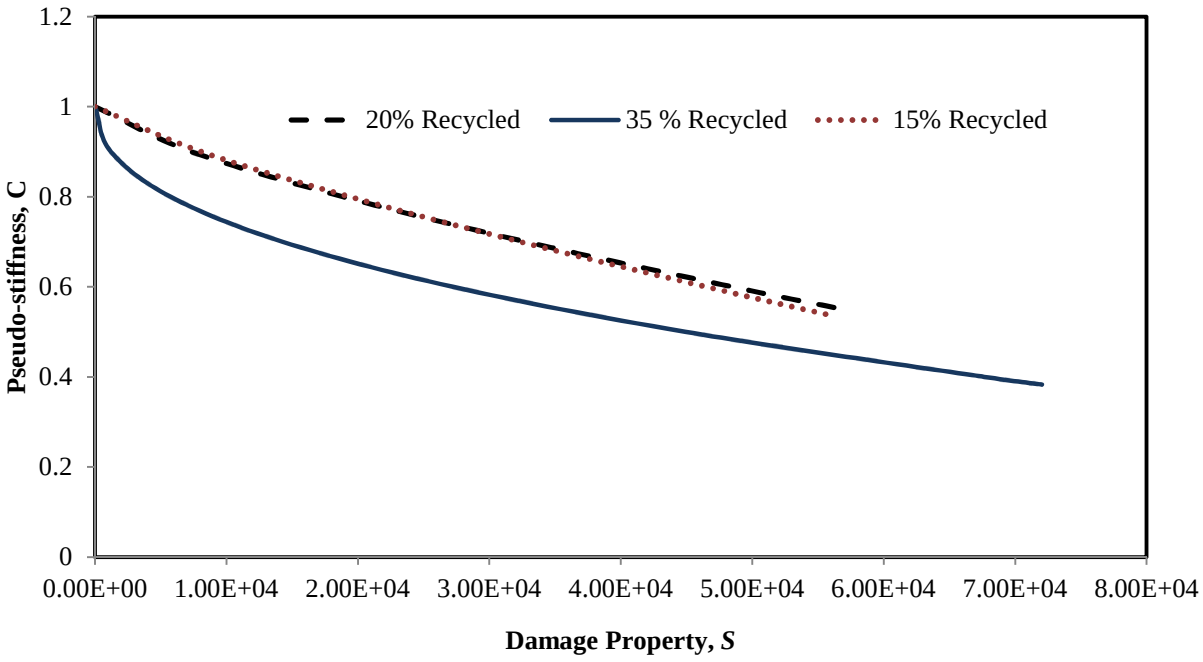

Figure 4.20 C versus S curves for US-59-surface

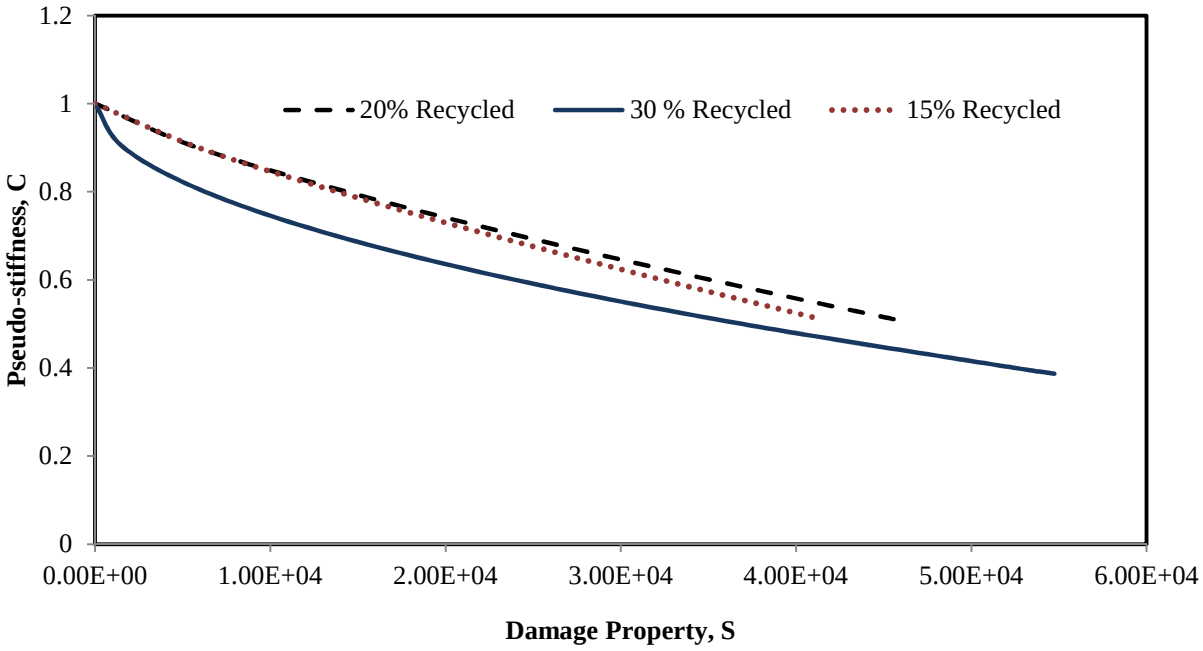

Figure 4.21 C versus S curves for US-59-intermediate

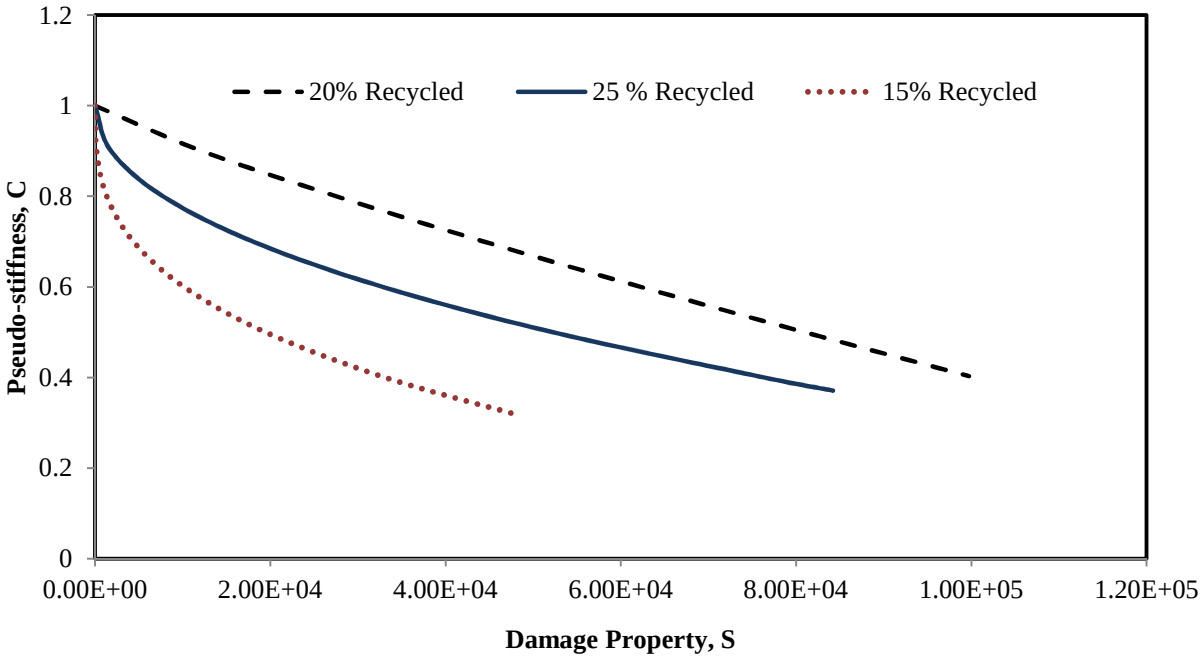

Figure 4.22 C versus S curves for US-36

4.6 Statistical Analysis

The analysis of variance (ANOVA) and Dunnett test were conducted on the moisture susceptibility test results. Also, statistical analysis was performed with the HWTD and FN test results to assess rutting behavior of the mixtures with respect to virgin binder content. Statistical Analysis Software (SAS) (SAS, 2011) was used to perform the analysis and develop the prediction models for rut depths.

4.6.1 Statistical Analysis of KT-56 Test Results

For moisture susceptibility test, there was only one value of TSR for each mixture, thereby preventing statistical estimation of mixture behavior as a function of the TSR values. However, ANOVA and Dunnett test were conducted on the tensile strength results of this test. Dunnett method is a procedure for comparing several treatments simultaneously with a control or standard treatment (Kuehl, 2000). In this study, for each project, mixture with 15% recycled materials was selected as the control mixture. Different virgin binder percentages were considered as the treatments and tensile strength values were taken as response variables. Tensile strength values of conditioned and unconditioned samples were evaluated separately. Table 4.7 and Table 4.8 summarize the results of ANOVA for the conditioned and unconditioned samples, respectively. Table 4.9 summarizes the results of the Dunnett test.

Results of the F test at 95% confidence level, as shown in ANOVA tables, indicate that all the treatments were effective.

Table 4.7 ANOVA table for tensile strength of conditioned samples

Mixture	Source of Variance	DF	Sum of Squares	Mean Square	$F_{Statistics}$	$F_{Critical}$
US-59-surface	Treatment	2	34430	17215	30.59	5.14
	Error	6	3377	563		
	Total	8	37807	-		
US-59-int.	Treatment	2	49291	24645	56.57	5.14
	Error	6	2614	436		
	Total	8	51905	-		
US-36-int.	Treatment	2	217817	108908	33.46	5.79
	Error	5	16273	3255		
	Total	7	234089	-		

Table 4.8 ANOVA table for tensile strength of unconditioned samples

Mixture	Source of Variance	DF	Sum of Squares	Mean Square	$F_{Statistics}$	$F_{Critical}$
US-59-surface	Treatment	2	38047	19023	29.18	5.14
	Error	6	3911	652		
	Total	8	41958	-		
US-59-int.	Treatment	2	64572	32286	14.75	5.14
	Error	6	13132	2189		
	Total	8	77704	-		
US-36-int.	Treatment	2	135888	67944	11.42	5.14
	Error	6	35701	5950		
	Total	8	171589	-		

Table 4.9 Dunnett test for tensile strength of samples

Mixture		Contrast	Difference in Mean $\lvert\mu i - \mu c\rvert$	d(0.05, 2, 6)	D(2, 0.05)	Simultaneous 95% Confidence Limits	
US-59-surface	Cond.	0.75 vs. 0.79	126	2.86	55	71	182
		0.62 vs. 0.79	-9	2.86	55	-65	46
	Uncond.	0.75 vs. 0.79	143	2.86	60	84	203
		0.62 vs. 0.79	11	2.86	60	-48	71
US-59-int	Cond.	0.70 vs. 0.79	103	2.86	49	54	152
		0.60 vs. 0.79	-78	2.86	49	-126	-29
	Uncond.	0.70 vs. 0.79	122	2.86	109	13	231
		0.60 vs. 0.79	-85	2.86	109	-194	25
US-36-int	Cond.	0.58 vs. 0.86	381	3.03	141	240	522
		0.52 vs. 0.86	175	3.03	141	34	317
	Uncond.	0.58 vs. 0.86	296	2.86	180	116	476
		0.52 vs. 0.86	195	2.86	180	15	375

Note:

* Numbers shown under the "Contrast" column represent the percentage of the virgin binder in each mixture. For example, 0.75 vs. 0.79 indicates that mixture with 75% virgin binder was compared to the control mixture with 79% virgin binder.

Based on the Dunnett test results, difference in the estimated mean for the US-59-surface course mixture with 75% virgin binder was shown to be bigger than the Dunnett criterion ($D_{(k,\alpha)}$). Therefore it was concluded that mixture with 75% virgin binder produced different tensile strengths when compared with that for the control mixture (mixture with 79% virgin binder content). Also, all values for the simultaneous 95% confidence intervals were positive numbers; showing that higher values of tensile strength were expected for the mixture with 75% virgin binder. For mixture with the lowest virgin binder content of 62%, difference in estimated mean was smaller than critical value ($D_{(k,\alpha)}$) in the Dunnett test. Thus there was no evidence of a treatment effect when compared to the control mixture. For US-59-int mixture, the same trend as for the US-59-surface was observed. Higher values of tensile strength as compared to the control

mixture were expected for the mixture with 70% virgin binder content. For mixture with the lowest (62%) virgin binder content, data set could not provide any evidence of the treatment (virgin binder content) effect.

For US-36 mixtures, $D_{(k,\alpha)}$ was smaller than the difference in estimated means for all comparisons. Thereby, it was concluded that treatment (virgin binder content) was effective. Based on the simultaneous 95% confidence intervals, higher tensile strengths were expected for the mixtures with 58% and 52% virgin binder content as compared to the control mixture with 86% virgin binder.

4.6.2 Statistical Analysis of HWTD Test Results

In this study, virgin binder percentages and aggregate blends were considered to be treatments and measured rut depths were the response variables. Data was used to develop a regression model to estimate rutting in the HWTD test as a function of the mixture's virgin binder content. US-59-surface, US-59-intermediate, and US-36 mixtures were considered to be source 1, 2, and 3 of aggregates, respectively.

A model was selected to evaluate how virgin binder content influences rut depth. Due to the quadratic form of the data and a Box-Cox procedure that recommends a log transformation on the response, the following model was proposed to estimate rut depth of mixtures as a function of the percent virgin binder:

$$\ln(y) = \beta_0 + \beta_1\tau_1 + \beta_2\tau_2 + \beta_3 x + \beta_4\tau_1 x + \beta_5\tau_1 x + \beta_7\tau_1 x^2 + \beta_8\tau_2 x^2 + \epsilon \quad (4.1)$$

where:

y = average rut depth,

x = percentage of virgin binder,

$\tau_1 = 1$ if aggregate is from source 1, otherwise 0, and

$\tau_2 = 1$ if aggregate is from source 2, otherwise 0.

The data set was examined to determine if variables in the proposed model significantly affected rutting depth (with a 0.95 level of confidence). Based on Chi-Square values shown in Table 4.10, all parameters and interactions had significant effects on measured rut depth.

Table 4.10 LR statistics for type 3 analysis of HWTD

Source	DF	Chi-Square	Pr > ChiSq
Agg	2	10.76	0.0046
Percent	1	6.33	0.0119
Percent*Agg	2	10.60	0.0050
Percent*Percent	1	6.12	0.0134
Percent*Percent*Agg	2	10.62	0.0049

Estimates for β_i values from the SAS output are shown in Table 4.11. The fitted model is illustrated in Figure 4.23.

Table 4.11 Analysis of maximum likelihood parameter estimates for HWTD

Parameter		DF	Estimate	Standard Error	Wald 95% Confidence Limits		Wald Chi-Square	Pr > ChiSq
Intercept		1	27.3069	15.2381	-2.5592	57.1731	3.21	0.0731
Agg.	1	1	9.1825	17.7425	-25.5921	43.9571	0.27	0.6048
Agg.	2	1	-36.0962	17.5475	-70.4886	-1.7038	4.23	0.0397
Agg.	3	0	0.0000	0.0000	0.0000	0.0000	.	.
Percent		1	-0.8020	0.4654	-1.7141	0.1102	2.97	0.0849
Percent*Agg.	1	1	-0.1495	0.5344	-1.1968	0.8978	0.08	0.7797
Percent*Agg.	2	1	1.1360	0.5302	0.0969	2.1751	4.59	0.0321
Percent*Agg.	3	0	0.0000	0.0000	0.0000	0.0000	.	.
Percent*Percent		1	0.0059	0.0034	-0.0007	0.0125	3.09	0.0789
Percent*Percent*Agg.	1	1	0.0007	0.0038	-0.0068	0.0083	0.04	0.8468
Percent*Percent*Agg.	2	1	-0.0084	0.0038	-0.0159	-0.0009	4.87	0.0273
Percent*Percent*Agg.	3	0	0.0000	0.0000	0.0000	0.0000	.	.
Scale		1	1.6695	0.2361	1.2653	2.2027		

Note:

* Agg. 1, 2, and 3 refer to US-59-surface, US-59-intermediate, and US-36.
* Percent stands for the percent of virgin binder.

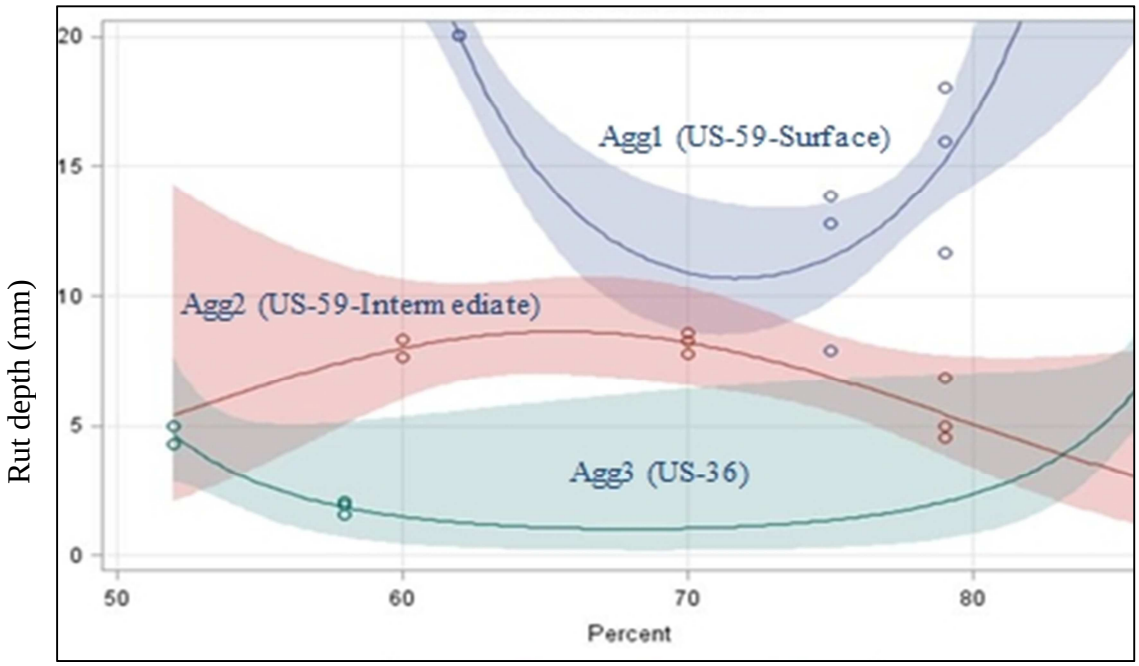

Figure 4.23 Fit for rut depth with 95% confidence limits

The model in Figure 4.23 indicates that minimum rut depth was expected for the 70%–75% virgin binder for the US-59-surface course. For US-36, 60%–75% virgin binder provided optimum rutting performance. Results for the US-59-intermediate mixture showed that maximum rut depth was predicted for 60%–70% of virgin binder. This mixture was expected to perform better with increased virgin binder content.

4.6.3 Statistical Analysis of Flow Number Test Results

The following model was used to estimate FN as a function of virgin binder content in the recycled mixture:

$$\ln(y) = \beta_0 + \beta_1\tau_1 + \beta_2\tau_2 + \beta_3 x \quad (4.2)$$

where:

y = average flow number,

x = percentage of virgin binder,

$\tau_1 = 1$ if aggregate is from source 1, otherwise 0, and

$\tau_2 = 1$ if aggregate is from source 2, otherwise 0.

This model was chosen after fitting a full model and using backwards stepwise model parameter selection in which parameters that were not significant were removed. A Box-Cox procedure recommended a log transformation on the responses. The fitted model and estimates for β_i from SAS output are shown in Figure 4.24 and Table 4.12, respectively.

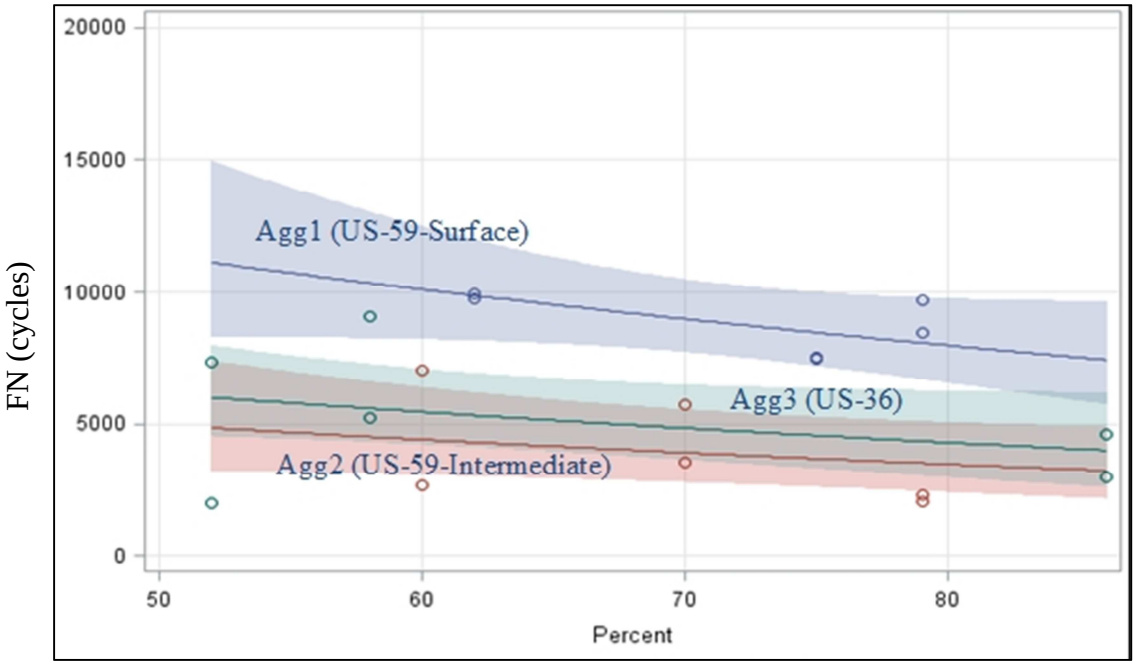

Figure 4.24 Fit for FN with 95% confidence limits

Table 4.12 Analysis of maximum likelihood parameter estimates for FN

Parameter		DF	Estimate	Standard Error	Wald 95% Confidence Limits		Wald Chi-Square	Pr > ChiSq
Intercept		1	9.3164	0.4407	8.4527	10.1802	446.93	<.0001
Agg	1	1	0.6179	0.1691	0.2864	0.9494	13.35	0.0003
Agg	2	1	-0.2118	0.2287	-0.6601	0.2365	0.86	0.3545
Agg	3	0	0.0000	0.0000	0.0000	0.0000	.	.
Percent		1	-0.0119	0.0069	-0.0255	0.0017	2.93	0.0872
Scale		1	1706.093	284.3488	1230.653	2365.209		

Final results, as shown in type 3 analysis in Table 4.13, showed that, although the mixture type had significant effect, the percentage of virgin binder appears to have no effect on flow point (at a 5% level of significance). However, the p-value was marginally not significant, suggesting that a larger sample size and/or more values for percentage of virgin binder may detect a significant effect.

Table 4.13 LR statistics for type 3 analysis for FN

Source	DF	Chi-Square	Pr > ChiSq
Agg	2	17.25	0.0002
Percent	1	2.89	0.0890

The purpose of statistical analysis in this study was to estimate mixture performance with respect to percentage of virgin binder. For the S-VECD fatigue cracking test, standard test results were damage characteristics curves, so they were not statistically evaluated.

Chapter 5 - Conclusions and Recommendations

5.1 Conclusions

The objective of this research was to investigate the effect of recycled binder from RAP and RAS incorporated into the Superpave HMA mixtures in order to identify minimum virgin binder content that would result in satisfactory mixture performance. Three KDOT mixture designs with 9.5 mm and 19 mm NMAS were selected as control mixtures. Mixtures with higher percentages of recycled materials were designed in the laboratory. A total of nine mixture designs with varying virgin binder contents were developed and evaluated for moisture susceptibility, rutting resistance, and fatigue cracking resistance. Based on test results, the following conclusions were drawn:

- Modified Lottman test results indicated that all mixtures, irrespective of virgin binder content, could achieve TSR values greater than 80% as required by KDOT.
- Moisture resistance for US-59 mixtures slightly decreased as virgin binder content decreased. For US-36 mixtures, moisture resistance improved when RAS was incorporated into the mixture; for virgin binder content below 60%, moisture susceptibility increased again.
- According to HWTD test results, all mixtures could pass the KDOT requirement of 12.5 mm rut depth at 10,000 wheel passes.
- Rutting performance of the mixtures was highly dependent on NMAS. SR-19A mixtures showed better rutting performance than SR-9.5A mixtures. A regression model developed from HWTD test results indicated that rutting performance is dependent on mixture type. For US-59 mixtures, optimal performance was found for virgin binder content above 70%; for SR-9.5A, higher values of virgin binder

content were required. For US-36, virgin binder contents above 60% were predicted to show optimum rutting performance.

- HWTD output parameters for stripping slope and stripping inflection point indicated low moisture resistance of SR-9.5A compared to SR-19A mixtures.
- FN results showed better shear flow resistance for SR-9.5A mixtures compared to SR-19A mixtures. However, for US-59 mixtures, no agreement was found between HWTD and FN test results.
- Based on statistical analysis, the FN test failed to predict any significant dependency of FN on virgin binder content.
- Dynamic modulus test results indicated stiffer mixture behavior at lower test temperatures and higher test frequencies. Based on master curves developed at 18 °C, SR-19A mixtures and SR-9.5A behaved differently. For SR-9.5A mixtures, stiffness was dependent on test frequency, but for SR-19A, a distinct pattern was observed for all frequencies. Mixtures with 70% and 60% virgin binder content showed highest stiffness for US-59-intermediate and US-36 mixtures, respectively.
- Fatigue cracking test results showed a significant relationship between predicted fatigue damage characteristics and aggregate source. For US-59, mixtures with 70%–79% virgin binder content performed approximately the same. Incorporation of higher recycled binder resulted in decreased fatigue performance. Based on S-VECD test results, virgin binder contents below 70% for SR-19A and 75% for SR-9.5A resulted in an increased propensity for fatigue cracking. For US-36, mixtures with RAP and RAS showed improved fatigue resistance compared to the

RAP-only mixture, even though those mixtures had lower virgin binder content. Virgin binder content of 60% showed optimal performance among all US-36 mixtures.

5.2 Recommendations

Based on results of this study, the following recommendations are made:

- Virgin binder requirement should be defined based on mixture type since varying performance was observed for SR-9.5A and SR-19A mixtures in this study.
- For SR-9.5A, virgin binder content higher than 75% showed satisfactory performances with respect to moisture damage, rutting potential, and fatigue cracking propensity.
- For SR-19A, virgin binder content close to 70% showed good performance, and this was shown to be optimum binder content. In addition, mixtures with virgin binder contents below 60% did not show good performance and are not recommended.
- Conclusions in this study were based on a limited number of virgin binder content observations ranging from 52% to 86%. Additional mixtures with varying virgin binder content are recommended for further study.
- Further assessment of RAS mixture performance is recommended since better performance of RAP and RAS mixtures compared to RAP-only mixtures was observed.

References

AASHTO, M 323-13 (2013). Standard specification for Superpave volumetric mix design. AASHTO Provisional Procedure, Washington, D.C.

AASHTO, MP 15-09 (2012). Standard specification for use of reclaimed asphalt shingles as an additive in Hot-Mix Asphalt (HMA). American Association of State and Highway Transportation Officials, Washington, DC.

AASHTO MP 23-15 (2015). Standard specification for reclaimed asphalt shingles for use in asphalt mixtures. American Association of State and Highway Transportation Officials, Washington, DC.

AASHTO PP 61-13 (2013). Standard practice for developing dynamic modulus master curves for hot mix asphalt (HMA) using the Asphalt Mixture Performance Tester (AMPT). AASHTO Proposed Protocol, Washington, D.C.

AASHTO PP 78-14 (2014). Standard practice for design considerations when using reclaimed asphalt shingles (RAS) in asphalt mixtures. American Association of State and Highway Transportation Officials, Washington, DC.

AASHTO T 283 (2007). Resistance of compacted asphalt mixtures to moisture-induced damage. AASHTO Standard Specification, Washington, D.C.

AASHTO TP 62-07 (2013). Standard method of test for determining dynamic modulus of hot-mix asphalt concrete mixtures. AASHTO Test Protocol, Washington, D.C.

AASHTO TP 79-13 (2013). Standard method of test for determining the Dynamic modulus and flow number for hot mix asphalt (HMA) using the asphalt mixture performance tester (AMPT). American Association of State and Highway Transportation Officials, Washington, DC.

AASHTO TP 107-14 (2014). Standard method of test for determining the damage characteristics curve of asphalt mixtures from direct tension cyclic fatigue test. AASHTO Test Protocol, Washington, D.C.

Ahmed, A. (2015). Evaluation of cracking potential of Superpave mixtures with high reclaimed asphalt pavement content (Master Thesis, Kansas State University).

Al-Qadi, I. L., Aurangzeb, Q., Carpenter, S. H., Pine, W. J., and Trepanier, J. (2012). Impact of high RAP contents on structural and performance properties of asphalt mixtures. FHWA-ICT-12-002.

Al-Qadi, I. L., Elseifi, M., and Carpenter, S. H. (2007). Reclaimed asphalt pavement-a literature review. Illinois Center for Transportation (FHWA-ICT-07-001).

Anderson, D. A., Dukatz, E. L., and Petersen, J. C. (1982). The effect of antistrip additives on the properties of asphalt cement. In Association of Asphalt Paving Technologists Proceedings (Vol. 51).

Aschenbrener, T. (1994). Influence of refining processes and crude oil sources used in Colorado on results from the Hamburg Wheel-Tracking Device. Colorado Department of Transportation (No. CDOT-DTD-R-94-7).

Bonaquist, R. (2012). Evaluation of Flow Number (Fn) as a discriminating HMA mixture property. Wisconsin Highway Research Program (No. WHRP 12-01).

Brown, E. R., Kandhal, P. S., Roberts, F. L., Kim R., Lee, D. Y., and Kennedy, T. W. (2009). Hot mix asphalt materials, mixture design and construction. Third Edition, NAPA Research and Education Foundation.

Button, J. W., Williams, D., and Scherocman, J. (1996). Roofing shingles and toner in asphalt mixtures. Research Report 1344-2F, Texas Transportation Institute, Texas A&M University, College Station, Texas.

Cascione, A. A., Williams, R. C., Buttlar, W. G., Ahmed, S., Hill, B., Haugen, D. S., and Gillen, S. (2011). Laboratory evaluation of field produced hot mix asphalt containing post-consumer recycled asphalt shingles and fractionated recycled asphalt pavement. Journal of the Association of Asphalt Paving Technologists, 80.

Cascione, A., Williams, R. C., Gillen, S., and Haugen, D. (2010). Utilization of post-consumer recycled asphalt shingles and fractionated recycled asphalt pavement in hot mix asphalt. In Proceedings of the 2010 Mid-Continent Transportation Research Forum.

Collins, R., Shami, H., and Lai, J. (1996). Use of Georgia loaded wheel tester to evaluate rutting of asphalt samples prepared by Superpave gyratory compactor. Transportation Research Record: Journal of the Transportation Research Board, (1545), 161-168.

Cominsky, R. J., Huber, G. A., Kennedy, T. W., and Anderson, M. (1994). The Superpave mix design manual for new construction and overlays. Washington, DC: Strategic Highway Research Program (No. SHRP-A-407).

Cooley A. L., Kandhal, P. S., Buchanan, M. S., Fee, F., and Epps, A. (2000). Loaded wheel testers in the United States: State of the practice. Transportation Research Board, National Research Council.

Copeland, A. (2011). Reclaimed asphalt pavement in asphalt mixtures: state of the practice. Federal Highway Administration (No. FHWA-HRT-11-021).

Daniel, J., and Lachance, A. (2005). Mechanistic and volumetric properties of asphalt mixtures with recycled asphalt pavement. Transportation Research Record: Journal of the Transportation Research Board, (1929), 28-36.

Doyle, J. D., Mejias-Santiago, M., Brown, E., and Howard, I. L. (2011). Performance of high RAP-WMA surface mixtures. Journal of the Association of Asphalt Paving Technologists, Vol. 80, pp 419-458.

Eisenmann, J., and Hilmer, A. (1987). Influence of wheel load and inflation pressure on the rutting effect at asphalt-pavements: experiments and theoretical investigations. Ann Arbor, Mich 6th International Conference on the Structural Design of Asphalt Pavements, Vol. I proceedings.

Elseifi, M. A., Mohammad, L. N., and Cooper III, S. B. (2011). Laboratory evaluation of asphalt mixtures containing sustainable technologies. Journal of the Association of Asphalt Paving Technologists, Vol. 80, pp 227-254.

Federal Highway Administration (FHWA). (2015). Aspahlt pavement recycling with reclaimed asphalt pavement (RAP). Retrieved from http://www.fhwa.dot.gov/paveemnt/recycling/index.cfm

Federal Highway Administration (FHWA). (2012). Performance testing for Superpave and structural validation. Chapter 6 (No. FHWA-HRT-11-045).

Foxlow, J. J., Sias Daniel, J., and Krishna Swamy, A. (2011). RAP or RAS? The differences in performance of HMA containing reclaimed asphalt pavement and reclaimed asphalt shingles. Asphalt Paving Technology-Proceedings Association of Asphalt Technologists, 80, 347.

Glover, C. J., Martin, A. E., Chowdhury, A., Han, R., Prapaitrakul, N., Jin, X., and Lawrence, J. (2009). Evaluation of binder aging and its influence in aging of hot mix asphalt concrete: literature review and experimental design (No. FHWA/TX-08/0-6009-1).

Hansen, K. R., and Newcomb, D. E. (2011). Asphalt pavement mix production survey on reclaimed asphalt pavement, reclaimed asphalt shingles, and warm-mix asphalt usage: 2009-2010. Information Series, 138, 21.

Hofstra, A., and Klomp, A. J. G. (1972) Permanent deformation of flexible pavements under simulated traffic conditions. Proceedings for the Third International Conference on the Structural Design of Asphalt Pavements, Vol. I, London, pp. 613-621.

Huang, B., Shu, X., Dong, Q., and Shen, J. (2010). Laboratory evaluation of moisture susceptibility of hot-mix asphalt containing cementitious fillers. Journal of Materials in Civil Engineering, 22(7), pp. 667-673.

Huber, G. (2013). History of asphalt mix design in north america, Part 1 and II, Asphalt Institute Journal: Asphalt, Vol. 28, pp. 15-20 and pp. 25-29.

InstroTek, Inc. (2012). Asphalt pavement hieratical analysis toolbox-fatigue program. InstroTek, Inc. Raleigh, NC.

Izzo, R., and Tahmoressi, M. (1999). Use of the Hamburg wheel-tracking device for evaluating moisture susceptibility of hot-mix asphalt. Transportation Research Record: Journal of the Transportation Research Board, (1681), pp. 76-85.

Johnson, E., Johnson, G., Dai, S., Linell, D., McGraw, J., and Watson, M. (2010). Incorporation of recycled asphalt shingles in hot mixed asphalt pavement mixtures. Minnesota Department of Transportation, St. Paul, MN, pp. 58-28.

Kandhal, P., and Cooley Jr, L. (2002). Coarse-versus fine-graded Superpave mixtures: Comparative evaluation of resistance to rutting. Transportation research record: journal of the transportation research board, (1789), 216-224.

Kandhal, P. S. (1994). Field and laboratory investigation of stripping in asphalt pavements: State of the art report. Transportation Research Record, (1454).

Kansas Standard Test Method KT-1 (2004). Sampling and splitting of aggregates. Kansas Department of Transportation, Topeka, Kansas.

Kansas Standard Test Method KT-2 (2004). Sieve analysis of aggregates. Kansas Department of Transportation, Topeka, Kansas.

Kansas Standard Test Method KT-6 (2004). Specific gravity and absorption of aggregates. Kansas Department of Transportation, Topeka, Kansas.

Kansas Standard Test Method KT-15 (2004). Bulk specific gravity and unit weight of compacted hot mix asphalt. Kansas Department of Transportation, Topeka, Kansas.

Kansas Standard Test Method KT-34 (2004). Sieve analysis of extracted aggregate. Kansas Department of Transportation. Topeka, Kansas.

Kansas Standard Test Method KT-39 (2004). Theoretical maximum specific gravity of asphalt paving mixtures. Kansas Department of Transportation. Topeka, Kansas.

Kansas Standard Test Method KT-56 (2004). Resistance of compacted asphalt mixtures to moisture induced damage. Kansas Department of Transportation, Topeka, Kansas.

Karlsson, R., and Isacsson, U. (2006). Material-related aspects of asphalt recycling-state-of-the-art. Journal of Materials in Civil Engineering, 18(1), pp. 81–92.

Kiggundu, B. M., Roberts. F. (1988). Stripping in HMA mixtures: State-of-the-art and critical review of test methods. Auburn, AL: National Center for Asphalt Technology (No. NCAT Report No. 88-2).

Kim, Y. R., Little, D. N., and Lytton, R. L. (2003). Fatigue and healing characterization of asphalt mixtures. Journal of Materials in Civil Engineering, 15(1), pp. 75-83.

Kim, Y. R., Lee, H. J., and Little, D. N. (1997). Fatigue characterization of asphalt concrete using viscoelasticity and continuum damage theory (with discussion). Journal of the Association of Asphalt Paving Technologists, Vol. 66, pp. 520-569.

Kim, Y. R., Little, D. N., and Benson, F. C. (1990). Chemical and mechanical evaluation on healing mechanism of asphalt concrete (with discussion). Journal of the Association of Asphalt Paving Technologists, Vol. 59, pp. 240-275.

Kuehl, R.O., (2000). Design of experiments: statistical principles of research design and analysis. Pacific Grove, CA: Duxbury/Thomson Learning.

Lancaster, I. M., and Khalid, H. A. (2015). Viscoelastic continuum damage analysis of polymer modified asphalt in the cyclic semi-circular bending test. Bituminous Mixtures and Pavements, Vol. I, pp. 21-26.

Li, J., Oh, J., Naik, B., Simate, G. S., and Walubita, L. F. (2014). Laboratory characterization of cracking-resistance potential of asphalt mixes using overlay tester. Construction and Building Materials, Vol. 70, pp. 130-140.

Li, X., Marasteanu, M., Williams, R., and Clyne, T. (2008). Effect of reclaimed asphalt pavement (proportion and type) and binder grade on asphalt mixtures. Transportation Research Record: Journal of the Transportation Research Board, (2051), pp. 90-97.

Li, X., Clyne, T. R., and Marasteanu, M. O. (2004). Recycled asphalt pavement (RAP) effects on binder and mixture quality.

Little, D. N., Bhasin, A., Darabi, M. K., (2015). Damage healing in asphalt pavements: theory, mechanism, measurement, and modeling. Advances in Asphalt Materials: Road and Pavement Construction,Woodhead Publishing, PP. 205-344.

Little, D. N., and Petersen, J. C. (2005). Unique effects of hydrated lime filler on the performance-related properties of asphalt cements: physical and chemical interactions revisited. Journal of Materials in Civil Engineering, 17(2), pp. 207-218.

Little, D. N., Epps, J. A., and Sebaaly, P. E. (2001). The benefits of hydrated lime in hot mix asphalt. National Lime Association.

LL Pelling Co. (2015). Asphalt shingle recycling. Retrieved from http://www.llpelling.com/divisions/ras/

Mamlouk, M. S., and Zaniewski, J. P. (2006). Materials for civil and construction engineers. ,3rd edition, Pearson Prentice Hall (SBN-13: 978-0136110583).

McDaniel, R. S., Soleymani, H., Anderson, R. M., Turner, P., and Peterson, R. (2000). Recommended use of reclaimed asphalt pavement in the Superpave mix design method. NCHRP Web document, 30.

Miró, R., Valdés, G., Martínez, A., Segura, P., and Rodríguez, C. (2011). Evaluation of high modulus mixture behaviour with high reclaimed asphalt pavement (RAP) percentages for sustainable road construction. Construction and Building Materials, 25(10), pp. 3854-3862.

Mogawer, W., Austerman, A., Bonaquist, R., and Roussel, M. (2011). Performance characteristics of thin-lift overlay mixtures: high reclaimed asphalt pavement content, recycled asphalt shingles, and warm-mix asphalt technology. Transportation Research Record: Journal of the Transportation Research Board, (2208), pp. 17-25.

Moghaddam, T. B., Karim, M. R., and Abdelaziz, M. (2011). A review on fatigue and rutting performance of asphalt mixes. Scientific Research and Essays, 6(4), pp. 670-682.

National Asphalt Pavement Association (NAPA). (2015). Engineering overview. Retrieved from http://www.asphaltpavement.org

National Center for Asphalt Technology (NCAT). (2014). Demystifying the dynamic modulus master curve. Asphalt technology E-News, Volume 26.

Newcomb, D., Stroup-Gardiner, M., Weikle, B., and Drescher, A. (1993). Influence of roofing shingles on asphalt concrete mixture properties. Final report (No. MN/RC-93/09).

Ozer, H., Al-Qadi, I., Kanaan, A., and Lippert, D. (2013). Performance characterization of asphalt mixtures at high asphalt binder replacement with recycled asphalt shingles. Transportation Research Record: Journal of the Transportation Research Board, (2371), pp. 105-112.

Ozer, H., Al-Qadi, I. L., and Kanaan, A. (2012). Laboratory evaluation of high asphalt binder replacement with recycled asphalt shingles (RAS) for a low N-design asphalt mixture. (FHWA-ICT-12-018).

Palvadi, S., Bhasin, A., Motamed, A., and Little, D. N. (2012). Quantifying healing based on viscoelastic continuum damage theory in fine aggregate asphalt specimen. In 7th RILEM International Conference on Cracking in Pavements, pp. 1115-1123, Springer Netherlands.

Putman, B. J., and Amirkhanian, S. N. (2006). Laboratory evaluation of anti-strip additives in hot mix asphalt. Final Report, SCDOT and Clemson University (No. FHWA-SC-06-07).

Rahman, F. (2010). Performance evaluation of 4.75-mm NMAS Superpave mixture. (Doctoral dissertation, Kansas State University).

Roberts, F. L., Kandhal, P. S., Brown, E. R., Lee, D. Y., and Kennedy, T. W. (1996). Hot mix asphalt materials, mixture design and construction. National Asphalt Pavement Association Research and Education Foundation.

Sabahfer, N., and Hossain, M. (2015). Effect of Fractionation of Reclaimed Asphalt Pavement on Properties of Superpave Mixtures with Reclaimed Asphalt Pavement. In Advances in Civil Engineering Materials (Vol. 4, No. 1, pp. 47-60). ASTM International.

Sabhafer, N., & Hossain, M. (2014). Volumetric properties of Superpave mixtures with reclaimed asphalt pavement. In T&DI Congress 2014@ sPlanes, Trains, and Automobiles (pp. 14-23). ASCE.

Sabahfar, N., Aziz, S. R., Hossain, M., & Schieber, G. (2014). Evaluation of Superpave mixtures with high percentages of reclaimed asphalt pavement. In Transportation Research Board 93rd Annual Meeting (No. 14-3146).

Sabahfar, N. (2012). Use of high-volume reclaimed asphalt pavement (RAP) for asphalt pavement rehabilitation (Master Thesis, Kansas State University).

Samoo, F. A. (2011). Initial performance assessment for implementation of hot mix asphalt containing recycled asphalt shingles in Oregon. (Master Thesis, Oregon State University).

SAS (2011). SAS user guide for Windows, Release 9.3. SAS Institute, Inc. Cary, NC. 2011.

Schapery, R. A. (1975). A theory of crack initiation and growth in viscoelastic media. International Journal of Fracture, 11(1), 141-159.

Scholz, T. V. (2010). Preliminary investigation of RAP and RAS in HMAC. Oregon Department of Transportation (No. OR-RD-10-12).

Shami, H., Lai, J., D'Angelo, J., and Harman, T. (1997). Development of temperature-effect model for predicting rutting of asphalt mixtures using Georgia loaded wheel tester. Transportation Research Record: Journal of the Transportation Research Board, (1590), 17-22.

Shu, X., Huang, B., Shrum, E. D., and Jia, X. (2012). Laboratory evaluation of moisture susceptibility of foamed warm mix asphalt containing high percentages of RAP. Construction and Building Materials, Vol. 35, pp. 125-130.

Shu, X., Huang, B., and Vukosavljevic, D. (2008). Laboratory evaluation of fatigue characteristics of recycled asphalt mixture. Construction and Building Materials, 22(7), pp. 1323-1330.

Sondag, M. S., Chadbourn, B. A., and Drescher, A. (2002). Investigation of recycled asphalt pavement (RAP) mixtures. Minnesota Department of Transportation (MN/RC-2002-15).

Sousa, J. B., Craus, J., and Monismith, C. L. (1991). Summary report on permanent deformation in asphalt concrete (No. SHRP-A-318).

Stuart, K.D. and W.S. Mogawer, (1997). Effect of compaction method on rutting susceptibility measured by wheel-tracking devices, Presented at the 76th Annual Meeting of the Transportation Research Board, Washington, D.C.

Stuart, K. D., and Izzo, R. P. (1995). Correlation of Superpave G*/sin δ with rutting susceptibility from laboratory mixture tests. Transportation Research Record, (1492), pp. 176-183.

Tayfur, S., Ozen, H., and Aksoy, A. (2007). Investigation of rutting performance of asphalt mixtures containing polymer modifiers. Construction and Building Materials, 21(2), pp. 328-337.

TRB Superpave committee. (2005). Superpave performance by design final report of the TRB Superpave committee. Transportation Research Board (ISBN 0-309-09414-3)

Uppu, K. K. (2012). Durable superpave hot-mix asphalt mixes in Kansas (Master Thesis, Kansas State University).

Valdés, G., Pérez-Jiménez, F., Miró, R., Martínez, A., and Botella, R. (2011). Experimental study of recycled asphalt mixtures with high percentages of reclaimed asphalt pavement (RAP). Construction and Building Materials, 25(3), pp. 1289-1297.

Visintine, B. (2011). An Investigation of various percentages of reclaimed asphalt pavement on the performance of asphalt pavements. (Doctoral Dissertations, NC State University).

Wen, H., Wu, S., Zhang, K., Tumwater, W. A., Waste, K. C. S., and Renton, W. A. (2015). Performance evaluation of hot mix asphalt containing recycled asphalt shingles in Washington State, Journal of Materials in Civil Engineering, ASCE (ISSN 0899-1561/04015088(10)).

Wen, H., Wu, S., Zhang, K., Tumwater, W. A., Waste, K. C. S., and Renton, W. A. (2014) Performance evaluation of hot mix asphalt containing recycled asphalt shingles in Washington State. Washington Department of Transportation.

West, R. C. (1999). A ruggedness study of the asphalt pavement analyzer rutting test. Memorandum to the Asphalt Pavement Analyzer Group and New APA Owners.

Williams, R. C., Cascione, A. A., Yu, J., Haugen, D., Marasteanu, M., and McGraw, J. (2013). Performance of recycled asphalt shingles in hot mix asphalt. In Trans Project Reports. Paper 19, TPF-5(213).

Williams, R. C., Cascione, A., Haugen, D. S., Buttlar, W. G., Bentsen, R. A., and Behnke, J. (2011). Characterization of hot mix asphalt containing post-consumer recycled asphalt shingles and fractionated reclaimed asphalt pavement. Final report for the Illinois State Toll Highway Authority.

Williams, S. G. (2003). The effects of HMA mixture characteristics on rutting susceptibility. Transportation Research Board.

Witczak, M. W. (2005). Simple performance tests: Summary of recommended methods and database, Transportation Research Board, Vol. 46.

Witczak, M. W., Kaloush, K., Pellinen, T., El-Basyouny, M., and Von Quintus, H. (2002). Simple performance test for superpave mix design, NCHRP Report 465. Transportation Research Board, Washington, DC, USA.

Xie, Z., Shen, J., Earnest, M., Li, B., Jackson, M. (2015). Fatigue performance evaluation of porous European mix (PEM) with crumb rubber modified binders using simplified Viscoelastic Continuum Damage model." 94th Annual Meeting: Transportation Research Board, Washington D. C.

Yildirim, Y., Jayawickrama, P. W., Hossain, M. S., Alhabshi, A., Yildirim, C., Smit, A. D. F., and Little, D. N. (2007). Hamburg wheel-tracking database analysis (No. FHWA/TX-05/0-1707-7).

Zhang, Q. S., Chen, Y. L., and Li, X. L. (2009). Rutting in asphalt pavement under heavy load and high temperature in asphalt material characterization, accelerated testing, and highway management. Selected papers from the 2009 GeoHunan International Conference, ASCE (pp. 39-48).

Zhao, S., Bowers, B., Huang, B., and Shu, X. (2013). Characterizing rheological properties of binder and blending efficiency of asphalt paving mixtures containing RAS through GPC. Journal of Materials in Civil Engineering, 26(5), pp. 941-946.

Zhao, S., Huang, B., Shu, X., Jia, X., and Woods, M. (2012). Laboratory performance evaluation of warm-mix asphalt containing high percentages of reclaimed asphalt pavement. Transportation Research Record: Journal of the Transportation Research Board, (2294), 98-105.

Zhou, F., Hu, S., and Scullion, T. (2013). Balanced RAP/RAS mix design and performance evaluation system for project-specific service conditions. Texas A&M Transportation Institute, College Station, Texas (No. FHWA/TX-13/0-6092-3).

Zhou, F., Button, J. W., and Epps, J. A. (2012). Best practice of using RAS in HMA. Vol. 7, College Station: Texas Transportation Institute.

Zhou, F., Hu, S., and Scullion, T. (2006). Integrated asphalt (overlay) mixture design, balancing rutting and cracking requirements. Texas Department of Transportation (No. FHWA/TX-06/0-5123-1).

Zhou, F., Scullion, T., and Sun, L. (2004). Verification and modeling of three-stage permanent deformation behavior of asphalt mixes. Journal of Transportation Engineering, 130(4), pp. 486-494.